PNL--8167

DE93 006605

HYDROGEOLOGIC CONTROLS ON GROUND-WATER AND CONTAMINANT DISCHARGE TO THE COLUMBIA RIVER NEAR THE HANFORD TOWNSITE

S. P. Luttrell
D. R. Newcomer
S. S. Teel
V. R. Vermeul

November 1992

Prepared for
the U.S. Department of Energy
under Contract DE-AC06-76RLO 1830

Pacific Northwest Laboratory
Richland, Washington 99352

SUMMARY

In 1990, the U.S. Department of Energy, Richland Field Office, authorized Pacific Northwest Laboratory to begin a study to describe ground-water and contaminant discharge to the Columbia River in the Hanford Townsite vicinity. Ground-water and contaminant discharge from the unconfined aquifer is the emphasis of this study, which focuses primarily on the period from June 1990 through March 1992.

Results demonstrate that ground-water movement, contaminant distribution, and discharge to the Columbia River in the Hanford Townsite study area are influenced by the local geology, by regional ground-water conditions, and significantly by river-stage fluctuations. These results led to the following major conclusions.

Ground water containing tritium concentrations greater than the Drinking Water Standard of 20,000 pCi/L discharges to the Columbia River via several springs within the study area. The concentration of tritium in these springs is less than the concentration of tritium in ground water from wells because of dilution from bank storage from the Columbia River.

Regional ground-water velocity and tritium migration rate appear to be greater in the east-central part of the study area than in the southeast part of the study area. This region of higher hydraulic conductivity appears to be continuous to the river.

Fluctuations in Columbia River discharge (and stage) affect ground-water elevations and tritium concentrations in wells located as far as 800 m from the river. Statistical analyses indicate a high correlation between the river-stage fluctuations and well water-level fluctuations, with an increase in ground-water elevations during high river stage and a decrease in ground-water elevations during low river stage. The magnitude of the average horizontal hydraulic gradient across the study area also is affected by fluctuations in river stage. Fluctuations in Columbia River discharge and associated bank storage affect concentrations of tritium in wells. As the river stage rises, water from the river moves inland, resulting in dilution of

tritium concentrations in wells near the river. The water-level responses in wells are observed farther from the river than are the dilution effects of the river.

The majority of ground-water discharge to the Columbia River is from the Hanford formation aquifer. This formation has higher transmissivity and higher contaminant concentrations than the underlying Ringold Formation. The aquifer is not present in the northwest portion of the study area where the Elephant Mountain basalt subcrops above the water table, and in two locations adjacent to the Columbia River in the east portion of the study area where clay- and silt-dominated facies of the Ringold Formation subcrop above the water table. Ground-water flow and the areas of greatest discharge to the river very likely are controlled by these areas. Ground water is diverted around these areas where the Hanford formation aquifer is not present and discharges to the river in one (and quite possibly a second) restricted region.

The total ground-water discharge to the Columbia River was calculated to be approximately 6.6×10^6 m^3/year. The total tritium mass discharge to the Columbia River was calculated to be approximately 1400 Ci/year. The total uncertainty factor assigned to the calculated contaminant mass discharge calculations is plus or minus five. Although ground-water and contaminant discharge fluctuates in relation to changes in the Columbia River stage, no estimates of the time-variant nature of contaminant discharge were made.

ACKNOWLEDGMENTS

The authors want to acknowledge a number of individuals who contributed to this report. We thank Karl Pohlod, who made countless trips to the Hanford Townsite study area to install equipment and collect water-level data. We also thank Alan Pearson for performing geophysical logging of numerous wells. We appreciate David Lanigan's efforts to compile an exhaustive volume of well completion information and to graph river-stage data. We thank Paul Thorne and Michelle Chamness for their technical reviews. Last, but certainly not least, we thank Debra Perez for her very thorough editorial reviews and coordination.

CONTENTS

FIGURES

TABLES

1.0 INTRODUCTION

Pacific Northwest Laboratory (PNL)[a] has conducted studies to evaluate ground-water/surface-water relationships and contaminant discharge to the Columbia River in the vicinity of the abandoned Hanford Townsite. In 1990, the U.S. Department of Energy, Richland Field Office, authorized PNL to begin the present study, which continued through March 1992. Earlier studies were conducted in this vicinity from 1981 through 1983.

1.1 PURPOSE AND OBJECTIVES

The purpose of this study is to quantify ground-water and contaminant discharge to the Columbia River in the Hanford Townsite vicinity. The location of the Hanford Townsite study area within the regional setting is shown in Figure 1.1.

The primary objectives of the work are to

- describe the hydrogeologic setting and controls on ground-water movement and contaminant discharge to the Columbia River
- understand the river/aquifer relationship and its effects on contaminant discharge to the Columbia River
- quantify the ground-water and contaminant mass discharge to the Columbia River
- provide data that may be useful for a three-dimensional model of ground-water flow and contaminant transport in the Hanford Townsite study area.

The location of the Hanford Townsite study area (see Figure 1.1) corresponds with the region of highest tritium concentration and one of the regions of highest nitrate concentration in ground water discharging directly to the Columbia River. The majority of ground-water contamination occurs within the unconfined aquifer; therefore, ground-water and contaminant discharge from the unconfined aquifer is the emphasis of this study. The period of study is primarily from June 1990 through March 1992.

(a) PNL is operated for the U.S. Department of Energy by Battelle Memorial Institute.

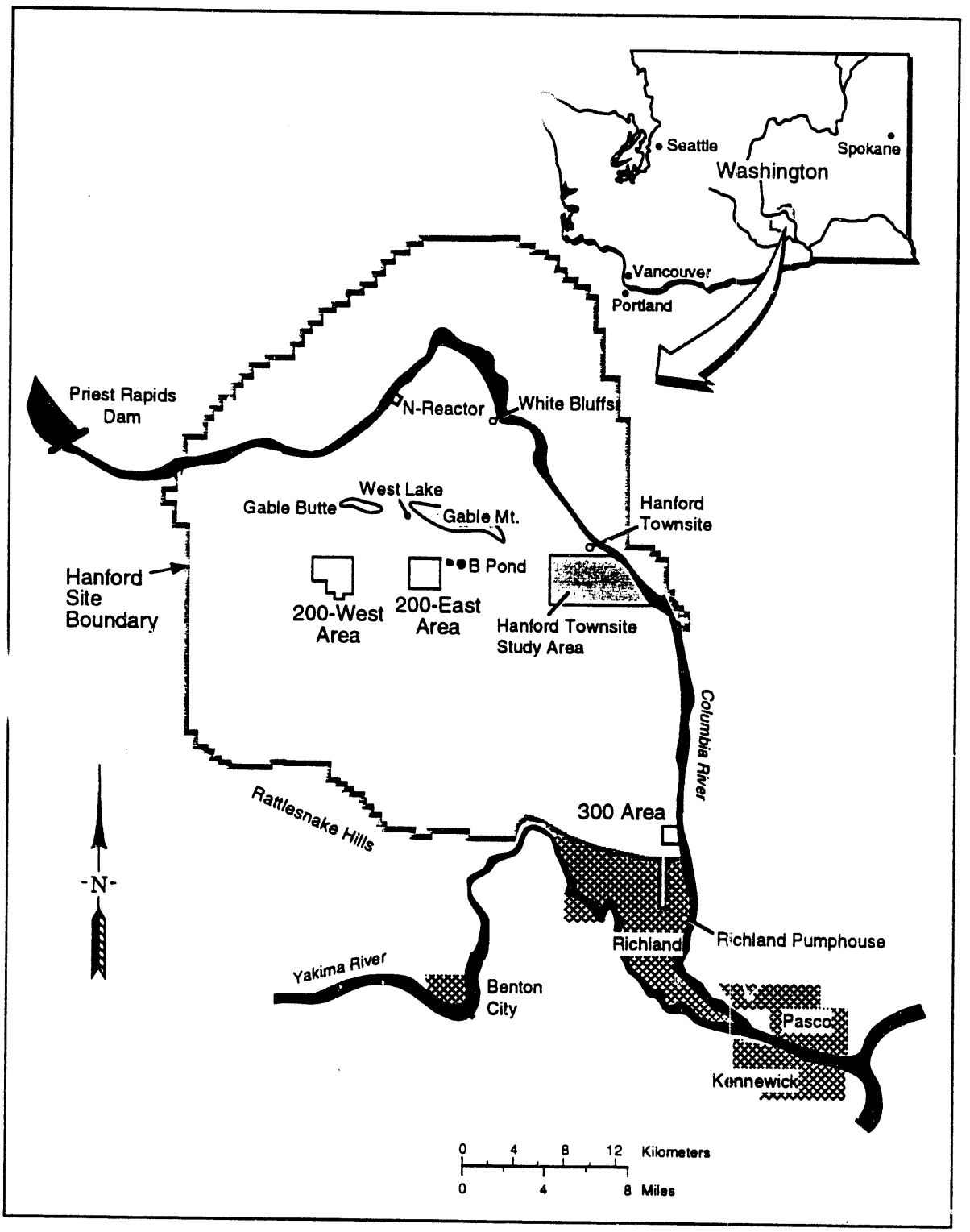

S9204082.5a

FIGURE 1.1. Hanford Site Location Map Showing the Location of the Hanford Townsite Study Area

1.2 BACKGROUND

The U.S. Department of Energy's operations on the Hanford Site have resulted in large volumes of waste water that were discharged to the ground (and the soil column) through cribs, ditches, and ponds. These discharges contaminated the ground water and influenced ground-water flow and contaminant movement in the unconfined aquifer beneath the Site. Discharge of waste water to the ground at Hanford began in the mid-1940s and reached a peak in 1955. After 1955, discharge to cribs declined because of improved treatment of waste streams and deactivation of various facilities.

Approximately 23.7 billion liters of liquid effluent, primarily cooling water, was disposed to the ground in the 200 Areas (see Figure 1.1) during 1988. This value is indicative of the magnitude of previous years' discharges to ground. Data on the volume and radionuclide inventory of waste water released to various discharge facilities are documented in annual reports prepared by the operating contractor, currently Westinghouse Hanford Company (WHC) (e.g., Cooney and Thomas 1989).

Some mobile constituents such as tritium percolate through the soil column to eventually enter the ground water. They then move downgradient in the same direction and at a rate nearly equal to ground-water flow, although their concentrations are reduced by dispersion and radioactive decay (Jaquish and Bryce 1990).

Each year, ground-water samples are collected from wells within the Hanford Site for monitoring and surveillance programs. Samples are analyzed for radiological and chemical constituents to determine the level and extent of contamination. Results of sample collection and analysis are reported annually by both PNL and WHC (e.g., Serkowski and Jordan 1989; Evans et al. 1990). The distribution of tritium in the unconfined aquifer during 1990 is shown in Figure 1.2.

Figure 1.2 shows that tritium concentrations as high as 200,000 picocuries per liter (pCi/L) may discharge to the Columbia River in the vicinity

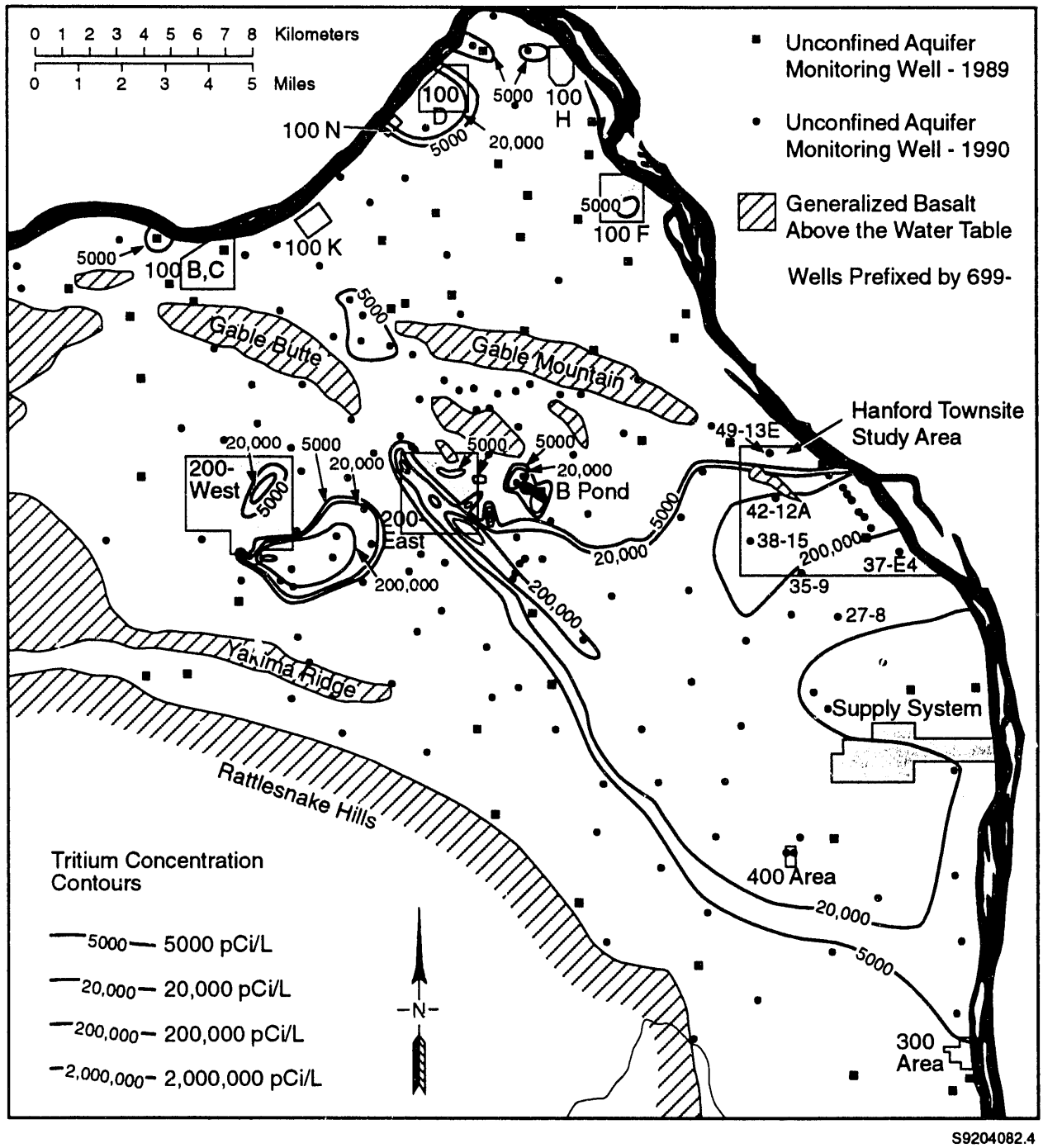

FIGURE 1.2. Distribution of Tritium in the Hanford Site Unconfined Aquifer, 1990

of the Hanford Townsite study area. This concentration exceeds the current Environmental Protection Agency (EPA) National Interim Drinking Water Standard (DWS) of 20,000 pCi/L (EPA 1976).

Ground-water discharge is known to occur via springs, many located near the Hanford Townsite. The accessibility of these springs to the public (e.g., recreational users of the river) has prompted close inquiry and review by special-interest groups and other government agencies, including the U.S. Geological Survey.

This report contains eight sections. In Section 2.0, the regional geographic, geologic, and hydrologic setting of the Hanford Site is discussed. Previous investigations pertaining to aquifer/river relationships and contaminant movement near the Hanford Townsite study area are summarized in Section 3.0. The geology of the area is detailed in Section 4.0. Section 5.0 discusses the methods and results of data collection and analysis. In Section 6.0, a conceptual model of the Hanford Townsite study area is provided, along with mechanisms and estimates of discharge to the river. The research conclusions are provided in Section 7.0, and the references cited in the report are listed in Section 8.0.

2.0 REGIONAL SETTING

This section primarily discusses the regional geographic, geologic, and hydrologic setting of the Hanford Site primarily. Most of this discussion comes from Jaquish and Bryce (1990).

2.1 GEOGRAPHY AND CLIMATE

The Hanford Site is located in a sparsely populated region of south-central Washington State and occupies an area of about 1500 km^2 (570 mi^2). The population in the area surrounding the Site is rural, with the exception of the area near the Site's southeast boundary where the major cities of Kennewick, Pasco, and Richland are located (see Figure 1.1).

The climate is dry and mild; the area receives approximately 16 cm of precipitation annually. About 40% of the total precipitation occurs during November, December, and January; only 10% falls in July, August, and September. The average minimum and maximum temperatures in July are 16°C and 32°C. The average minimum and maximum temperatures for January are -6°C and 3°C. Monthly average wind speeds range from about 15 km/h in summer to 10 km/h in winter. The prevailing regional winds are from the northwest.

The semiarid land on which the Hanford Site is located has a sparse covering of desert shrubs and drought-resistant grasses. The type of vegetation most broadly distributed on the Site is the sagebrush/cheatgrass/bluegrass community.

2.2 GEOLOGY

The Hanford Site lies within the Pasco Basin, one of many topographic and structural basins within the Columbia Plateau. Principal geologic units beneath the Hanford Site include, in ascending order, the Columbia River Basalt Group, the Ringold Formation, and a series of deposits informally referred to as the Hanford formation. These units are covered locally by a few meters or less of recent alluvial or wind-blown deposits. Older geologic

units have been deformed into a series of roughly east-west trending folds. The stratigraphic and structural relationships between these units are displayed conceptually in Figure 2.1.

Emplacement of Columbia River basalt flows was followed by a period of river and lake sedimentation. These deposits, which belong to the Ringold Formation, contain a wide range of sediment types, with beds ranging from weakly cemented coarse sandy gravel to compacted silt and clay. The Hanford formation was deposited later as a result of giant floods associated with the sudden draining of glacier-dammed lakes located northeast of the Columbia Plateau. Within the Pasco Basin, the Hanford formation consists of mostly coarse gravel and sand, and overlies the eroded surface of the Ringold Formation, but in places the Hanford formation directly overlies basalt. Deposits associated with these two formations show considerable lateral and vertical variability as a result of changing river courses over time.

2.3 HYDROLOGY

The Columbia River flows through the northern part of the Hanford Site and forms part of the Site's eastern boundary (see Figure 1.1). Priest Rapids is the nearest dam upstream of the Site and controls flow rate in the Columbia River at the Hanford Townsite study area. The Hanford Reach of the Columbia River extends from Priest Rapids Dam to the head of Lake Wallula near Richland and is the last stretch of the Columbia River above Bonneville Dam that remains unimpounded. The State of Washington Department of Ecology has designated a stretch of the river that includes the Hanford Reach as Class A (Excellent). This designation requires that all industrial uses of this water be compatible with other uses, including drinking, wildlife habitat, and recreation.

Flows in the Hanford Reach fluctuate significantly because of the relatively small storage capacities and the operational practices of upstream dams. Flow rate of the Columbia River through the Site is regulated primarily by Priest Rapids Dam. Typical daily flows range from 1000 to 7000 cubic meters per second (m^3/s), with peak spring runoff flows of up to 12,600 m^3/s.

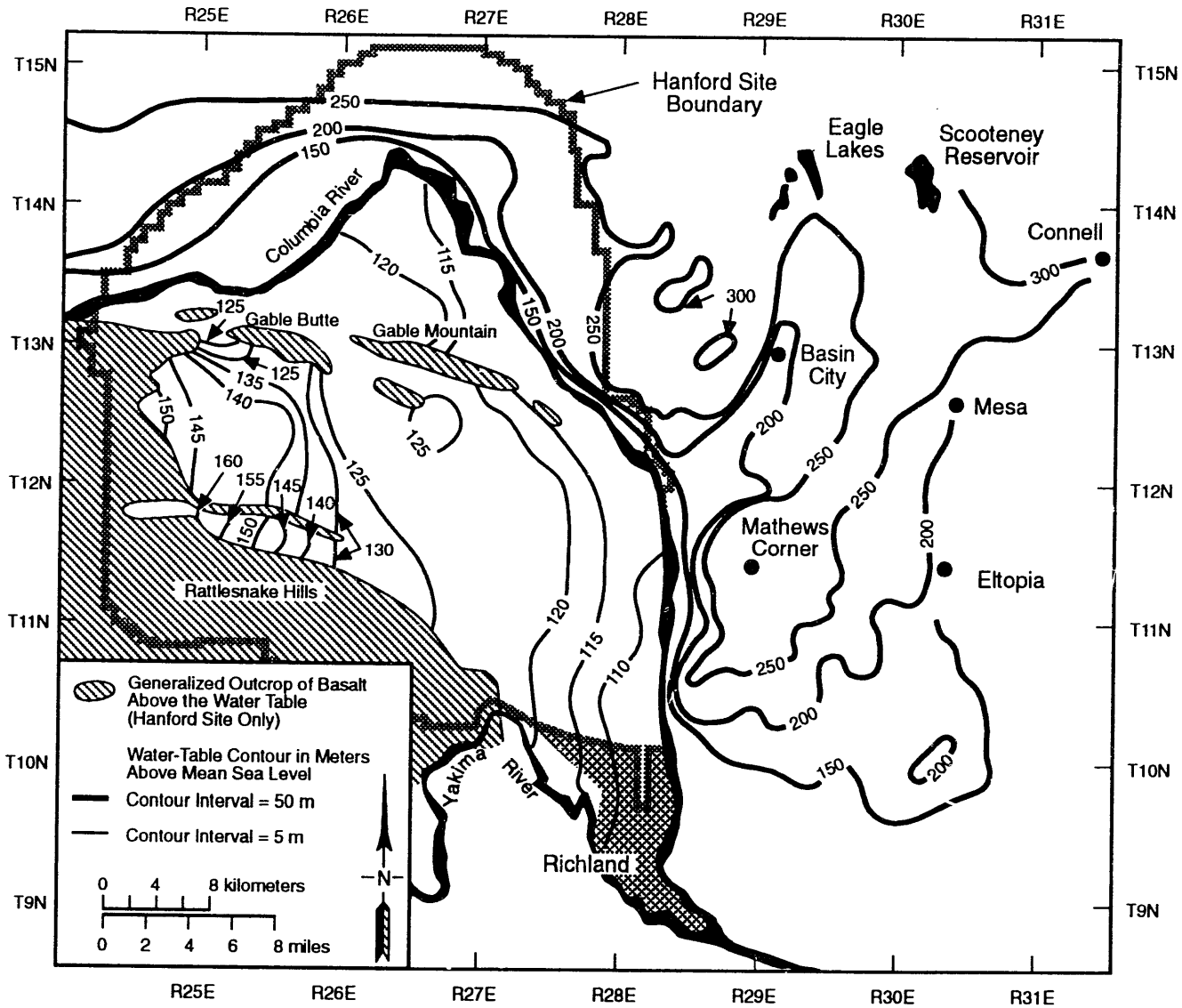

FIGURE 2.2. Water-Table Elevations for the Unconfined Aquifer at Hanford, June 1990 (after Woodruff and Hanf 1991)

Dry Creek to the west. The Columbia River recharges the unconfined aquifer, if only temporarily, during high stages when river water is transferred to the aquifer along the riverbank (bank storage). Gee (1987) reviewed available information and concluded that minimum recharge (<0.1 cm/year) occurs where soils are fine textured and surfaces are vegetated with deep-rooted plants, while maximum recharge (10 cm/year) occurs where there are coarse soils or gravel and no vegetation is present at the surface.

Large-scale artificial recharge occurs from off-site agricultural irrigation and from on-site liquid-waste disposal in the operating areas. Recharge from irrigation in the Cold Creek Valley enters the Hanford Site as ground-water flow across the western boundary. Artificial recharge from waste-water disposal occurs principally in the 200 Areas (see Figure 1.1). The operational discharge of water has created ground-water mounds and altered the aquifer's local flow pattern, which is generally from the recharge areas in the west to the discharge areas (primarily the Columbia River) in the east. Ground-water levels have continued to change during Site operations, and the movement of ground water and associated constituents also has changed with time.

2.4 GROUND-WATER MONITORING

Radiological and chemical constituents in ground water are monitored by the Ground-Water Surveillance Project to 1) determine the distribution of mobile radionuclides and selected chemicals, 2) relate the distribution of these constituents to Site operations, and 3) identify chemicals present in ground water as a result of Site operations. The distribution of tritium and nitrate in ground water within the Hanford Site is shown in Figures 1.2 and 2.3, respectively. Separate tritium pulses associated with two episodes of operations within the 200-East Area can be distinguished. The lobe that encompasses a portion of the Hanford Townsite study area is a result of discharges to ground from 1956 to 1972 (Evans et al. 1990).

Approximately 11 wells in the Hanford Townsite study area have been sampled several times for the Ground-Water Surveillance Project. Ground water with tritium concentrations greater than 200,000 pCi/L exists within the

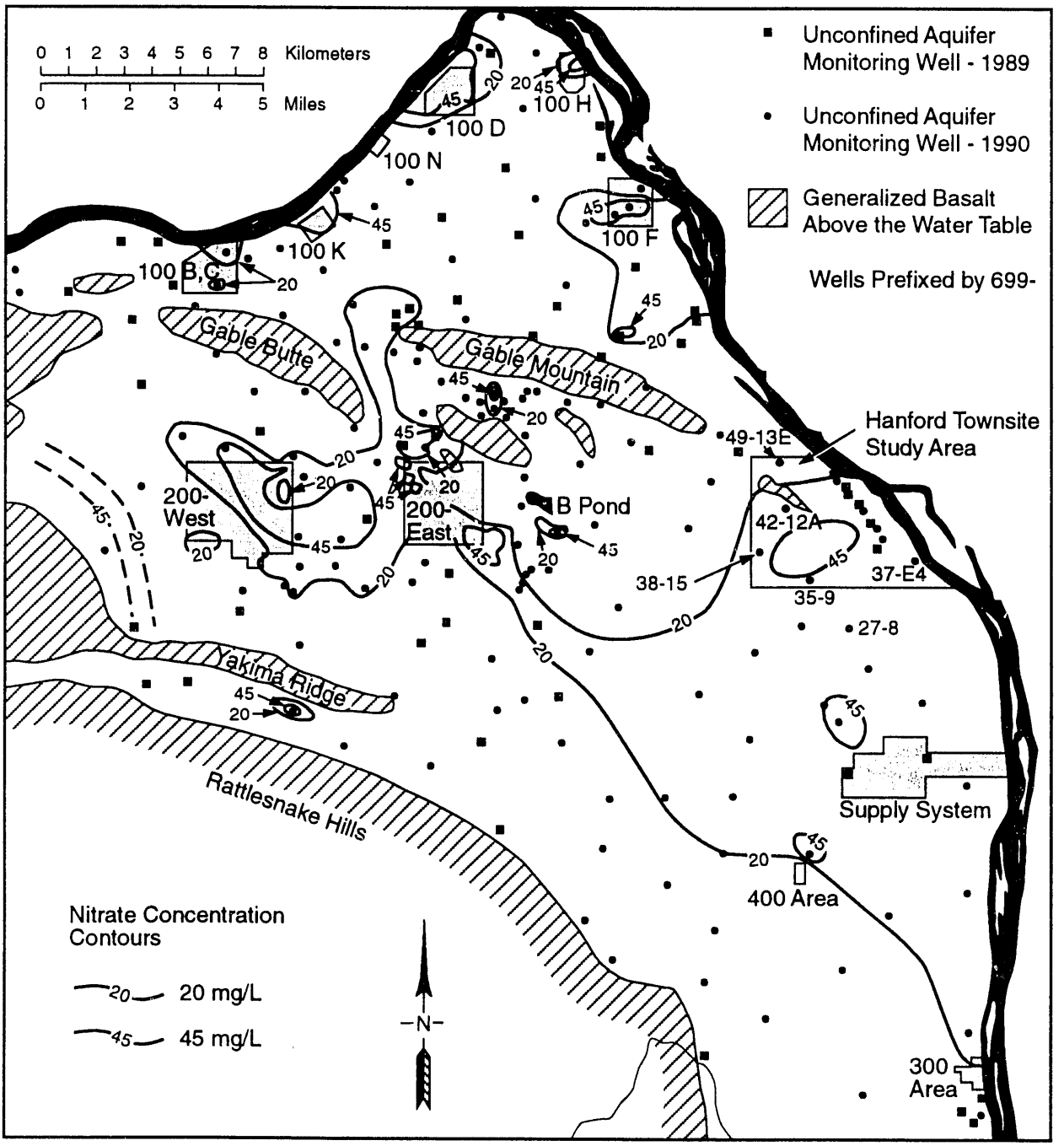

FIGURE 2.3. Distribution of Nitrate in the Hanford Site Unconfined Aquifer, 1990

Hanford Townsite study area and in fact appears to discharge to the river. Nitrate concentration in ground water within the Hanford Townsite study area is near 45 mg/L, which is the EPA DWS for nitrate. The northern edge of the tritium contamination plume is distinctly defined near the north side of the Hanford Townsite study area; however, the southern portion of the plume extends south to the 300 Area, and the concentration appears to decrease gradually toward the south.

3.0 PREVIOUS INVESTIGATIONS

A large number of reports have been prepared concerning Hanford Site geology, hydrogeology, and contaminant source, movement, and distribution. This discussion pertains primarily to those reports that have a particular bearing on aquifer/river relationships and contaminant distribution and movement near the Hanford Townsite study area.

The U.S. Geological Survey discussed the geology and ground-water characteristics of the Hanford Site (Newcomb et al. 1972). The discussion on effects of the Columbia River on ground-water levels in wells near the river is of particular interest to the present study. The authors concluded that within a 3-km (2-mi)-wide belt in which the ground water rises during flood stage in the river, a great deal of water is recharged to bank storage and then discharged back to the river during its declining stages. The high level of bank-stored water causes a ground-water gradient inland away from the river in some areas. Newcomb and Brown (1961) gave 10^8 m^3 (84,000 acre-feet) of water as the probable volume of the annual bank storage along the west bank of the Columbia River beneath the Hanford Site, and determined that about 99% is infiltrated from the river. It is apparent that bank storage will affect both contaminant distribution and ground-water and contaminant discharge to the river.

Evaluation of bank storage in the vicinity of the Hanford Townsite study area began in October 1981 in support of the Ground-Water Surveillance Project to obtain information about interactions of the Columbia River and the unconfined aquifer (Eddy et al. 1982, 1983; Prater et al. 1984). The authors found a strong direct relationship between the Columbia River flow rate and ground-water levels in wells near the river. The influence of the river on ground-water levels was found to decrease with increasing distance from the river. The authors indicated that the maximum extent of the influence is approximately 1.2 km (0.75 mi). They also found a strong inverse relationship between the Columbia River flow rate and tritium concentrations in one well approximately 200 m (700 ft) from the river; tritium concentrations were reduced by the influence of bank storage. The authors concluded that

contaminant concentrations in samples from wells near the river will be influenced by bank storage, and that this should be taken into consideration when determining sampling schedules and interpreting analytical results from these wells.

Search Technical Services (Search) collected water-chemistry data from springs in the Hanford Townsite study area vicinity to estimate ground-water discharge to the river (Buske and Josephson 1986). The authors, using data collected in 1986, asserted that the average ground-water discharge to the river from 260 m (852 ft) of Columbia River shoreline is greater than 0.2 m^3/s (6 ft^3/s). The authors further maintained that ground water flows from the 200-East Area to the Columbia River primarily through a boulder-filled channel connecting the 200-East Area to the river and that the travel time for ground water to move from the 200-East Area to the river is less than 3 years.

The U.S. Geological Survey (USGS) reviewed selected work and suggested further study related to transport of radionuclides in the upper aquifer on the Hanford Site (USGS 1987). In particular, the USGS reviewed the results presented by Search. The USGS authors concluded that available data did not confirm or refute the existence of a narrow, boulder-filled channel as proposed by Search. They did, however, state that the data suggest an alternative hypothesis allowing for large, localized ground-water discharge and longer travel times between the 200-East Area and the river than proposed by Search. The USGS concluded that such travel time is probably on the order of 10 to 20 years.

The USGS recommended further studies to characterize movement of radionuclides. The suggestions offered by the USGS include 1) installing additional wells for geologic and hydrologic characterization and mapping the extent and thickness of the saturated Hanford formation deposits; 2) using an improved mass-balance method (improved over the method used by Search) to estimate ground-water discharge to the river; and 3) conducting three-dimensional ground-water flow and contaminant transport modeling, based on reliable water-level and water-chemistry data.

Estimates of ground-water travel time from waste-water source areas to discharge areas within the Hanford Site have been calculated by several

researchers. These estimates were reviewed by Freshley and Graham (1988). These authors indicate that contaminant movement and travel times in the unconfined aquifer are influenced by the pattern of natural recharge, the locations and volumes of artificial recharge in the operating areas, the distribution of hydraulic properties within the aquifer, the starting and ending locations for flow paths, and the chemical composition of liquid contaminants and geochemical behavior of contaminants in Hanford Site ground water. All of these factors may interact over the length of the flow path. Recent applications of ground-water flow and contaminant transport models have considered the distribution of arrival times as well as the distribution of outflow quantities. These distributions have been used to estimate the dose to individuals at outflow locations such as the Columbia River (Murthy et al. 1983; DOE 1987).

Pacific Northwest Laboratory has evaluated, on two different occasions, the discharge of ground water to the Columbia River along the Hanford Reach via springs. Both of these studies included investigation of spring discharges in the Hanford Townsite study area. The first, conducted in fall 1982 and fall 1983, provided qualitative descriptions of physical characteristics and relative magnitudes of the spring discharges, and tritium, iodine-129, and nitrate analysis results from spring samples (McCormack and Carlile 1984). One significant conclusion of this study was that monitoring the unconfined aquifer is the most effective method of monitoring ground-water discharges to the Columbia River, primarily because river water can mix with ground water and produce diluted concentrations in spring discharges.

The second study, conducted primarily in fall 1988, sampled a smaller number of springs in the Hanford Townsite study area; however, a much more comprehensive list of constituents was analyzed for (Dirkes 1990). The results of this work confirmed that the type and concentrations of contaminants in the riverbank springs along the Hanford shoreline are within the range known to exist in ground water near the river. Tritium concentration from some springs in the Hanford Townsite study area was above the DWS of 20,000 pCi/L. River samples collected near some spring discharge zones also exceeded the DWS for tritium.

4.0 GEOLOGY

This section discusses the geology of the Hanford Townsite study area, including a discussion of previous work and a description of the suprabasalt sediments.

4.1 PREVIOUS WORK

Investigations of the geology of the Hanford Townsite study area include those of Puget Sound Power and Light Company (PSPL 1982) and Poeter and Gaylord (1990). PSPL (1982) included the results of an extensive study connected with the siting of a proposed nuclear power plant. Numerous boreholes were drilled in the Hanford Townsite vicinity for this study. Golder Associates supervised the installation of these wells, which are informally referred to as "Golder wells."

Poeter and Gaylord (1990) constructed lithofacies percentage maps and geologic cross sections of the upper 25 m of the saturated zone and compared these with contour maps of tritium concentrations at various times. Two types of lithofacies maps were constructed, gravel dominated and mud dominated. The mud-dominated map appeared to be more effective than the gravel-dominated map at predicting potential paths of contaminant migration, thereby suggesting that mud-dominant areas are significant in controlling contaminant migration. Areas where mud-dominated lithofacies intersect the water table may be especially important. The cross sections constructed by these authors showed the lateral correlation of mud-dominated lithofacies. However, some of the wells used in the cross sections of Poeter and Gaylord were spaced at distances of up to 7.5 km; correlation of thin, mud-dominated lithofacies over such distances can be speculative. Nevertheless, the study suggests that lithofacies trends can be helpful in predicting contaminant migration paths.

In addition, Gaylord and coworkers at Washington State University (WSU) in 1990 and 1991 examined drill logs, geophysical logs, and core samples; constructed cross sections; and performed grain size analyses and limited petrographic analyses. They also described analog lithofacies via measured sections along the White Bluffs (along the east side of the Columbia River).

They used this information as input for a multiple indicator conditional stochastic simulation along a 3.7-km-long two-dimensional cross section. This simulation is a geostatistical technique that estimates aquifer heterogeneity and the spatial distribution of lithofacies. This technique is discussed in more detail in Sections 4.2.1 and 5.7.

4.2 SUPRABASALT SEDIMENTS IN THE HANFORD TOWNSITE STUDY AREA

The following brief description of the suprabasalt sediments summarizes the previous work mentioned in Section 4.1, with additional examination of geologic logs from the many boreholes and wells in the study area. Figure 4.1 is a map showing the locations of all wells within the study area. Table 4.1 summarizes the available well construction information for these wells. Construction details are sketchy at best for many of the Golder wells because these wells often were used as shotholes (i.e., blasting) for geophysical investigations. Some of these wells have been geophysically logged by PNL. A summary of geophysical logging performed by PNL to date (including camera surveys) is provided in Appendix A.

Three geologic cross sections were constructed to illustrate the stratigraphy of the study area (see Figure 4.1). These cross sections are shown in Figures 4.2 through 4.4.

4.2.1 Ringold Formation

The Ringold Formation consists of a variety of lithologies that include 1) clast-supported, pebble-cobble gravels with a sand matrix that includes varying degrees of mud (silt and clay); 2) sands to gravelly sands; 3) silt to silty sands; and 4) clay to silty clay with minor sand and gravel. The Ringold Formation ranges from 0 to 104 m thick in the study area. This variable thickness is a result of a combination of erosion by post-Ringold Pleistocene catastrophic flood events and bedrock topography. It ranges from unconsolidated to consolidated and can be locally cemented. The age of the Ringold Formation is Miocene-Pliocene and ranges from about 8.5 to 3.4 million years ago (Fecht et al. 1987).

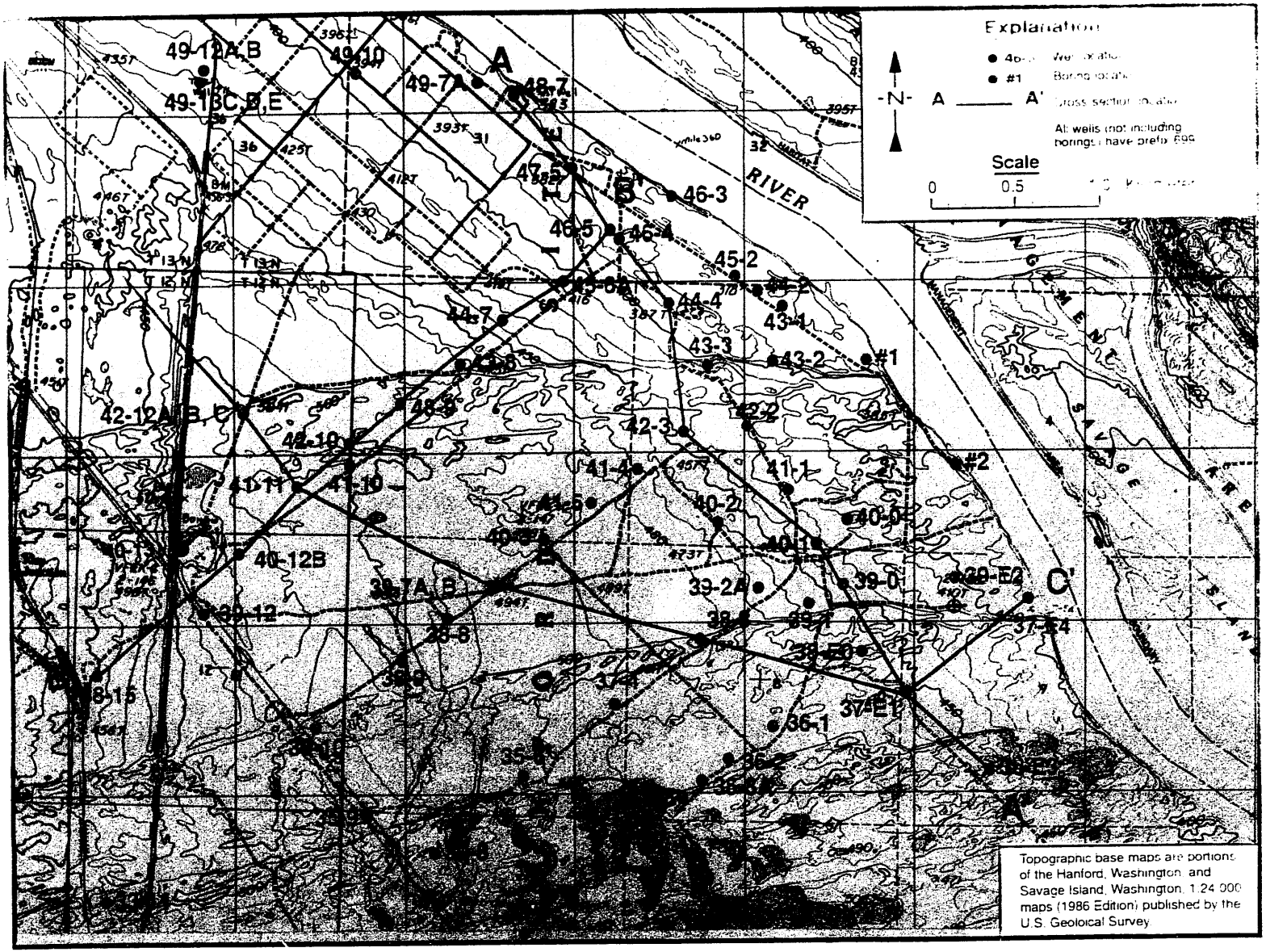

FIGURE 4.1. Location Map of Wells and Cross Sections Within the Hanford Townsite Study Area

TABLE 4.1. Hanford Townsite Well Table

Hanford Well Number	Golder Well Number	Drill Depth (m)	Depth to Bottom (m)	Date Completed	Casing Diameter (cm)	Type of Casing	Casing Interval (m)	Monitored Interval (m)	Casing Elevation (m)
699-33-6	52	180.1	54.9	6/80	15.2	CS[a]	+0.5 - 54.2	Bottom of Casing	153.41
					10.2	PVC[b]	0 - 180.1		
699-33-14	30	174.7	36.6	5/80	15.2	CS	0 - 36.6	Bottom of Casing	144.24
					10.2	PVC	0 - 174.3		
699-34-8	119	175.3	28	1/81	15.2	CS	0 - 90.8	Bottom of Casing	148.21
					10.2	PVC	0 - 175		
699-35-3	53	146.3	0	5/80	15.2	None		Abandoned	
699-35-3A		?	?	1/81	?	?	?	?	146.35
699-35-6	118	161.5	0	1/81	15.2	CS	+1 - 60.1	Bottom of Casing	153.28
					10.2	PVC	0 - 161.5		
699-35-9		53.6	53.6	10/50	20.3	CS		33.5 - 41.1	152.35
699-36-E3	100	114.3	114.3	12/80	15.2	CS	0 - 78.6	Bottom of Casing	141.94
					10.2	PVC	0 - 114.3		
699-36-1	54	91.0	34.7	5/80	15.2	CS	+0.2 - 44.5	Bottom of Casing	148.08
					10.2	PVC	0 - 90.8		
699-36-2	111	93.9	86.9	11/80	15.2	CS	+0.8 - 66.1	Bottom of Casing	147.50
					10.2	PVC	+0.8 - 88.4		
699-36-10	115	183.8	43.0	12/80	20.3	CS	+0.7 - 73.1	Bottom of Casing	160.63
					15.2	CS	4.3 - 136.5		
					10.2	PVC	0 - 183.8		
699-37-E1	94	94.3	50.6	8/80	15.2	CS	+1.0 - 30.0	Bottom of Casing	140.34
					10.2	PVC	9.1 - 49		
699-37-E4		29.9	9.1	7/82	15.2	CS	+0.3 - 25	25.0 - 29.9	117.99
699-37-4	101	84.9	35.8	10/80	15.2	CS	+0.4 - 32.6	Bottom of Casing	149.01
699-38-E0	55	82.3	33.5	6/80	15.2	CS	0 - 41.8	Bottom of Casing	143.14
					10.2	PVC	0 - 82.3		
699-38-3	102	81.4	3.8	11/80	15.2	CS	+1 - ?	Bottom of Casing	152.22
699-38-8	122A	141.7	?	2/81	15.2	CS	0 - 42.1	Bottom of Casing	146.33
					10.2	PVC	0 - 140		
699-38-9	113	166.1	28.3	12/80	15.2	CS	0 - 70.1	Bottom of Casing	153.51
					10.2	PVC	0 - 166.1		
699-38-15	4	149.4	38.1	12/79	15.2	CS	0 - 38.1	Bottom of Casing	138.61
699-39-E2	68	74.7	19.5	6/80	15.2	CS	0 - 25.9	Bottom of Casing	123.41
					10.2	PVC	0 - 74.7		
699-39-0		32.0	30.8	8/90	15.2	CS	+0.9 - 32	25.9 - 29.0	137.02
699-39-1	99	103.6	30.5	10/80	15.2	CS	0 - 66.4	Bottom of Casing	145.26
699-39-2A	103	93.6	30.8	11/80	15.2	CS	0 - 30	Bottom of Casing	142.52
699-39-7A	108	79.2	37.2	11/80	15.2	CS	41 - 59.7	Bottom of Casing	150.07
					10.2	PVC	52.2 - ?		
699-39-7B	125	137.6	46.3	6/81	15.2	CS	0 - 42.2	Bottom of Casing	149.23
699-39-12	2	46.9	0?	2/80	?	?	Abandoned?		161.96
699-40-0	120	114.3	30.5	1/81	15.2	CS	+0.7 - 67?	Bottom of Casing	128.27
					10.2	PVC	20 - 114?		
699-40-1		128.0	30.5	11/61	20.3	CS	+0.6 - 96.3	19.8 - 30.4	133.72
699-40-2	98	123.4	121.9	10/81	15.2	CS	+0.7 - 90.8	Bottom of Casing	
					10.2	PVC	+0.7 - 123.4		
699-40-6	109	86.3	32.0	11/80	15.2	CS	+0.8 - 47.8	Bottom of Casing	148.69
					10.2	PVC	31 - 86		
699-40-12B	3	148.1	148.1	2/80	15.2	CS	0 - 45	Bottom of Casing	157.59
					10.2	CS	0 - 95		
699-40-13	1	153.6	24.0	2/80	15.2	CS	?	?	
699-41-1		26.7	25.9	8/79	15.2	CS	+0.4 - 27	20.1 - 25.9	131.85
699-41-4	123	116.4	115.8	2/81	15.2	CS	0 - 41.7	Bottom of Casing	
					10.2	PVC	0 - 116.6		
699-41-5	110	83.2	79.9	11/80	15.2	CS	+0.7 - 54.0	Bottom of Casing	147.46
					10.2	PVC	0 - 82.3		
699-41-10	5	89.3	?	11/79	25.4	CS	0 - 6.1	Bottom of Casing	153.02
					20.3	CS	0 - 82.5		

TABLE 4.1. (contd)

Hanford Well Number	Golder Well Number	Drill Depth (m)	Depth to Bottom (m)	Date Completed	Casing Diameter (cm)	Type of Casing	Casing Interval (m)	Monitored Interval (m)	Casing Elevation (m)
699-41-11	104	131.1	?	10/80	15.2	CS	+0.4 - 85.1	Bottom of Casing	156.30
					10.2	PVC	0 - 131		
699-42-2		30.5	29?	8/79	15.2	CS	+0.7 - 29?	22.6 - 27.4	132.13
699-42-3	116	128.0	45.1	12/80	15.2	CS	0 - 82	Bottom of Casing	135.41
					10.2	PVC	0 - 127.4		
699-42-10	112	67.1	67.1	11/80	15.2	CS	0 - 53.8	Bottom of Casing	151.03
					7.6	PVC	0 - 67.0		
699-42-12A		106.7	54.9	12/57	20.3	CS	+0.3? - 97.5	36.6 - 54.9	156.75
					15.2	KAI[c]	30.8 - 55.8	55.2 - 55.8	
699-42-12B		79.2		4/76	30.5	CS	+0.3? - 79.2	42.7 - 73.2	156.67
699-42-12C		47.2	27.1	5/76	15.2	CS	+0.3? - 47.2	?	141.41
699-43-1		19.8	0	9/80		None		Abandoned	
699-43-2	117	118.9	118.9	12/80	15.2	CS	0 - 85.3	Bottom of Casing	123.66
					10.2	PVC	0 - 118.9		
699-43-3		26.7	23.8	7/79	20.3	CS	+0.6 - 26.5	19.8 - 25.0	127.91
699-43-8	7	86.3	0	11/79			Abandoned		144.24
699-43-9	105	67.1	66.5	10/80	15.2	CS	+0.4 - 49.4	Bottom of Casing	149.58
					7.6	PVC	0 - 67.0		
699-44-2		21.3	0	9/80		None		Abandoned	132.13
699-44-4		16.8		7/79	15.2	CS	+0.7 - 16.8	9.8 - 16.5	119.26
699-44-7	106	144.8	144.2	11/80	15.2	CS	+1.0 - 103.6	Bottom of Casing	133.44
					7.6	PVC	+1.0 - 144.8		
699-45-2		14.6	13.7	9/80	15.2	CS	+0.5 - 14.8	7.9 - 11.6	115.79
699-45-6A		?	?	12/79	15.2	CS	0 - 36	Bottom of Casing	125.59
					10.2	PVC	0 - 40		
699-46-3	11	98.5	15.5	12/79	15.2	CS	+1.2 - 26.5	Bottom of Casing	116.29
					7.6	PVC	0 - 99		
699-46-4		14.6	13.7	7/79	15.2	CS	+0.3 - 14.1	7.0 - 14.0	116.57
699-46-5	114	115.8	116.7	12/80	15.2	CS	+0.79 - 92	Bottom of Casing	117.13
					10.2	PVC	0 - 116.7		
699-46-15	34	18.3	9.1	3/80	15.2	CS	+0.7 - 8.8	Bottom of Casing	135.35
					10.2	PVC	0 - 18.0		
699-47-5		13.7	12.8	7/79	15.2	CS	+0.3 - 13.4	6.4 - 13.4	116.51
699-48-7		16.5	14.6	9/43?	30.5	CS	+0.3? - 15?	3.7 - 9.8	117.26
699-49-7A		16.8	0	6/43	35.6	CS	?	Abandoned	117.1
699-49-10		13.7	0	1/44	15.2	CS	?	Abandoned?	120.75
699-49-12A		31.1	?	3/44	15.2	CS	+0.4 - 28.0	Abandoned?	125.29
699-49-12B		29.6	?	2/44	15.2	CS	+0.4 - 28.0	Abandoned?	125.34
699-49-13C		21.6	?	2/44	15.2	CS	+0.3 - 20.7	Abandoned?	126.15
699-49-13D		28.2	?	3/44	50.8	CS	+0.6 - 27.4	Abandoned?	125.69
699-49-13E		25.6	24.4	3/44	50.8	CS	0 - 24.4	16.8 - 22.9	125.80
Boring #1		20.4		7/82		None		Abandoned	
Boring #2		44.5		7/82		None		Abandoned	

(a) CS = carbon steel.
(b) PVC = polyvinyl chloride.
(c) KAI = KAI well casing.

Vertical Sequence

On the Hanford Site, the Ringold Formation has been subdivided in several different ways. For many years, the dominant scheme was that of Tallman et al. (1979) which divided the Ringold into basal, lower, middle, and upper units. Other schemes include that of Webster and Crosby (1982), who defined four units based on fining-upward cycles. Recently, Lindsey (1991) proposed a new subdivision based on sediment facies associations. Because of the inconsistency among the types of data available for the Hanford Townsite study area (Golder well logs versus drillers logs from a variety of drilling companies), and the fact that the sediments in the study area do not necessarily fit easily into defined subdivisions, a detailed subdivision of the Ringold Formation will not be attempted for this report. The emphasis will be placed on lateral major lithology changes within the unit. However, the established subdivisions will be referred to when appropriate.

The Ringold Formation unconformably overlies the Elephant Mountain Member of the Columbia River Basalt Group (Webster and Crosby 1982). Immediately overlying the Elephant Mountain Member is generally a clay/silty-clay/clayey-silt unit; however, sand or silty sands may occur locally. This unit probably was deposited under either overbank or lacustrine conditions (Lindsey 1991). Overlying this unit are interfingering gravel-, sand-, and silt-dominated units. Gravel-dominated units probably represent stream-channel deposits, sand-dominated units are probably stream deposits or near-overbank deposits, and silt-dominated units probably were deposited as overbank deposits (Lindsey 1991). The Ringold Formation is capped frequently by silts, silty sands, and/or sandy silts with varying amounts of clay. This uppermost unit corresponds to the upper Ringold unit of Tallman et al. (1979) and the upper mud unit of Lindsey (1991). Fining-upward sequences are common in the middle and upper portions of the Ringold Formation (Webster and Crosby 1982).

Based on boreholes installed by PNL from 1979 to 1982, Eddy et al. (1983) described a clay deposit in the Ringold Formation (upper mud unit?) that intersects the water table and appears to act as a partial barrier to ground-water flow. Logs of these borings have been examined; this clay deposit appears to be present in wells 699-43-1 and 699-43-2, and borings #1

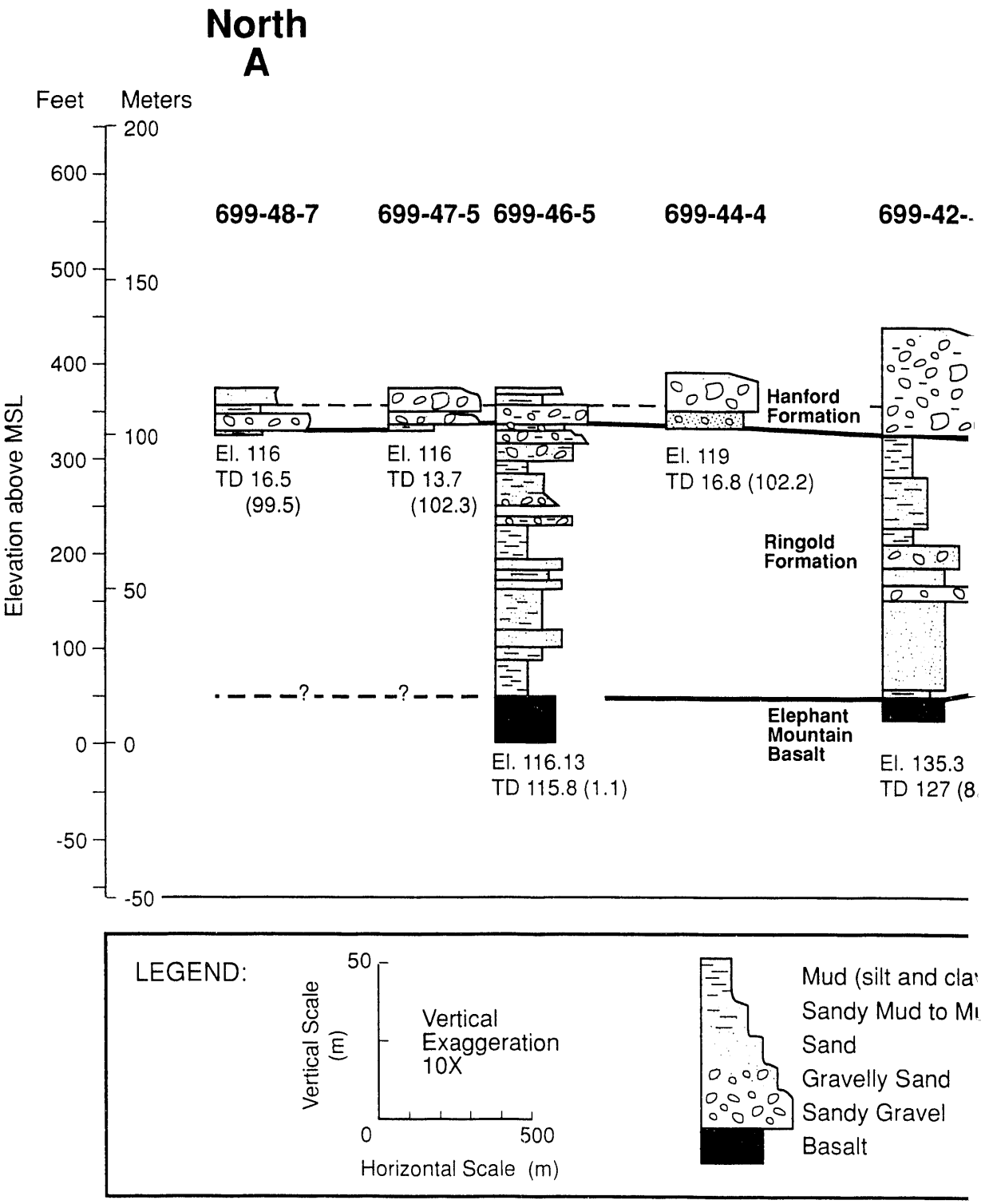

FIGURE 4.2. Cross Section A

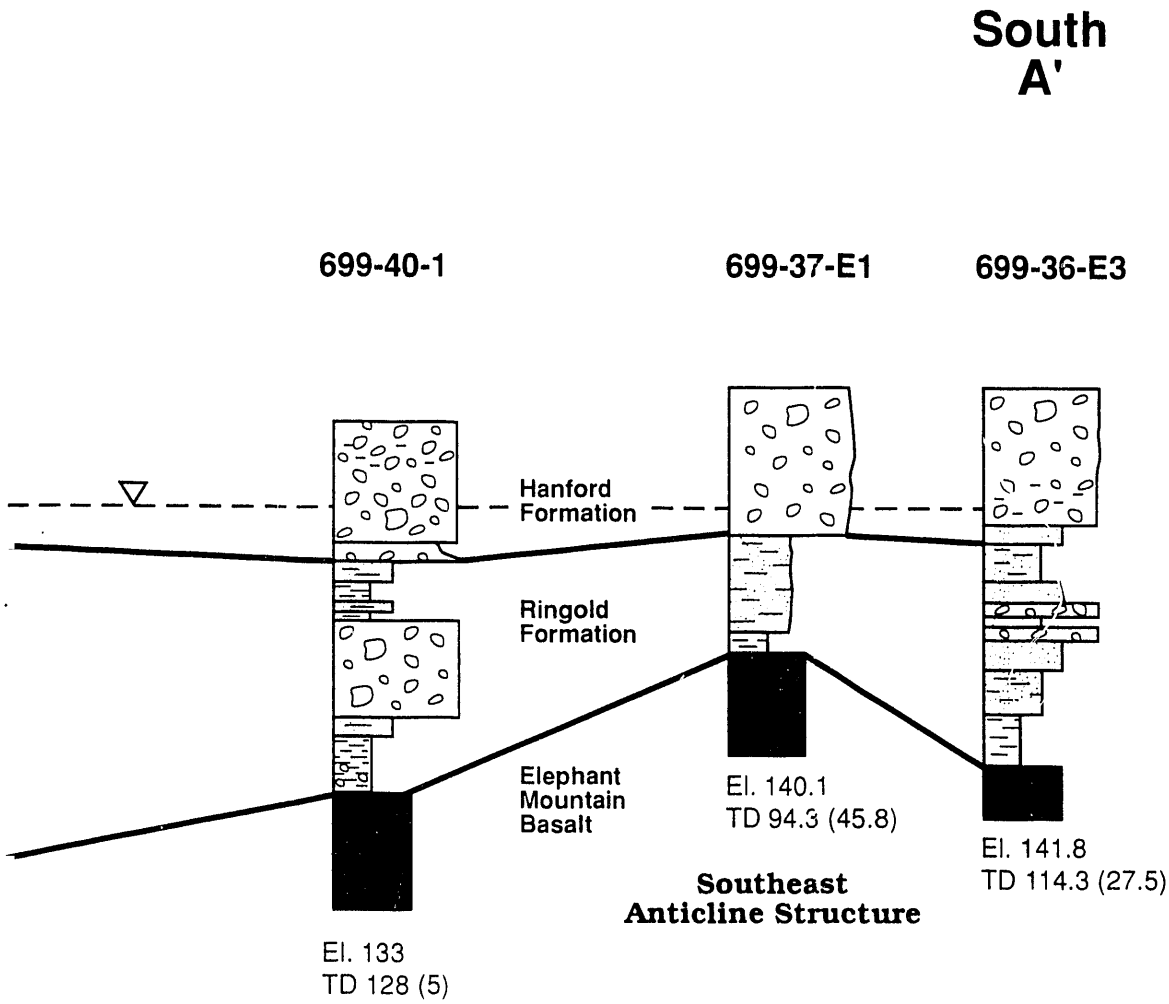

S9205013.2

	Formation boundaries
	Approximate elevation of water-table surface
El.	Surface elevation (m above MSL)
TD 81.4 (70.3)	Total depth (elevation of TD) (m)
MSL	Mean sea level

idy Sand

' (location shown in Figure 4.1)

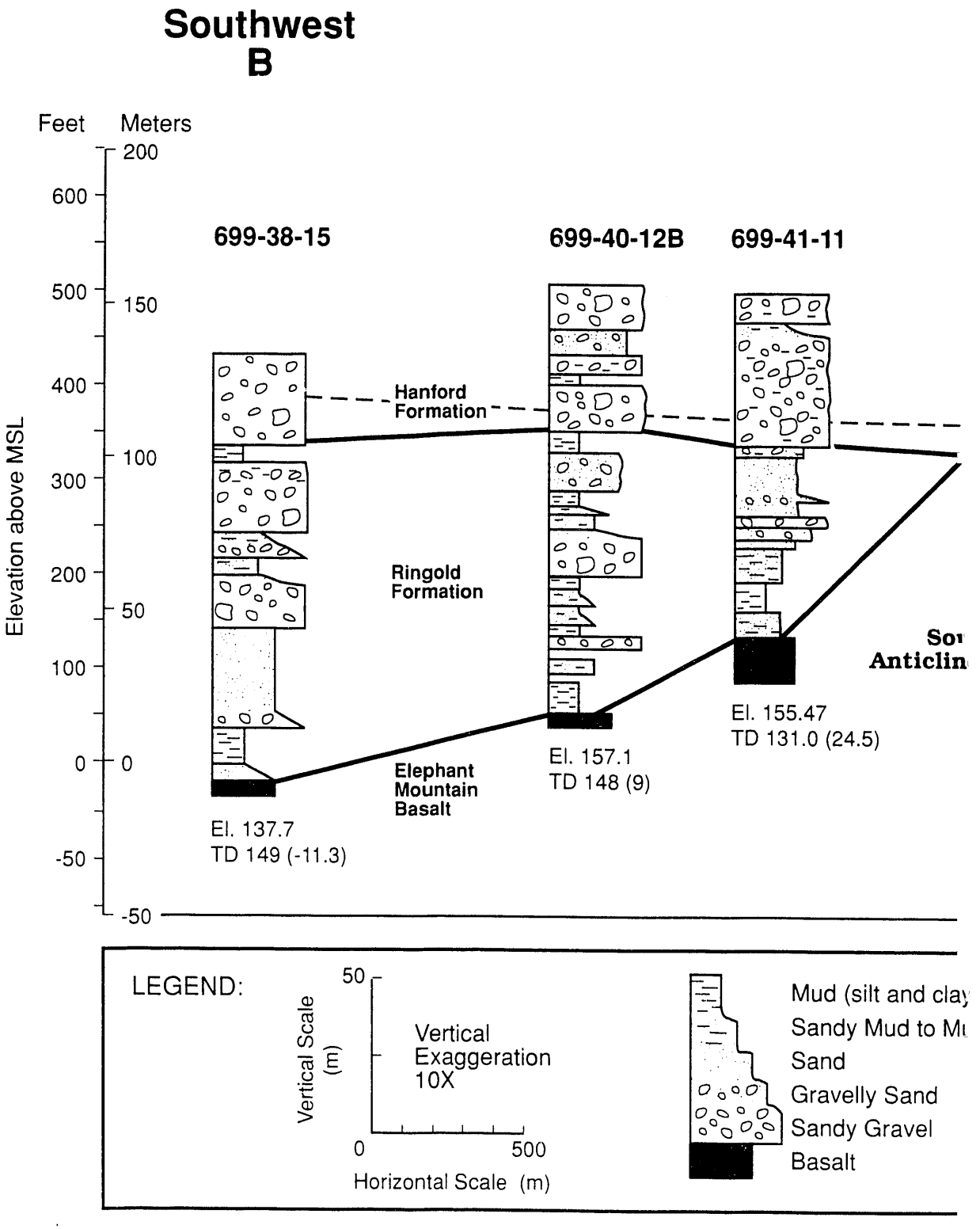

FIGURE 4.3. Cross Section B-

Northeast
B'

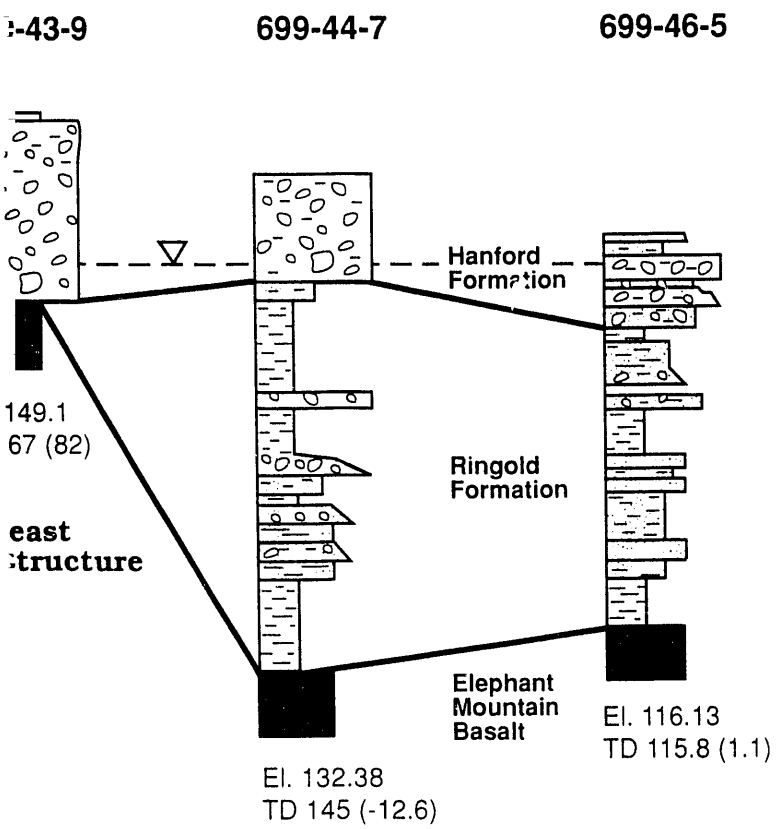

S9205013.3

	Formation boundaries
ly Sand	Approximate elevation of water-table surface
El.	Surface elevation (m above MSL)
TD 81.4 (70.3)	Total depth (elevation of TD) (m)
MSL	Mean sea level

(location shown in Figure 4.1)

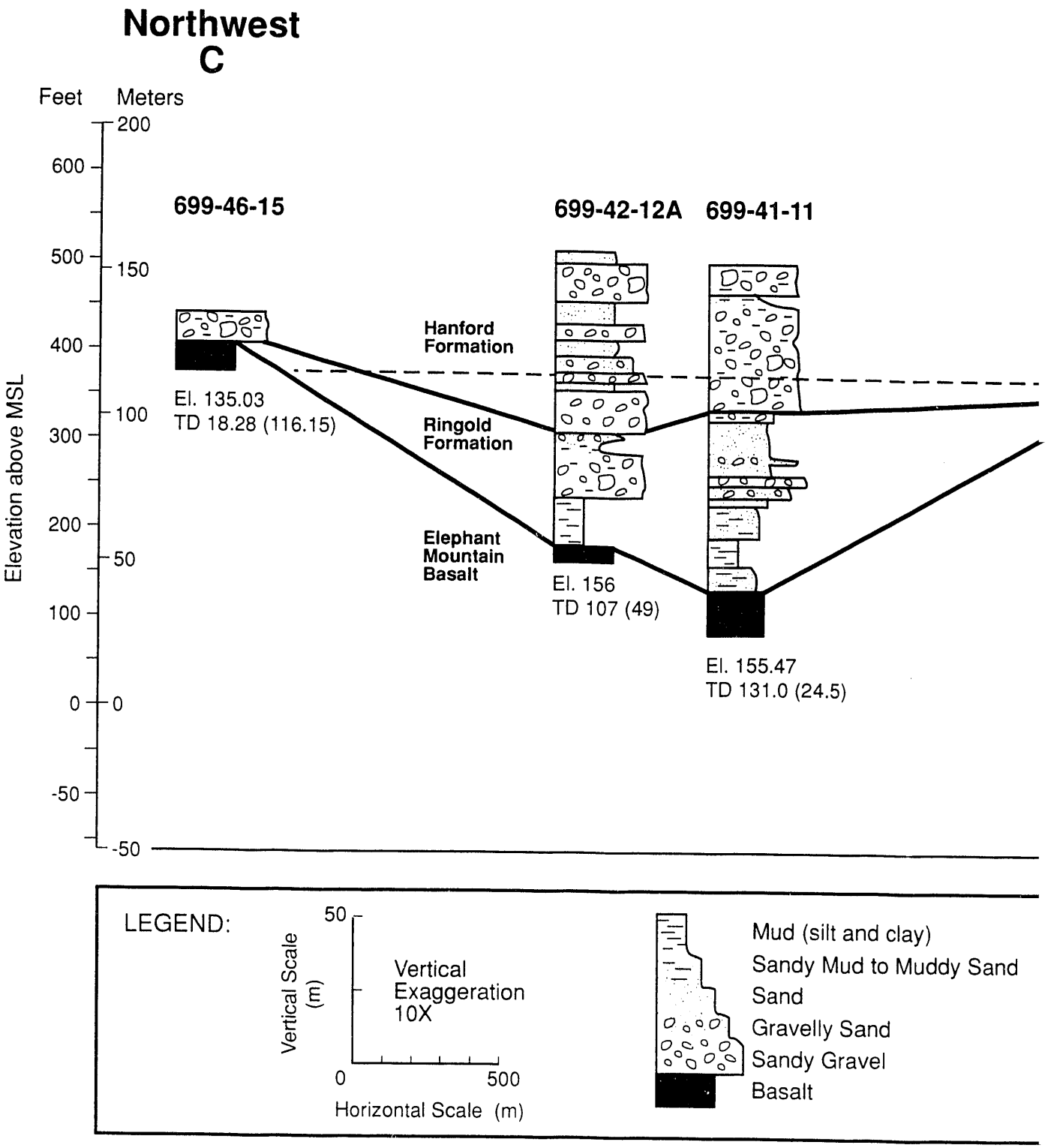

FIGURE 4.4. Cross Section C-C

Southeast C'

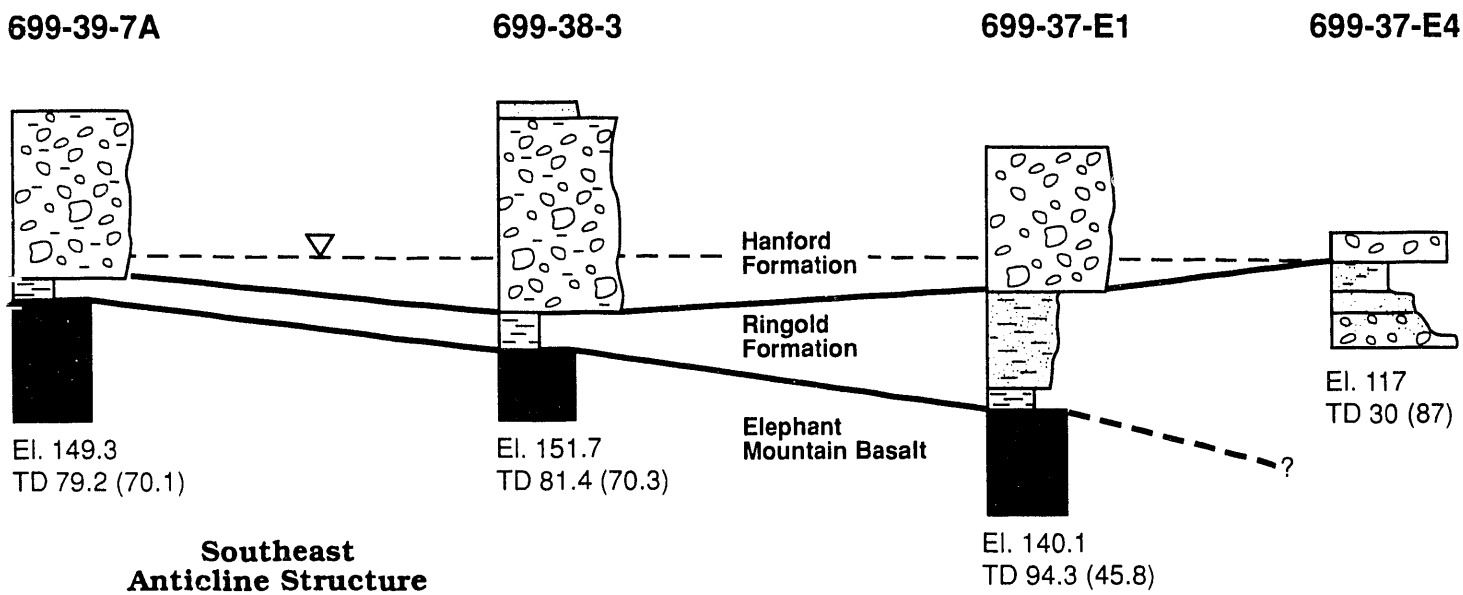

Southeast Anticline Structure

S9205013.1

———	Formation boundaries
_ _ ▽ _ _	Approximate elevation of water-table surface
El.	Surface elevation (m above MSL)
TD 81.4 (70.3)	Total depth (elevation of TD) (m)
MSL	Mean sea level

(location shown in Figure 4.1)

and #2. A similar clay deposit is also present in well 699-37-E4 (see Figure 4.4). These two clay lenses appear to represent uneroded portions of the upper part of the Ringold Formation and appear to be separated by a paleochannel (see discussion on paleochannels in Section 4.2.2).

Influence of Bedrock Topography

The topography of the surface-underlying basalt units may have been very important in influencing the nature of the sediments deposited during Ringold time. A structure contour map of the top of basalt is shown in Figure 4.5 (the elevations observed in the wells used to construct this map are provided in Appendix B). The most obvious feature on this map is the large basalt high that trends northwest-southeast across the center of the study area. This feature is the Southeast Anticline segment of the Umtanum Ridge–Gable Mountain structural trend (PSPL 1982) and is thought to have developed concurrently with Ringold Formation deposition (Bjornstad 1985).

In 1990 and 1991, D. R. Gaylord and coworkers at WSU observed that deposits north and east of the Umtanum Ridge–Gable Mountain structural trend are dominated by finer-grained (overbank) materials while deposits south of the trend are dominated by gravel, sandy gravel, and sand (channel deposits), although both types of deposits can be found on either side of the structure. This is illustrated in cross sections B-B′ (Figure 4.3) and C-C′ (Figure 4.4) and in stochastic simulation #99 (Figure 4.6). Figure 4.6 is a cross section of a stochastic simulation along most of the length of section B-B′. All three of the above cross sections cross the crest of the Southeast Anticline.

A structure contour map of the bottom of the Hanford formation is shown in Figure 4.7 (the elevations observed in the wells used to construct this map are provided in Appendix B). Comparison of this figure with Figure 4.5 indicates that the Ringold Formation reaches a maximum thickness of approximately 104 m near well 699-38-9, just to the south of the anticlinal crest. The Ringold thins to 0 to 10 m at the crest of the structure.

4.2.2 Hanford Formation

The Hanford formation commonly is divided into two subunits: the Pasco gravels and the Touchet Beds (Myers/Price et al. 1979). Within the study

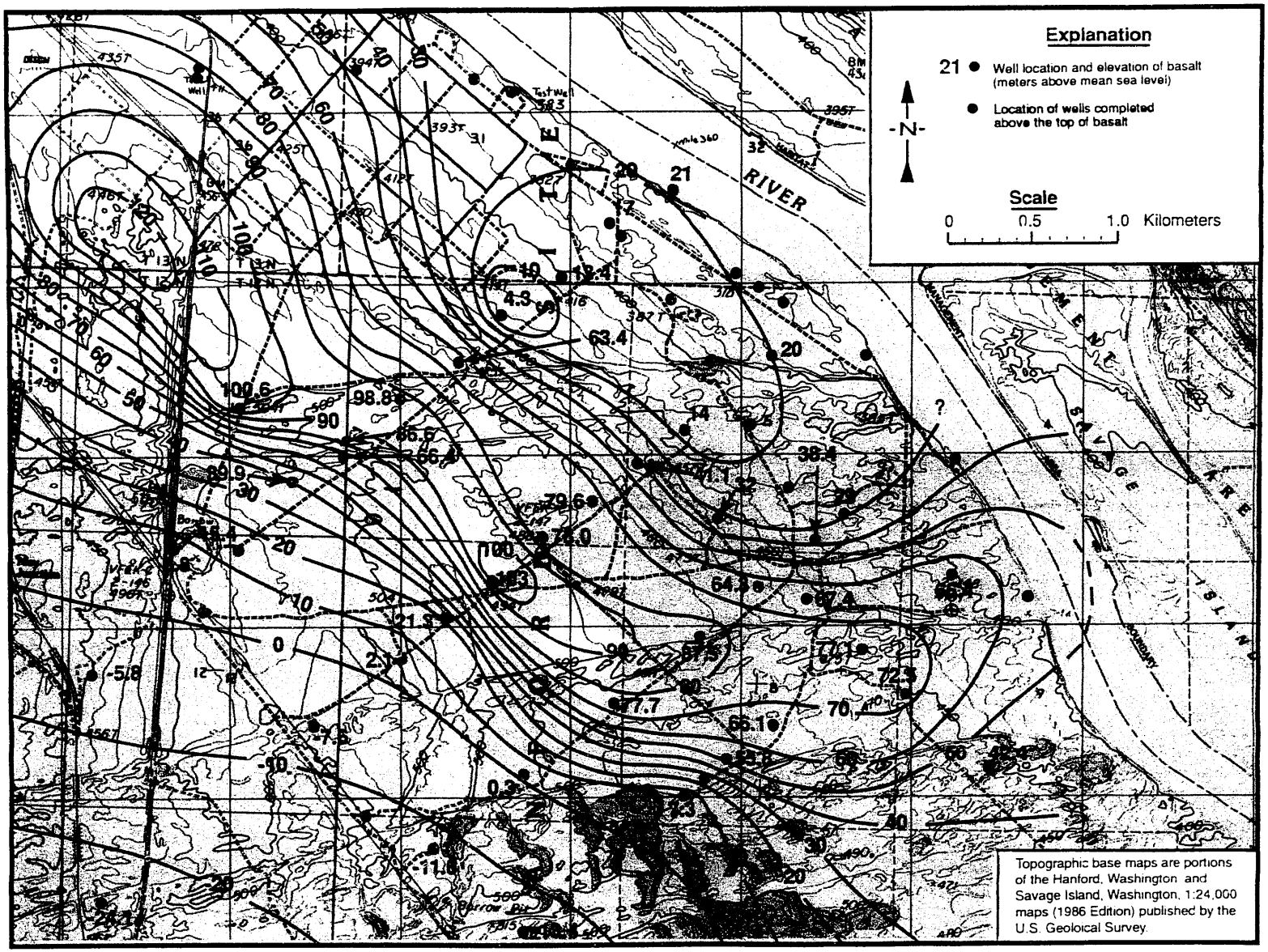

FIGURE 4.5. Structure Contour Map of the Top of Basalt in the Hanford Townsite Study Area

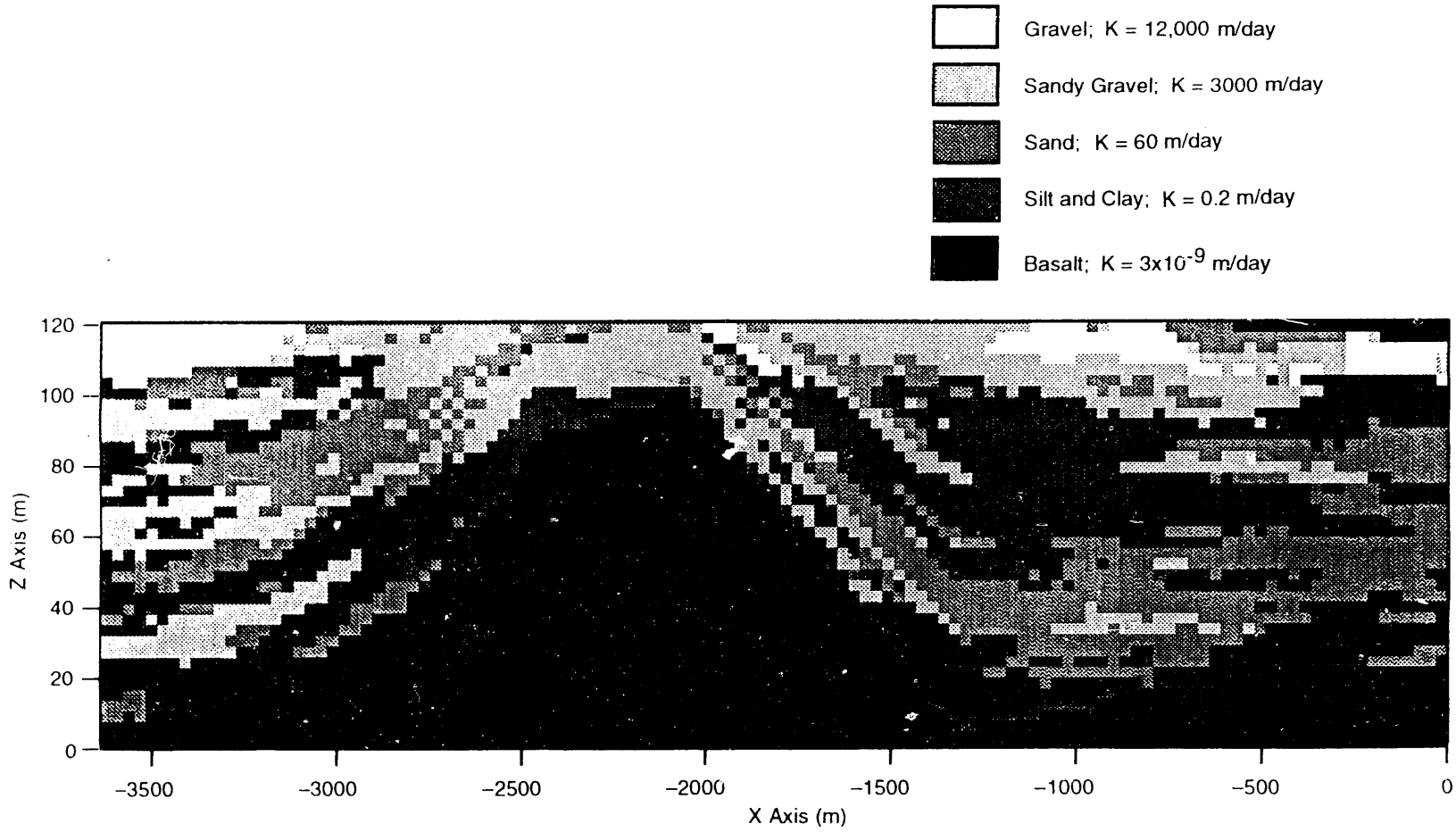

FIGURE 4.6. Example of a Stochastic Realization Along Cross Section B-B'

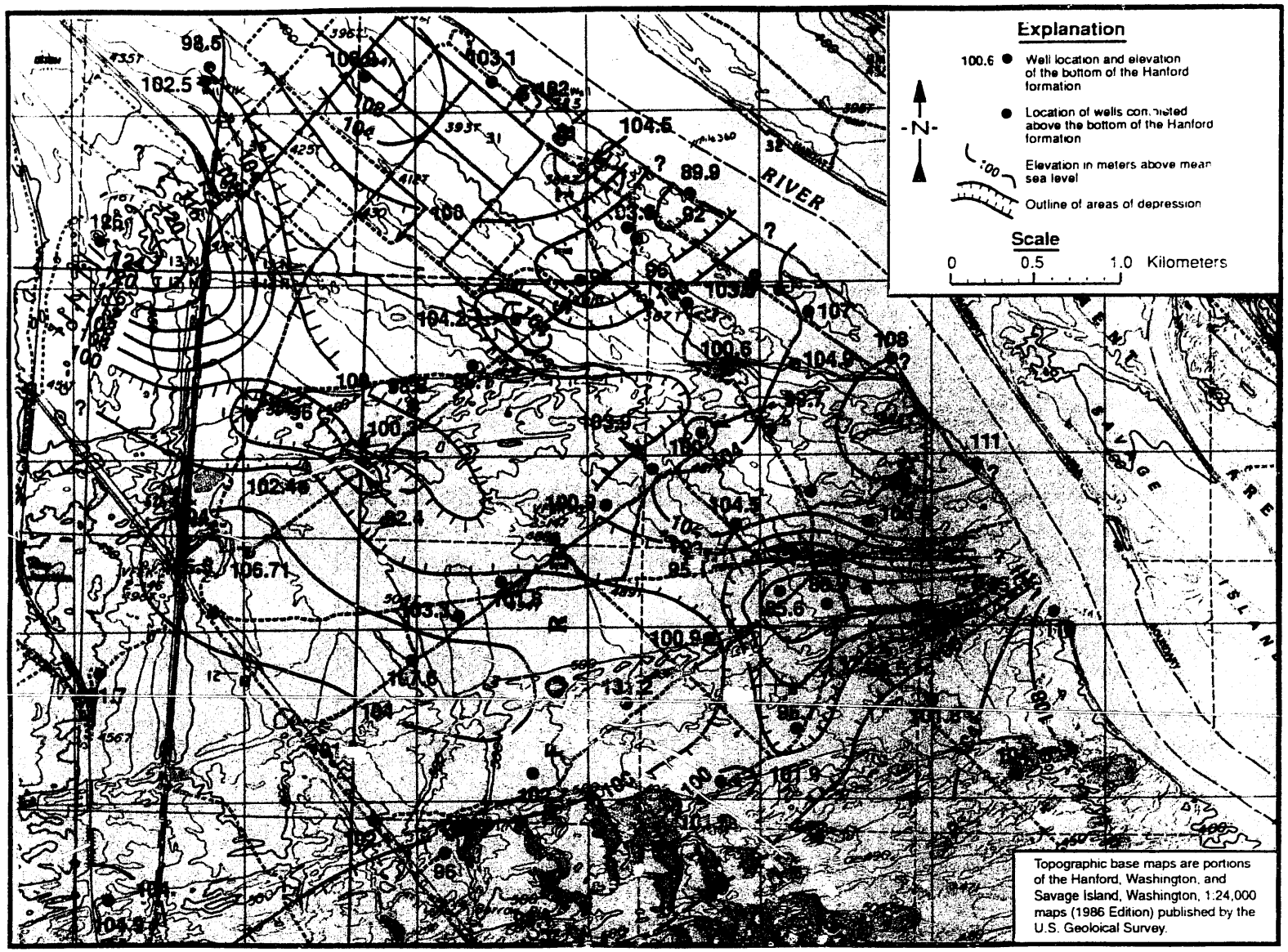

FIGURE 4.7. Structure Contour Map of the Bottom of the Hanford Formation in the Hanford Townsite Study Area

area, the Hanford formation consists of the Pasco gravels facies. Webster and Crosby (1982) divided the post-Ringold sediments into "Pre-Missoula Flood Gravels" and "Missoula Flood Gravels." The Missoula Flood Gravels are equivalent to the upper portion of the Pasco gravels; the Pre-Missoula Flood Gravels were deposited during a previous flood event and are equivalent to the basal portion of the Pasco gravels. Missoula Flood Gravels and Pre-Missoula Flood Gravels can be distinguished using Golder well log data; however, well logs from other sources do not permit such differentiation. For this report, therefore, the "Pasco gravels" terminology will be used. The Hanford formation is distinguished from the underlying Ringold Formation by its higher percentage of basalt fragments; unconsolidated, commonly open-work texture; and color. Bjornstad et al. (1991) provided more detailed information about regional Hanford formation stratigraphy.

The Pasco gravels were deposited from intermittent cataclysmic floods that occurred between 800,000 years ago (Bjornstad and Fecht 1989) and 13,000 years ago (Mullineaux et al. 1978). This unit is dominated by a gravel to sandy-gravel facies that commonly shows open-work fabric, large-scale foreset bedding, and a high concentration of basalt clasts. However, two other facies also are commonly found within this unit: sand dominated and silt dominated. The sand-dominated facies includes sands and gravelly sands that are commonly bedded subhorizontally. The silt-dominated facies includes silts with varying amounts of sand and minor clay to gravelly-clay units. These three facies are generally uncemented and unconsolidated, except for the silt-dominated facies, which may be semiconsolidated. Lateral distributions of these facies were shown on Figures 4.2 through 4.4.

A structure contour map of the bottom of the Hanford formation is shown in Figure 4.7. The higher-elevation area in the northwest quadrant of the map is due to a subcrop of basalt that occurs above the water table. The 108-m contour near boring #2 corresponds to the general area of the clay unit in the Ringold Formation that may restrict discharge to the river.

The cataclysmic floodwaters that deposited the Hanford formation scoured the surfaces of both the Columbia River basalt and the Ringold Formation. Brown (1960) was one of the earliest workers to suggest that the surface of

the Ringold Formation consisted of an "extensively channelled, highly irregular erosion surface." Possible paleoflow directions and locations of paleoflow channels associated with cataclysmic flooding on the Hanford Site are shown in Figure 4.8. The noticeable depressed areas in the structure contour map of the bottom of the Hanford formation (see Figure 4.7) may correspond to scouring by such paleoflow channels.

Overlying the Hanford formation are thin, discontinuous, Recent-age deposits of loess, dune sand, and alluvial sand.

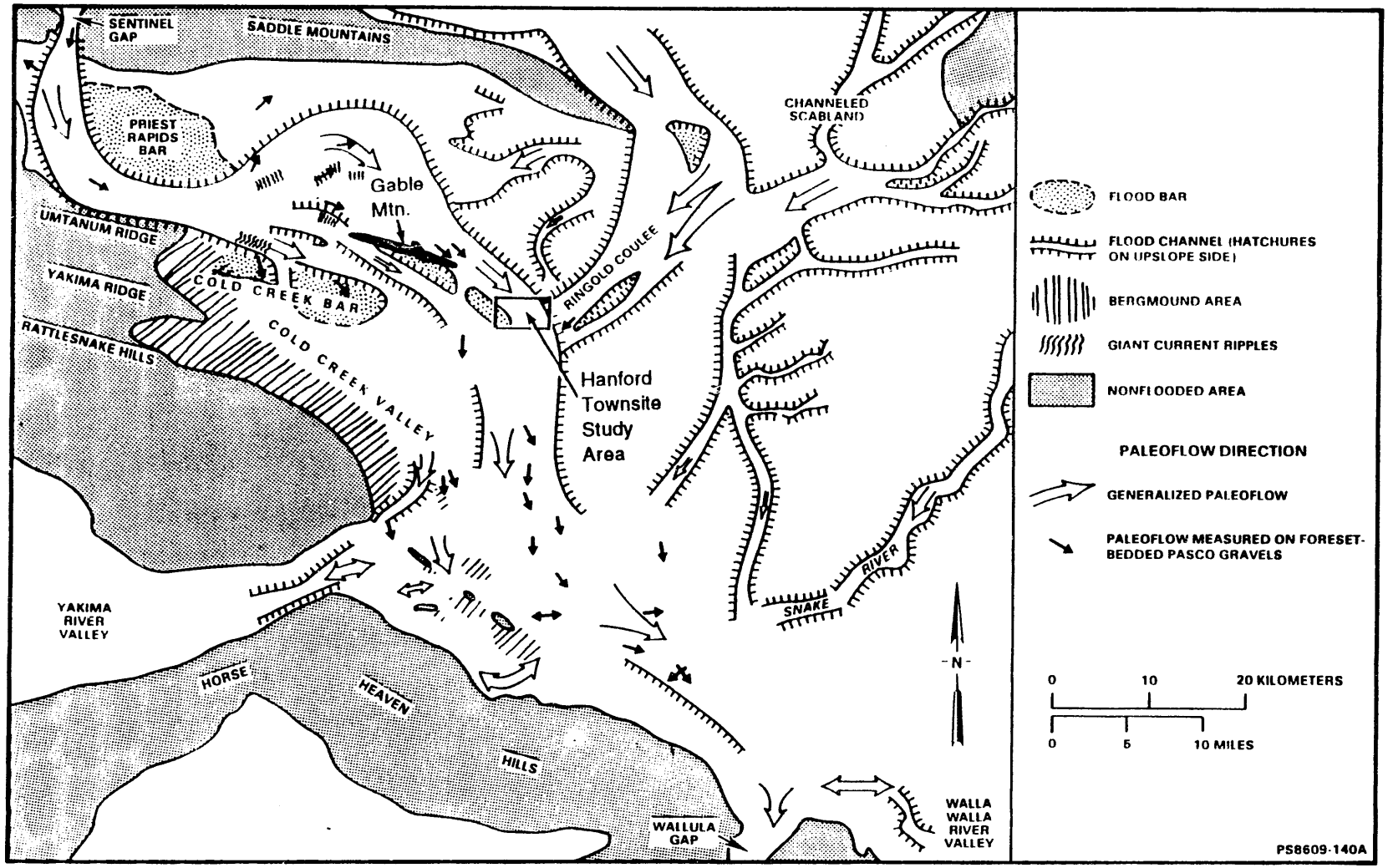

FIGURE 4.8. Paleoflow Directions and Landforms Associated with Proglacial Cataclysmic Flooding in the Central Columbia Plateau (from DOE 1988)

5.0 HYDROLOGY

This section discusses methods of data collection and analysis, presents results of the data collected, and discusses the results. Some of the specific data are presented in appendixes.

5.1 DATA COLLECTION AND ANALYSIS

All wells available for use in this study were shown on Figure 4.1 and listed in Table 4.1. Most of these wells have intervals open to the unconfined aquifer within the Hanford formation, and a very few wells have intervals open to upper portions of the Ringold Formation. Several boreholes installed for the Skagit/Hanford Nuclear Project by Golder Associates were drilled into basalt and are open to the basalt either as uncased boreholes or as cased, open-ended boreholes. The wells used in this study are those with open intervals within the Hanford formation and Ringold Formation. Water-level data were collected from several wells open to the basalt, and some of these data are presented; however, these data are not used in the evaluation of ground-water and contaminant discharge to the river.

Hydrologic data collection and analysis centered around measuring water-level elevations in wells, measuring river-level elevations in the Columbia River, collecting and analyzing samples from wells for tritium analysis, and analyzing and interpreting these data. Several limiting factors resulted in intermittent periods of data collection, as discussed later.

The data were interpreted to describe ground-water flow directions, river/aquifer relationships, hydrologic properties, and a general conceptual hydrogeologic model of the Hanford Townsite study area. An attempt also was made to model ground-water flow with a numerical model.

5.1.1 Water-Level Measurements in Wells

Depth-to-water measurements were made in a number of wells for the period from July 1990 to January 1992. The wells are listed in Table 5.1, along with the types of measurement made in each well and the formation

TABLE 5.1. Wells Used for Hydrologic Data Collection

Hanford Well Number	Screened Interval Depth (m)	Monitored Geologic Unit	Type of Hydrologic Data Collected
699-35-9	34 - 41	Hanford	W. L.[a] - Tape
699-37-E4	25 - 30	Ringold	W. L. - Tape, Trans.
699-38-15	38.1	Ringold	W. L. - Tape
699-39-0	25 - 28	Hanford	W. L. - Tape
699-40-1	20 - 30	Hanford	W. L. - Tape, Trans.
699-41-1	20 - 27	Hanford	W. L. - Tape
699-41-11	?	Elephant Mt.?	W. L. - Tape
699-42-2	23 - 27	Hanford	W. L. - Tape
699-42-10	67.1[b]	Elephant Mt.	W. L. - Tape
699-42-12A	37 - 55	Ringold/Hanford	W. L. - Tape, Rec.; W. Chem.[c]
699-42-12B	43 - 73	Ringold/Hanford	W. L. - Tape
699-43-3	20 - 25	Hanford	W. L. - Tape, Trans.; W. Chem.
699-44-4	10 - 16	Hanford	W. L. - Tape
699-44-7	144.8[b]	Elephant Mt.	W. L. - Tape, Rec.
699-45-2	8 - 12	Hanford	W. L. - Tape
699-46-4	7 - 14	Hanford	W. L. - Tape; W. Chem.
699-46-5	116.7[b]	Elephant Mt.	W. L. - Tape, Rec.
699-47-5	6 - 13	Ringold/Hanford	W. L. - Tape; W. Chem.
699-48-7	4 - 10	Hanford	W. L. - Tape, Rec.

(a) W. L. = water-level measurements were made using standardized steel tapes (Tape), chart-type recorders (Rec.), or pressure transducers (Trans.).
(b) No screen; open at bottom of casing.
(c) W. Chem. = water-chemistry samples were collected.

to which each well is open. The wells are shown in Figure 5.1. Measurements were made monthly or twice a month in 14 of these and were made intermittently in some. One or two reconnaissance water-level measurements were made in several wells, especially those open to the basalt. Data from these wells are provided in Appendix C, but they are not listed in Table 5.1 or shown on Figure 5.1.

The depth to water was measured from an established measuring point with standardized steel tapes according to procedures developed by PNL (1989). The depth to water was subtracted from the elevation of the measuring point to obtain the water-level elevation. The depth-to-water measurements and water-level elevations for the wells are presented in Appendix C. These water-level elevation data were used to plot hydrographs and construct water-level contour maps.

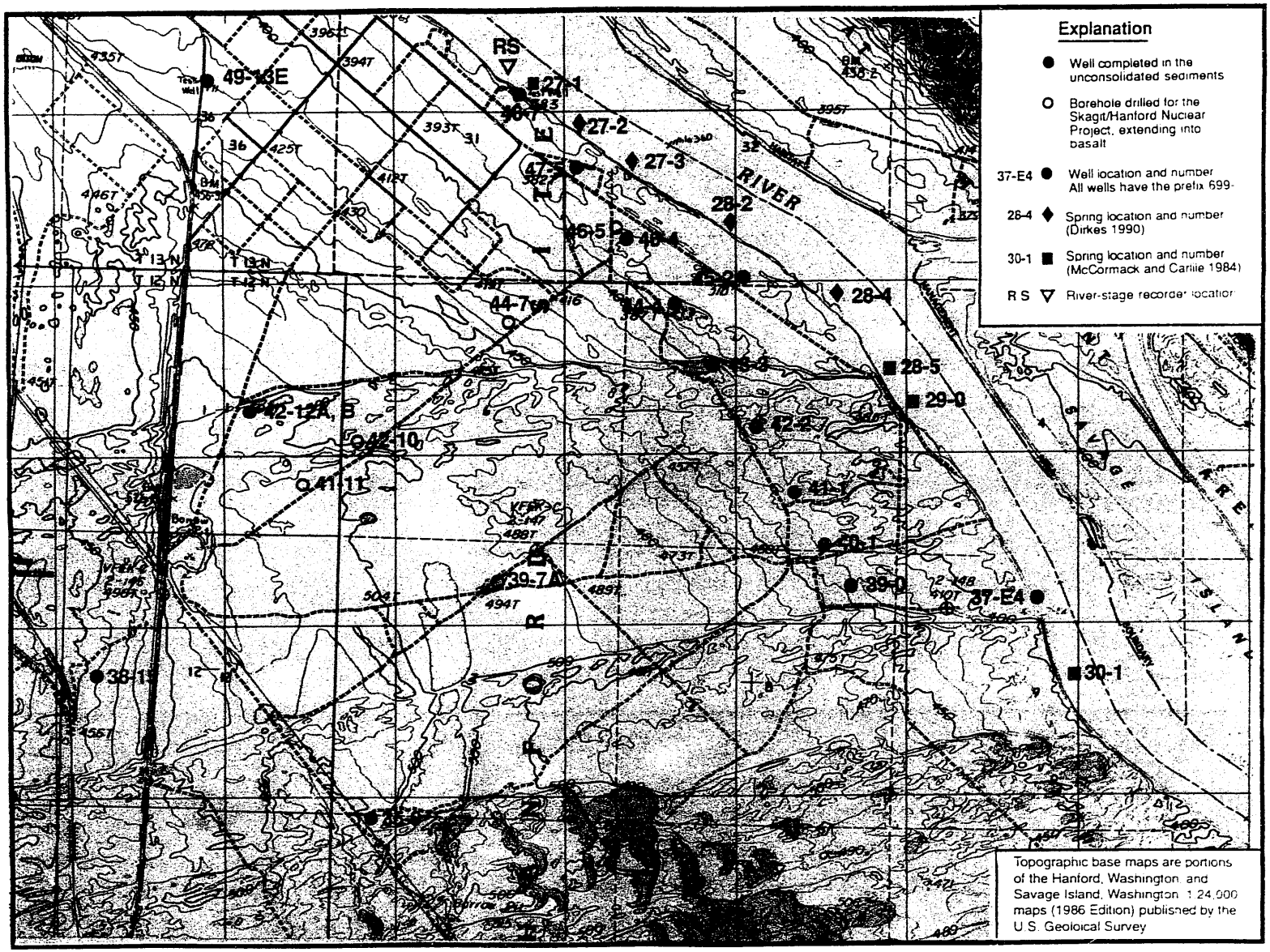

FIGURE 5.1. Locations of Wells, Springs, and the River-Stage Recorder Used for Hydrologic Data Collection in the Hanford Townsite Study Area

Chart-type recorders that continuously measure the depth to water were placed on three wells (699-44-7, 699-46-5, and 699-48-7) for the period July 1990 through mid-January 1992, and on one well (699-42-12A) for the period April 1990 through early January 1991. These wells are listed in Table 5.1 and shown in Figure 5.1. Depth-to-water measurements were taken with standardized steel tapes at a minimum of the start and end of each chart period, which is approximately 28 days. The continuous chart recorder data from well 699-48-7 were used to plot hydrographs and for quantitative analysis of river/aquifer relationships.

Pressure transducers were placed in three wells (699-37-E4, 699-40-1, and 699-43-3) from late January through mid-March 1992 (late March for 699-37-E4). These wells are included in Table 5.1 and are shown on Figure 5.1. The transducers were connected to data loggers that recorded pressure measurements at 2-hour intervals (wells 699-40-1 and 699-43-3) or 30-minute intervals (well 699-37-E4). The recording frequency was based on the response to river fluctuations; wells farther from the river had a dampened frequency and amplitude response to river fluctuations, while well 699-37-E4 had frequency responses similar to the river fluctuations. Functional, calibrated transducers and data loggers were not available much before the time they were actually placed in the wells, resulting in the short period of record beginning late in the study. These data were used for quantitative analysis of river/aquifer relationships and to estimate hydrologic properties.

5.1.2 River-Stage Measurements in the Columbia River

A pressure transducer was placed in the Columbia River near the upstream side of the Hanford Townsite study area (see Figure 5.1) from April 1991 through March 1992. The transducer was weighted and placed on the river bottom in a small natural embayment. The transducer cable, protected by plastic pipe, led to a data logger located on the riverbank. Pressure measurements were recorded at 30-minute intervals. A series of staff gauges, each approximately 1 m (3.3 ft) in length, was placed in the sediment adjacent to and in the river to accommodate the anticipated maximum river stage. Staff gauges were not set in the bank to accommodate anticipated minimum river stage until September 1991 because of access limitations. Also in September 1991, the

transducer was moved farther out into the river to measure the lower river stages. One staff gauge was surveyed relative to the casing elevation of well 699-48-7 to establish the river elevations. Staff gauges were read each time data were retrieved from the data logger. These readings were related to the elevation of the surveyed staff gauge to obtain elevations for each reading. The river elevation data were used for quantitative analysis of river/aquifer relationships.

5.1.3 Water-Chemistry Sampling and Analysis

Water samples were collected periodically from wells 699-42-12A, 699-43-3, 699-46-4, and 699-47-5 from late July 1990 through March 1991. The sample collection was as often as weekly (depending on the specific well) for the first 4 months and was every 2 weeks for the next 4 months. Selected samples (not all samples collected) were analyzed for tritium concentration. The sample analysis results are provided in Appendix C. The results were used to evaluate aquifer/river relationships.

5.1.4 Quantitative Hydrograph Analysis

This section summarizes the statistical methods used to analyze river-stage and well water-level data. The purpose of the statistical analysis was to correlate aquifer pressure-wave responses, observed from water-level fluctuations in wells, with river-stage fluctuations. Differences in elevation and timing of pressure waves between the river gauge and points on the river that form a perpendicular transect between the wells and the river are considered negligible for the statistical analyses.

Standard Statistics

Standard statistics were used to summarize well water-level data and river-stage data for specified periods. These statistics, which included arithmetic mean, variance, and sample standard deviation, described the distribution of well water-level and river-stage data.

Correlation and Covariance Statistics

Correlation and covariance statistics define the degree of similarity between two (or more) sets of time-series data. In this study, these

statistical analyses were used to quantify the timing and amplitude of changes in water levels observed in wells to the timing and amplitude of changes in river stage.

Bendat and Piersol (1986) used an unbiased estimator for the correlation function R_{xy} of two real time series x and y:

$$R_{xy}(r\Delta t) = \frac{1}{N-r}\sum_{n=1}^{N-r} x_n y_{n+r} \qquad (5.1)$$

where $R_{xy} = R_{xy}(\tau)$ = the correlation function at lags $\tau = r\Delta t$

r = lag number, integers with range $-N < r < N$

Δt = time interval between samples (constant for both series)

N = number of samples.

An unbiased estimator is one that has an expected value equal to the parameter being estimated. Because y is dependent on x, time series y is the well water-level data set and time series x is the river-stage data set for this study. Bendat and Piersol (1986) presented a normalized correlation coefficient Cor_{xy}, with values ranging from -1 to +1, as

$$Cor_{xy} = \frac{R_{xy}}{\sigma_x \sigma_y} \qquad (5.2)$$

where σ_x and σ_y are the sample standard deviations of time series x and y, respectively.

The covariance function Cov_{xy} of a pair of series x and y is defined as the correlation function R_{xy} of those series after the mean of each series has been de-meaned (that is, the mean of each series subtracted from its respective data series). Covariance can be calculated by substituting the de-meaned time series $x-\overline{x}$ and $y-\overline{y}$ for x and y, respectively, in Equation 5.1.

For computational efficiency, covariance was calculated using a fast Fourier transform procedure recommended by Press et al. (1986). This procedure applies a transformation to the data series by separating the waveforms into a sum of sinusoids of different frequencies. For computational convenience, the length of each time series was $N = 2^n$, where n is an integer. Covariances were then calculated by shifting one of the time series relative to the other time series in discrete steps of length $\pm N/4$ via circular convolution in the frequency domain, and correlations were calculated by Equation 5.2.

Correlation of two similar time series is a function of shifting the data at lag τ and usually has a maximum at some lag τ_{max}. If the two series are identical, then $Cor_{xy}(0) = 1$ at lag zero, and $Cor_{xy}(\tau)$ typically decreases symmetrically for increasing positive and negative lags τ. If the two time series are mirror images, $Cor_{xy}(0) = -1$. If the two time series are identical but one lags the other in time, Cor_{xy} will be 1 at time τ_{max}. In this case, $Cor_{xy}(0)$ is a measure of the overall similarity, and $Cor_{xy}(\tau_{max})$ is a measure of the similarity of the two time-series when they are aligned to produce the best match. Correlation and covariance statistics were applied to river-stage and well water-level time-series data to estimate the degree of well water-level responses to river-stage fluctuations. Also, for these data, τ_{max} provided an indication of the lag of the pressure-wave responses between the river and the well.

The correlation function also was used to calculate the attenuation factor, α_{xy}, which quantifies the reduction (or amplification) in series y, compared to series x at lag τ_{max} (Bendat and Piersol 1986). The attenuation factor is calculated as

$$\alpha_{xy} = Cor_{xy}(\tau_{max}) \frac{\sigma_y}{\sigma_x} \tag{5.3}$$

In this study, the attenuation factor was used to measure the reduction in water-level changes observed in wells, identified as time series y, compared with river-stage fluctuations, time series x. In this study, the

attenuation factor is a measure of the dampening effect that the aquifer matrix exerts on the pressure wave as it propagates from the river to the well.

Estimates of Aquifer Properties from River-Stage Fluctuations

Comparison of fluctuations in river stage and corresponding pressure-wave responses in wells provides an opportunity to estimate hydraulic properties of the unconfined aquifer adjacent to the river. Estimation of aquifer properties from water-level time-series data is an inverse problem that is based on the same principles of ground-water flow used for analyses of pump test data. In these "river-well tests," changes in river stage, rather than pumping at the well, is the stress mechanism.

The aquifer properties are estimated as model parameters by fitting model results of water-level changes to observed water-level changes. As noted by Bear (1979), models of aquifer behavior never completely represent reality, and simplifications in the model or unknown boundary conditions may add uncertainty to the results.

Both conventional pumping tests and river-well tests have advantages and disadvantages. A significant disadvantage of river-well tests is that no discharge information is available. However, river-well tests, which can support estimates from pumping tests, offer the following advantages: 1) they provide estimates of aquifer properties at natural flow rates; 2) they take place over longer periods, encompassing a wider range of water-level elevations; 3) the results are not biased by undersampling or by limited sampling under unique conditions; 4) they measure aquifer properties over a greater area; and 5) they are relatively inexpensive to perform.

Flow in the Unconfined Aquifer. An empirical coefficient of proportionality, the hydraulic conductivity K, relates specific discharge (discharge per unit area) to hydraulic gradient according to Darcy's law. Darcy's law states that $q = KJ$, where q is specific discharge, K is hydraulic conductivity (also called coefficient of permeability), and J is the hydraulic gradient

(Bear 1979). From Bear (1979), the continuity equation for flow in a one-dimensional, homogenous, unconfined aquifer can be written as

$$\frac{\partial}{\partial x}\left(h\frac{\partial h}{\partial x}\right)+\frac{N}{K} = \frac{S}{K}\frac{\partial h}{\partial t} \tag{5.4}$$

where $h = h(x,t)$ = height of the water table

$N = N(x,t)$ = an external source/sink term (positive downward)

K = hydraulic conductivity of the aquifer

S = storativity (specific yield) of the aquifer.

Equation 5.4 makes use of the Dupuit assumption, which requires small hydraulic gradients and assumes that all flow is horizontal. The equation also assumes that the base of the unconfined aquifer is horizontal and impermeable. The storativity S is the specific yield of the water-table aquifer and is defined as yield of the aquifer per unit height for a unit drop in water-table height (Bear 1979). The relatively small elastic storativity arising from expansion and contraction of pore spaces caused by pressure changes is neglected.

Despite the simplifications made in Equation 5.4, it is still difficult to solve because the $h(\partial h/\partial x)$ term is nonlinear. Linearization can be performed with a further simplification that replaces h in the nonlinear term with an average height $\bar{h}$:

$$\frac{\partial^2 h}{\partial x^2}+N = \frac{S}{T}\frac{\partial h}{\partial t} \tag{5.5}$$

where $T = K\bar{h}$ is the time- and space-averaged aquifer transmissivity.

Equation 5.5 is valid only when changes $\partial h/\partial x$ and $\partial h/\partial t$ are small relative to the total height h. After linearization, Equation 5.5 is equivalent to the equation for continuity in a homogenous, one-dimensional confined aquifer.

Numerical Solution. Numerical solution of Equation 5.4 or the linearized version, Equation 5.5, provides a reasonable technique for estimating diffusivity, T/S, from river-well interactions. Numerical solutions can incorporate the nonlinear variation $h(\partial h/\partial x)$, can specify more realistic initial and boundary conditions, can include spatial and temporal variability, and are computationally efficient. Equations 5.4 and 5.5 were solved using a one-dimensional, fully implicit finite-difference technique (Fletcher 1988). In finite-difference form, Equation 5.5 becomes

$$-\frac{K\bar{h}}{S}\frac{\Delta t}{(\Delta x)^2}h_{i-1}^{j+1}+\left(1+2\frac{K\bar{h}}{S}\frac{\Delta t}{(\Delta x)^2}\right)h_i^{j+1}-\frac{K\bar{h}}{S}\frac{\Delta t}{(\Delta x)^2}h_{i+1}^{j+1}=h_i^j \qquad (5.6)$$

where Δt is the constant time step, Δx is the constant grid spacing, and h_i^j is the water-table height at the i-th spatial node and the j-th time step.

Dirichlet boundary conditions were imposed at the boundaries by forcing constant h at x_i and $h_1^{j+1} = h_i^j + \Delta h$ at x_1. The i coefficients for the set of linear equations formed at each time step j in Equation 5.6 form a tridiagonal matrix that can be solved efficiently using the Thomas algorithm (Anderson et al. 1984).

The initial value of transmissivity was determined from an analytical solution to Equation 5.5, cited by Pinder et al. (1969), for an instantaneous change Δh_r in the water table at the river. This equation is analogous to the one-dimensional heat diffusion problem presented by Carslaw and Jaeger (1959) and is expressed as follows:

$$h_w = \Delta h_o \, \mathrm{erfc}\left(\frac{x}{2\sqrt{(T/S)t}}\right) \qquad (5.7)$$

where Δh_o is the impulse change in river stage at time t = 0, and erfc is the complementary error function. The nonlinear effect of changing aquifer thickness was approximated by using h from the previous time step.

5.2 GENERAL HYDROGEOLOGIC CHARACTERISTICS

The general hydrogeologic characteristics of the aquifer in the Hanford Townsite study area are discussed here. These include aquifer materials, thickness and geometry of the aquifer, water-level information, aquifer properties, and recharge/discharge.

5.2.1 Aquifer Materials and Geometry

The aquifer of primary interest for this study is contained within the sediments of the Hanford formation and the Ringold Formation. The aquifer within the Hanford formation generally has hydraulic conductivity values more than an order-of-magnitude greater than within the Ringold Formation (Graham et al. 1981). For this reason, the configuration of the Hanford formation is most important in terms of ground-water flow and contaminant migration and discharge to the Columbia River.

The bottom of the Hanford formation is shown in Figure 4.7 in Section 4.2. The aquifer is unconfined and is underlain primarily by lower-permeability sediments of the Ringold Formation. The Hanford formation is not present below the water table in some locations; in these locations, the aquifer is present only in the Ringold Formation. The aquifer within the Hanford formation ranges in thickness from zero to approximately 25 m. The saturated Hanford formation is not present at two locations adjacent to the Columbia River and in the northwest portion of the study area.

Some confined aquifers exist within the Ringold Formation, exhibited by more permeable sand and gravel facies overlain by silt and/or clay facies.

5.2.2 Hydrologic Properties

General hydrologic properties of the Ringold and Hanford formations have been documented by several sources, including Gephart et al. (1979) and Graham et al. (1981). Hydraulic conductivity for the Hanford formation ranges from 150 to 6100 m/day (500 to 20,000 ft/day), hydraulic conductivity for the Middle Ringold unit of the Ringold Formation ranges from 6 to 180 m/day (20 to 600 ft/day), and hydraulic conductivity for the undifferentiated Hanford and Middle Ringold unit ranges from 30 to 2100 m/day (100 to 7000 ft/day). The storativity of the unconfined aquifer is documented to range from 0.002 to 0.1. Hydrologic properties for specific wells have been documented by Kipp and Mudd (1973), as well as in other reports.

Transmissivity and, in some cases, hydraulic conductivity values are available from Kipp and Mudd (1973) or from PNL files for aquifer tests conducted in wells 699-35-9, 699-40-1, and 699-42-12A within the Hanford Townsite study area (see Figure 5.1). The data for wells 699-35-9 and 699-40-1 have been reanalyzed using data derivatives to evaluate time periods when radial flow dominates the responses. Data from well 699-42-12A were not reanalyzed.

The original analyses from well 699-35-9 indicate transmissivity values ranging from approximately 590 to 1000 m^2/day (6300 to 11,000 ft^2/day). The revised analyses resulted in transmissivity values ranging from approximately 650 to 1300 m^2/day (7000 to 14,000 ft^2/day). Based on an estimated aquifer thickness of approximately 15 m (50 ft), the hydraulic conductivity ranges from approximately 43 to 87 m/day (150 to 280 ft/day). These values lie within the range of hydraulic conductivity for the Middle Ringold or undifferentiated Hanford and Middle Ringold units.

The original analyses from well 699-40-1 indicated transmissivity values ranging from approximately 1560 to 3000 m^2/day (16,800 to 32,300 ft^2/day). The revised analysis yielded a transmissivity value of approximately 2800 m^2/day (30,000 ft^2/day). Based on an estimated aquifer thickness of approximately 15 m (50 ft), the hydraulic conductivity is approximately 190 m/day (600 ft/day). This value lies within the range of hydraulic conductivity for the Hanford formation.

The original analyses from well 699-42-12A indicated a transmissivity of approximately 6000 m^2/day (60,000 ft^2/day). Based on an estimated aquifer thickness of approximately 20 m (70 ft), the hydraulic conductivity is approximately 300 m/day (900 ft/day). This value lies within the range of hydraulic conductivity for the Hanford formation. These data are of generally poor quality; therefore, these results provide only an indication of the transmissivity for this well.

Hydrologic properties calculated from the numerical solutions also are discussed in Section 5.5.

5.2.3 Water-Level Conditions

The depth to water in the Hanford Townsite study area ranges from approximately 6 m (20 ft) near the Columbia River to more than 41 m (137 ft) in the western portion of the study area. The water-table elevation ranges from approximately 108 to 118 m (354 to 386 ft) above mean sea level (MSL); however, the water-table elevation near the Columbia River is highly dependent on river stage and fluctuates between approximately 108 and 111 m (354 and 363 ft) above MSL. The regional water-table map, which indicates general water-table and ground-water flow conditions, was shown in Figure 2.2. Water-table elevation maps within the study area for four time periods are shown in Figures 5.2 through 5.5. Each of these figures shows the same general configuration of the water table and the same general flow direction. Ground-water flow is toward the river, where it discharges. The average horizontal hydraulic gradient is greater during periods when the water-level elevations near the river are lower (e.g., October 10, 1990, shown on Figure 5.2) than when water-level elevations near the river are higher (e.g., May 24, 1991). The magnitude of the average horizontal hydraulic gradient for October 10, 1990, is approximately 3.1×10^{-3}; for December 6, 1990, is approximately 2.7×10^{-3}; for May 24, 1991, is approximately 2.4×10^{-3}; and for September 13, 1991, is approximately 3.0×10^{-3}.

Hydrographs indicating long-term changes in water levels influenced by both the magnitude of waste-water discharges and changes in the Columbia River stage are shown in Figures 5.6 and 5.7, respectively. The hydrograph for

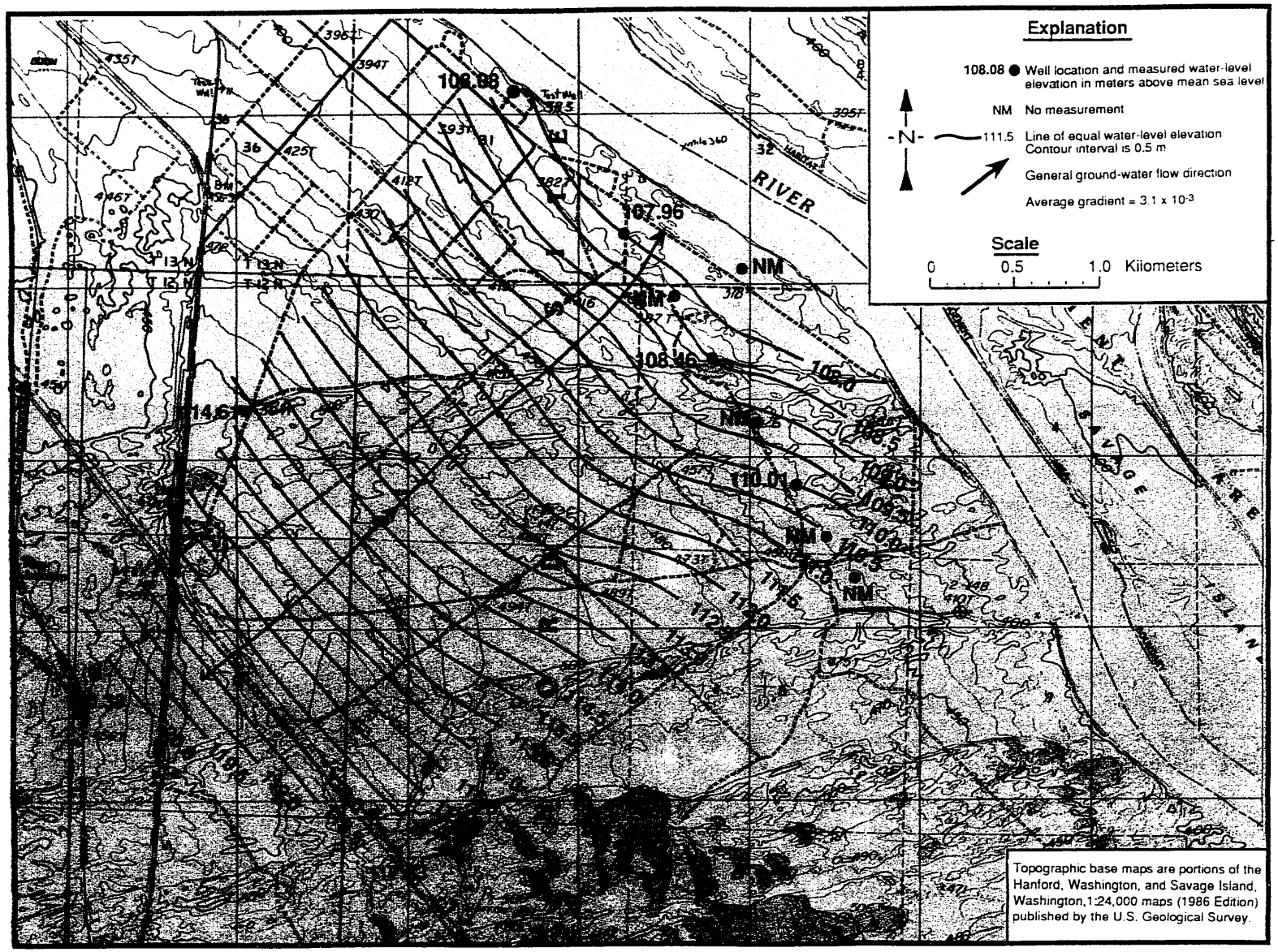

FIGURE 5.2. Generalized Water-Table Elevation Map for the Hanford Townsite Study Area, October 10-12, 1990

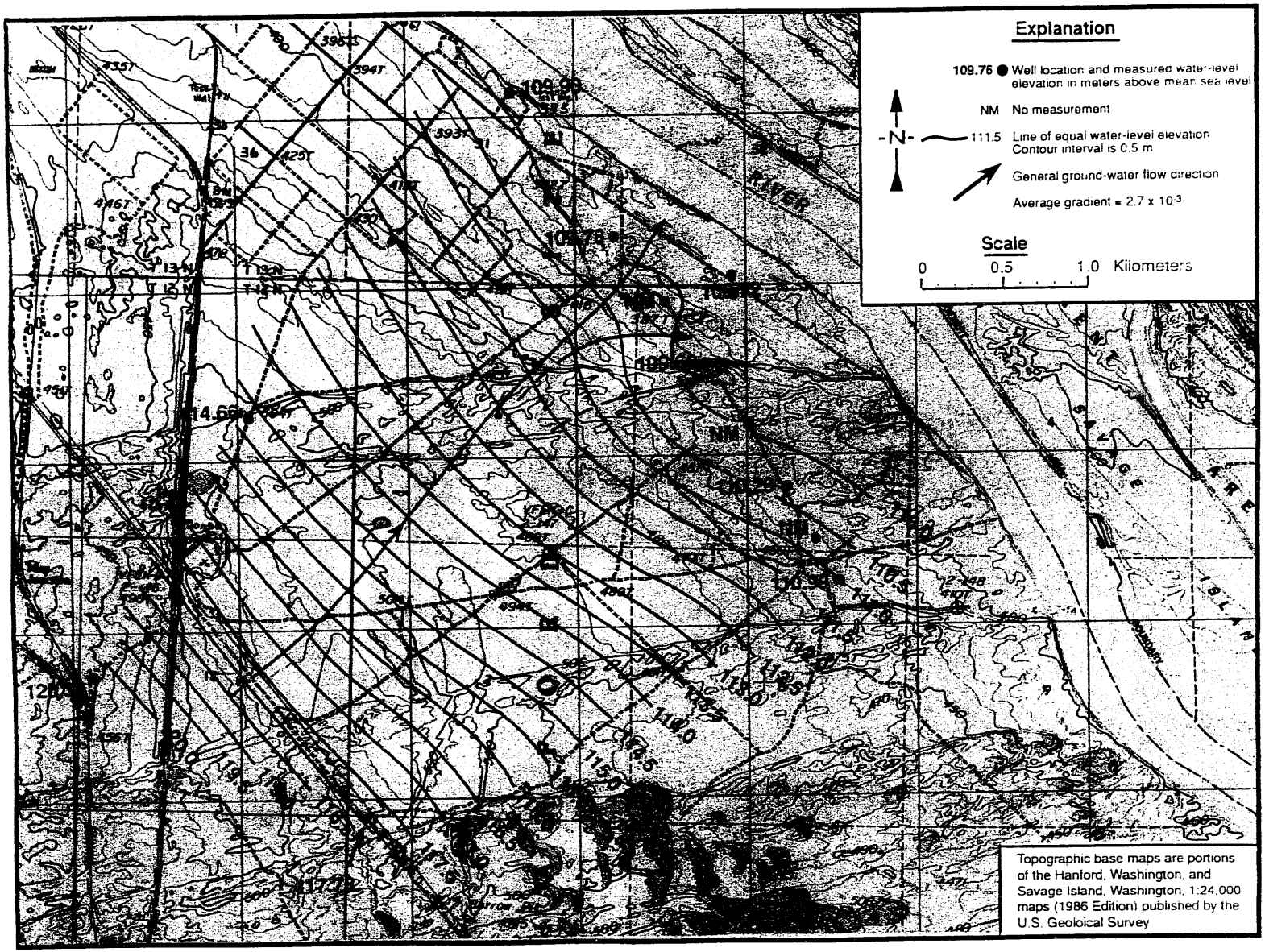

FIGURE 5.3. Generalized Water-Table Elevation Map for the Hanford Townsite Study Area, December 6, 1990

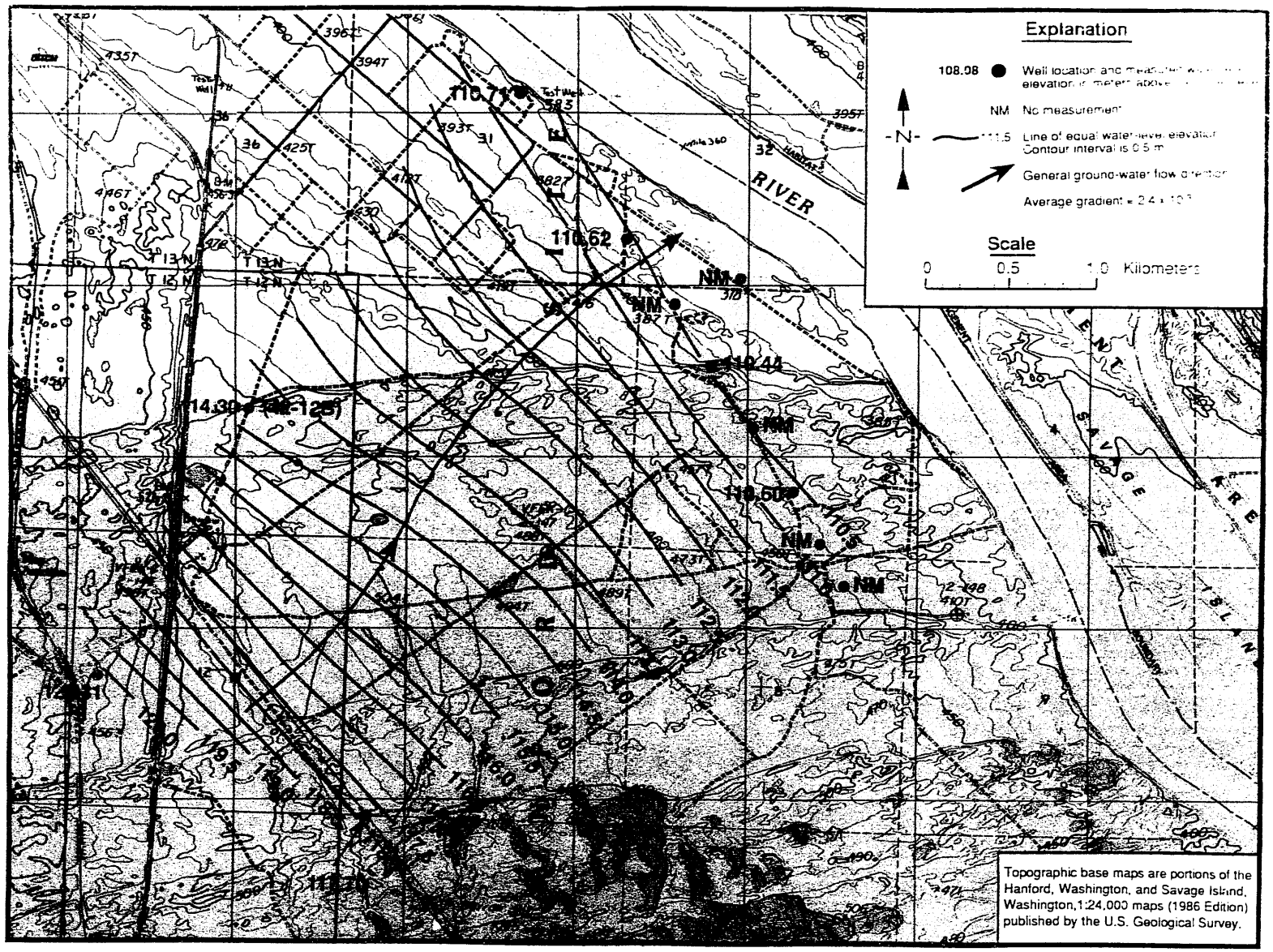

FIGURE 5.4. Generalized Water-Table Elevation Map for the Hanford Townsite Study Area, May 24, 1991

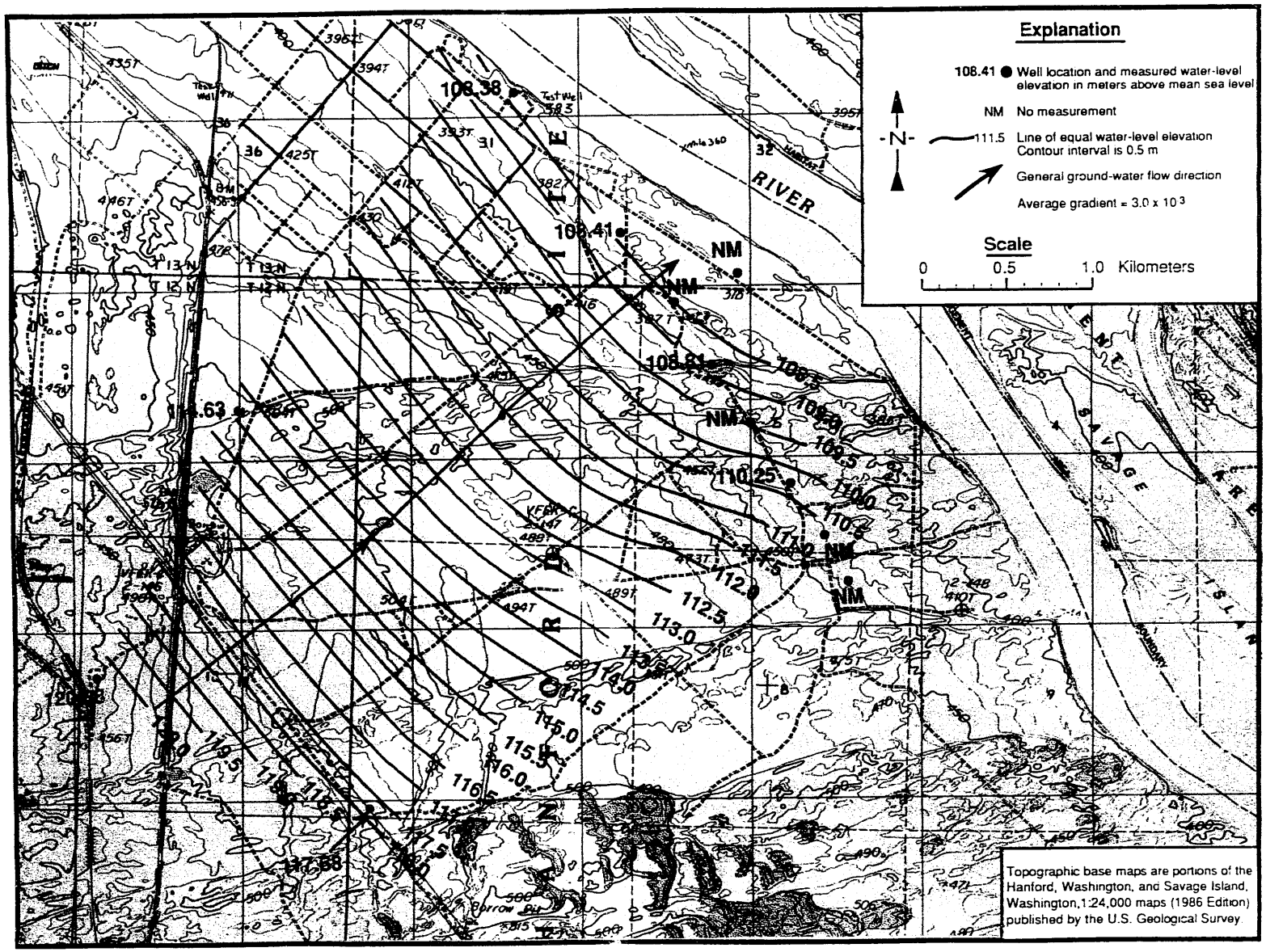

FIGURE 5.5. Generalized Water-Table Elevation Map for the Hanford Townsite Study Area, September 13, 1991

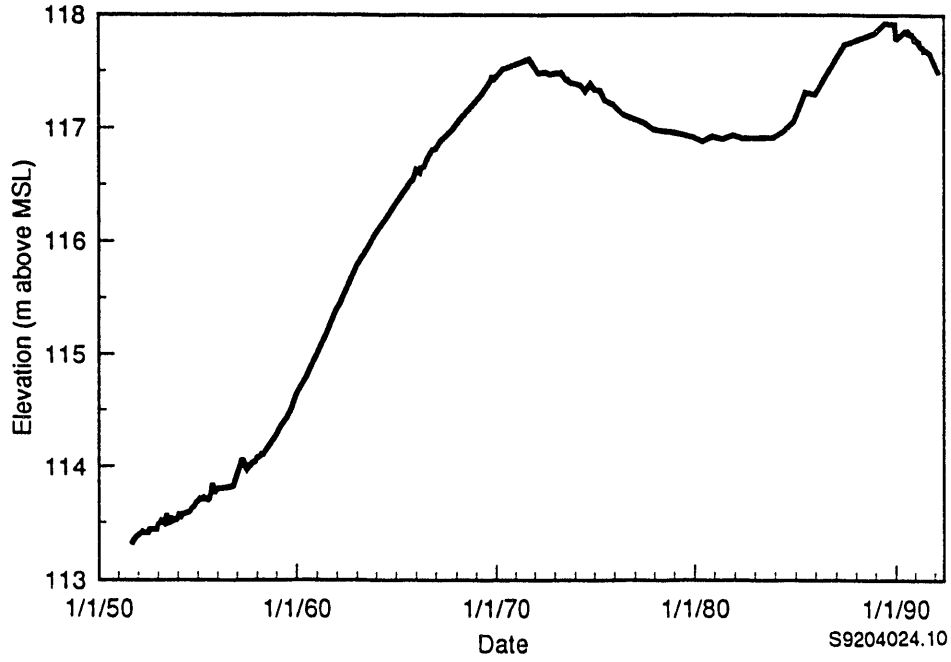

FIGURE 5.6. Long-Term Water-Level Elevation Trend in Well 699-35-9 (influenced by operational discharge volume)

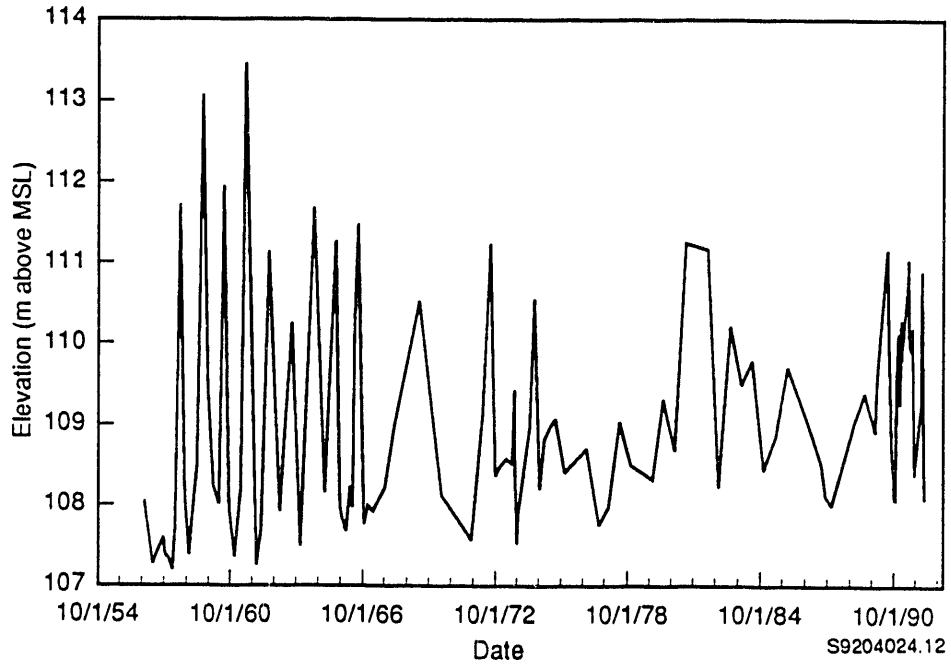

FIGURE 5.7. Long-Term Water-Level Elevation Trend in Well 699-48-7 (influenced by Columbia River stage)

well 699-35-9 illustrates the response of water-level elevations in the southwest portion of the study area to waste-water discharges; water-level elevations have increased nearly 5 m (15 ft) since 1952. The hydrograph for well 699-48-7 illustrates the response to the Columbia River of water-level elevations near the river; water-level elevations fluctuated more than 6 m (20 ft) within a single year before Priest Rapids Dam was constructed. Since that time, water-level elevations have fluctuated more than 3 m (10 ft) within a single year. No long-term increase in water-level elevation is apparent since the beginning of record (1957) in well 699-48-7. Water-level fluctuations and relationships are discussed in more detail in Sections 5.4 and 5.5.

Data are not available on the vertical distribution of hydraulic head within the aquifer in the sediments because wells have not been installed to monitor the hydraulic head deep within the aquifer or below confining units (an exception is well 699-37-E4; however, the Hanford formation is not present at this location). Near the river, the hydraulic head is expected to increase with depth because the Columbia River is a discharge area for the aquifer.

5.2.4 Recharge and Discharge

Significant ground-water recharge within the Hanford Townsite study area does not occur directly from infiltration and percolation; however, ground-water underflow occurs from water originating west of the study area. The primary source of this water is waste water from operations in the 200 Areas. Ground-water discharge is directly to the Columbia River via springs and seepage to the bed and banks of the river.

5.3 COLUMBIA RIVER

River flow through the Hanford Reach is highly controlled. Operations at Priest Rapids Dam exert immediate control over the flow in the Hanford Townsite study area. In turn, operation of Priest Rapids Dam is connected closely with operations of other mid-Columbia dams and with power demands. C. R. Sherwood and D. R. Newcomer at PNL recently have studied the operation of the mid-Columbia dams. The findings of this section are based largely on their work.

The average daily discharge from Priest Rapids Dam for the period of record from June 1990 through March 1992 is shown in Figure 5.8. These data were obtained from the Grant County Public Utility District.

5.3.1 Long-Term Changes

Daily river flow records are available beginning in 1959. These data indicate that maximum river flows decreased markedly between 1960 and 1978. Flow is now more evenly distributed throughout the year, and a wider range of flow is likely on a given day of the year.

5.3.2 Seasonal Changes

The average daily discharge record in Figure 5.8 shows peak river flow occurring during early to mid summer; however, a hydrograph for a typical year would show the peak flow occurring earlier, during spring runoff. The lowest flow occurs in late summer and fall. Over the last 30 years, flows during summer, fall, and winter have increased and flows during the normal runoff

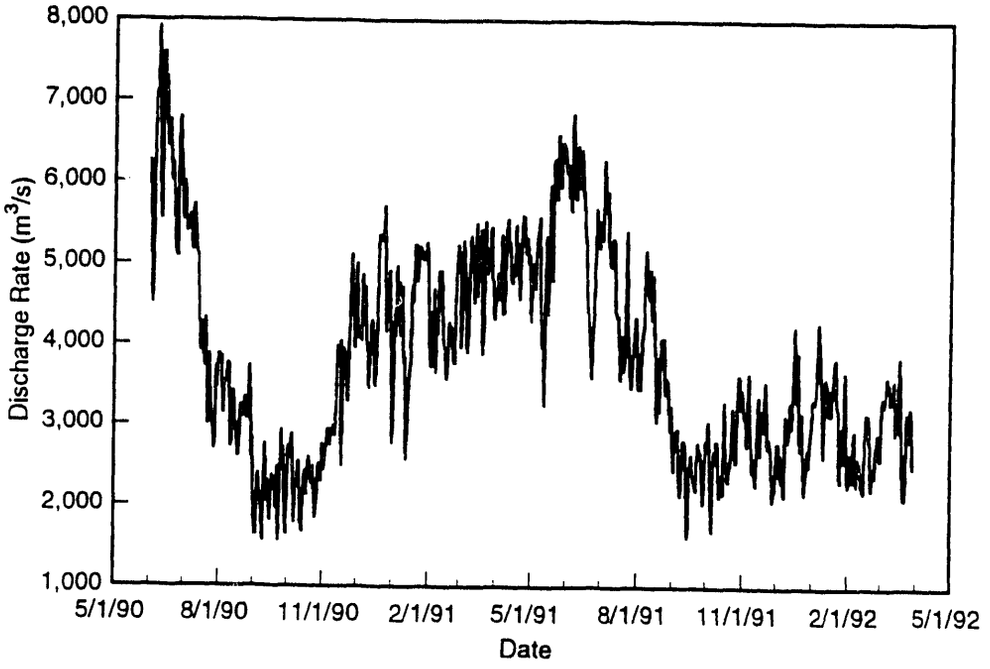

FIGURE 5.8. Average Daily Discharge in the Columbia River at Priest Rapids Dam

season have decreased. Spring runoff is now typically a 45- to 60-day period when discharges are increased to 3600 to 4200 m^3/s (120,000 to 140,000 ft^3/s).

5.3.3 Weekly and Daily Variations

Flow variations occur during the week as the mid-Columbia dams upstream of the Hanford Reach generate power to meet changing demands. Flows are lowest on Sundays, peak on Mondays, remain high during the weekdays, and drop again on Saturdays. A spectral power analysis of flow data indicates peaks of flow at periods of 7, 3.5, and 1.75 days. Daily variations in the river flow in the Hanford Reach typically produce 0.6- to 0.9-m (2- to 3-ft) changes in river stage in a 24-hour period; however, data collected by Sherwood and Newcomer indicate daily variations in river stage up to 2 m (8 ft). The actual shape of the daily variations changes with power demand and is somewhat irregular, but river stage typically peaks after midday when power demand is high and is low at night when power demand is low.

5.3.4 River Stage at the Hanford Townsite Study Area

River-stage gauges and a transducer were installed in the river near the north end of the Hanford Townsite study area (discussed in Section 5.1); however, difficulties in operation of the transducer/data logger system prevented collection of a full period of record (approximately 30% of the period of record is missing). In addition, perceived large uncertainties in staff gauge readings or large amounts of drift in the transducer prevented accurate representation of true river-stage elevation for approximately 30% of the period of record that is available. The record of data collected is provided in Appendix B. Portions of the data that have a low uncertainty associated with them are used for quantitative hydrograph analyses and are shown in Section 5.5. Daily river-stage fluctuations of up to 2 m (8 ft) were noted. The river stage fluctuates from less than 106 m (348 ft) above MSL to more than 111 m (367 ft) above MSL for the entire period of record.

5.4 TEMPORAL GROUND-WATER LEVEL CHANGES

Water-level fluctuations in wells within the Hanford Townsite study area are primarily a result of regional flow entering the area from the east,

Columbia River stage, or a combination of these effects. As discussed earlier, waste-water discharges associated with Hanford Site operations affect the regional ground-water system, and the Columbia River influences ground-water levels in wells near the river by inducing bank storage within the aquifer near the river. Water-level fluctuations in confined aquifers also may be influenced by tidal loading.

Hydrographs illustrating the transient character of water levels in a number of wells in the study area are shown in Figures 5.9 through 5.13. The locations of these wells were shown on Figure 5.1. Water levels from wells affected primarily by the regional flow system exhibit small changes and a slight downward trend for the period of record (see Figure 5.9). Water levels from wells affected by the Columbia River exhibit large changes of varying

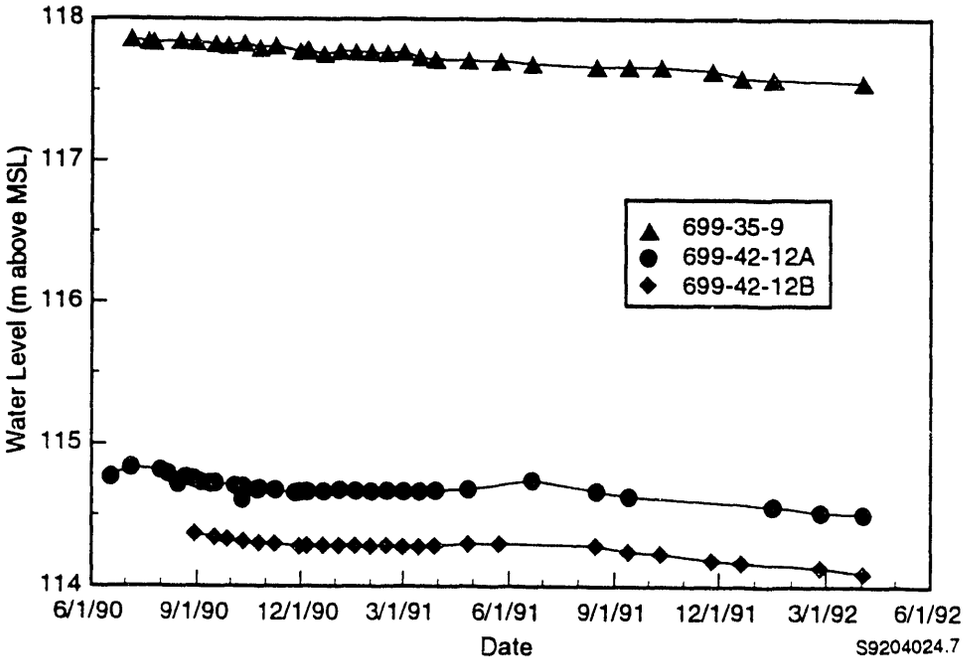

FIGURE 5.9. Water-Level Elevations in Wells Completed in the Unconfined Aquifer and Affected by Regional Ground-Water Flow

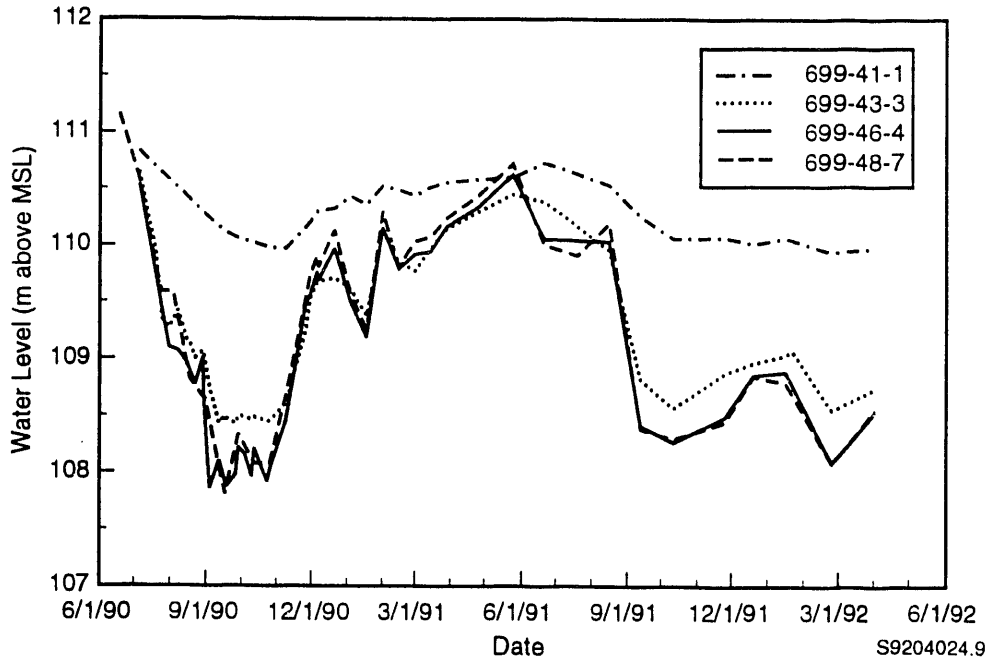

FIGURE 5.10. Water-Level Elevations in Wells Completed in the Unconfined Aquifer and Affected Strongly by the Columbia River

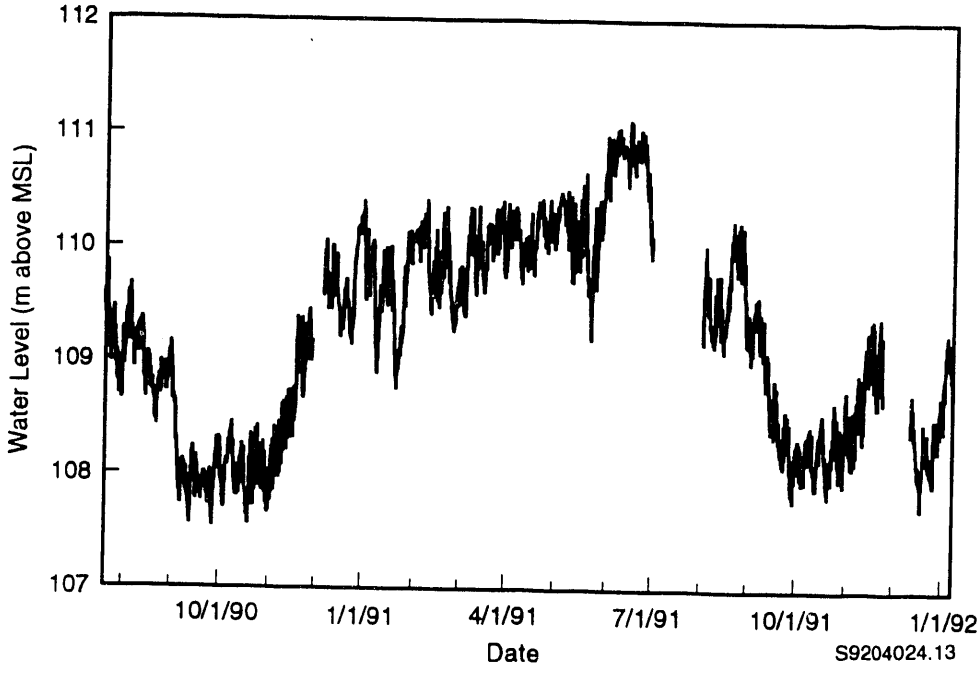

FIGURE 5.11. Water-Level Elevations in Well 699-48-7 Measured with a Continuous Recorder

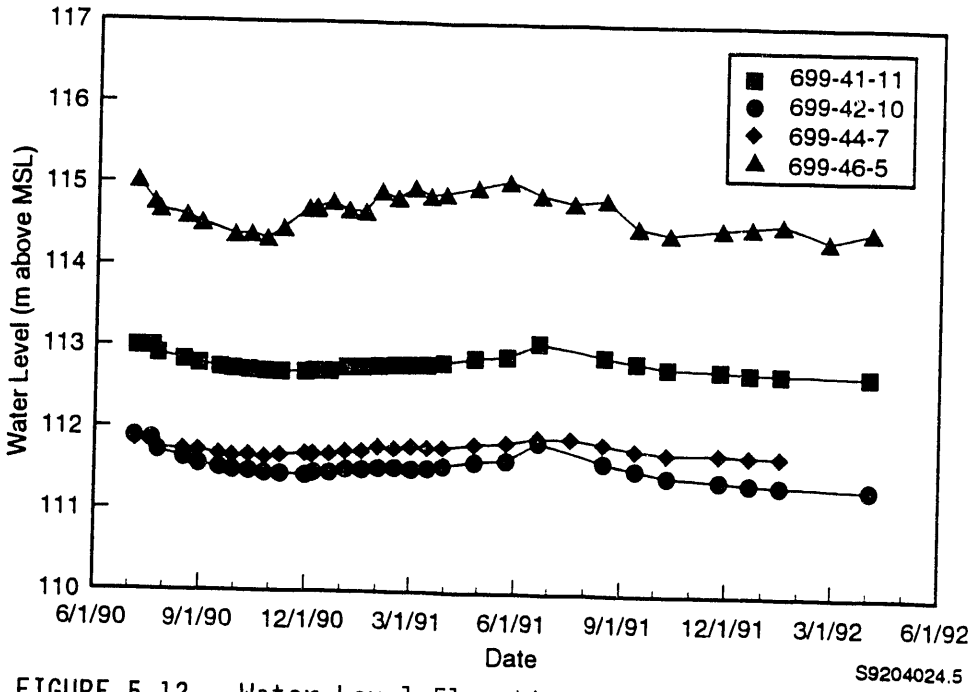

FIGURE 5.12. Water-Level Elevations in Wells Open Within the Elephant Mountain Basalt

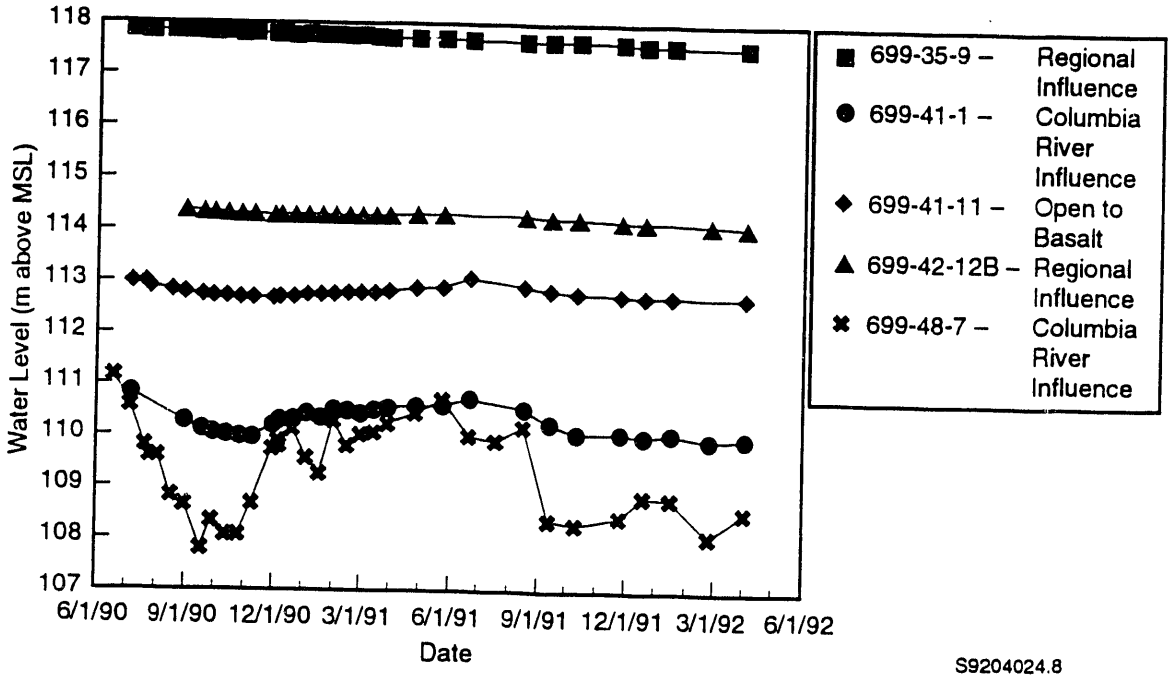

FIGURE 5.13. Water-Level Elevations in Wells Representing Each Major Condition Shown in Figures 5.9, 5.10, and 5.12

magnitude in direct response to the river (see Figure 5.10). The wells nearest the river (e.g., well 699-48-7) display much larger responses to Columbia River stage than do wells farther from the river (e.g., well 699-41-1). The continuous record of water-level elevations in well 699-48-7 recorded with a continuous chart recorder is shown in Figure 5.11. The hydrograph for well 699-48-7 shows clearly the strong relationship with the Columbia River stage; daily fluctuations as large as 0.6 m (2 ft) occur at times. The water-level hydrographs presented in Figure 5.10 must be regarded in view of the large daily fluctuations in water levels affected by the Columbia River. Measurements in all the wells were made within approximately a 2-hour period; therefore, for any given measurement period, the water-level differences between wells as a result of the river fluctuations is small.

The hydrographs shown in Figure 5.10 provide insight into the magnitude and frequency of bank storage influences and the direction of ground-water movement near the river. During several periods, the water-level elevations in wells near the river appear to be higher than those farther from the river. This is especially true on May 24, 1991, when the water-level elevation in well 699-48-7 was higher than the water-level elevation in all other wells shown in the hydrograph. The water-level elevation in well 699-48-7 was higher than the water-level elevation in well 699-43-3 during much of the period of high river stage. Well 699-43-3 is located more than 600 m (2000 ft) farther inland than well 699-48-7. This indicates that river stage affects ground-water movement up to 600 m (2000 ft) from the river during much of the high river stage. During this time, which may apparently range from a few days up to a few months, the river contributes to bank storage. The relationships discussed above are depicted on Figure 6.3 in Section 6.1. A time lag and reduced magnitude of hydrograph responses to the river fluctuations can be seen in the data for well 699-41-1. This may be due to distance from the river, as well as hydrologic properties of the materials (such as the low permeability of the clay unit located between this well and the river). River/aquifer relationships are evaluated quantitatively in Section 5.5.

Water levels from boreholes open to the basalt show dampened and time-lagged responses to the river (see Figure 5.12). These wells may be open to

different interflow units or flow interior units within the Elephant Mountain Member. Further, the condition of these boreholes, which were drilled by Golder Associates in support of nuclear power plant siting, is uncertain.

Water levels from several wells representing each of the conditions discussed above (regional flow, river influence, and confined basalt) are presented together on Figure 5.13 to provide a visual comparison of the influence of various factors on water levels in the study area.

5.5 QUANTITATIVE HYDROGRAPH ANALYSIS

5.5.1 Statistical Analysis Results

This section presents the results of the statistical analyses of river-stage and well water-level data from the Hanford Townsite study area. The periods of data selected were based on these criteria: continuity of simultaneous data for both river stage and well water levels, data quality, and length of time series available. The largest numbers of data points possible for N for the analyses were $2^9 = 512$ and $2^{11} = 2048$. Strip-chart data from well 699-48-7 were digitized in unequal time increments. The digitized data were then used to interpolate between adjacent data points to estimate the water level at equal time increments of 0.5 hour.

5.5.2 Standard Statistics

Results of the standard statistics are presented in Table 5.2. Standard statistics were applied to water-level data from well 699-48-7 for the period September 13 to October 26, 1991; from well 699-37-E4 for the period March 18 to March 29, 1992; and from well 699-43-3 for the period January 30 to March 12, 1992. Results for river stage also are shown for each period. The largest variability in river stage for the three periods was 2.56 m (8.39 ft).

5.5.3 Correlation and Covariance Statistics

The correlation and covariance statistics are presented in Table 5.3. These analysis results quantify similarities between the river stage and water-level changes observed in wells 699-48-7, 699-37-E4, and 699-43-3 for the same periods selected for the standard statistics. Negative lag indicates that water-level changes in the wells lag behind river-stage changes.

TABLE 5.2. Standard Statistics of River-Stage Data with Corresponding Water-Level Data for Wells 699-48-7, 699-37-E4, and 699-43-3

	9/13/91 - 10/26/91 N = 2048, Δt = 0.5 hour		3/18/92 - 3/29/92 N = 512, Δt = 0.5 hour		1/30/92 - 3/12/92 N = 2048, Δt = 2 hours	
	River	699-48-7	River	699-37-E4	River	699-43-3
Arithmetic Mean (m)	107.26	108.20	107.59	109.09	107.51	108.65
Standard Deviation (m)	0.56	0.18	0.55	0.18	0.50	0.12
Minimum (m)	105.93	107.78	106.87	108.84	106.86	108.47
Maximum (m)	108.49	108.73	108.55	109.40	108.65	108.95
Range (m)	2.56	0.95	1.68	0.56	1.79	0.48
Variance (m^2)	0.314	0.033	0.298	0.033	0.255	0.015

TABLE 5.3. Correlation and Covariance Statistics Between the Columbia River Stage and Water Levels at Wells 699-48-7, 699-37-E4, and 699-43-3

	9/13/91 - 10/26/91 699-48-7	3/18/92 - 3/29/92 699-37-E4	1/30/92 - 3/12/92 699-43-3		
			Data	1-Day Average	7-Day Average
Distance from River (m)	91	88	730	730	730
$Cor_{xy}(0)$	0.58	0.99	0.42	0.51	0.62
$Cov_{xy}(0)$ (m^2)	0.059	0.099	0.026	0.027	0.026
Lag (hours)	-2.5	-0.50	-56	-54	-64
Attenuation Factor	0.27	0.33	0.15	0.20	0.26
$Cor_{xy}(\tau_{max})$	0.81	0.99	0.61	0.71	0.74
$Cov_{xy}(\tau_{max})$ (m^2)	0.084	0.098	0.038	0.038	0.032

Among the three time series, the water-level changes in well 699-37-E4 had the highest correlation with river stage and responded within 0.5 hour (the time interval of measurement) of river-stage fluctuations. The water-level changes in well 699-48-7, located approximately the same distance from the river as well 699-37-E4, correlated highly with the river stage, but less than those of well 699-37-E4. Also, a lower attenuation factor for well 699-48-7 indicates that water-level changes in well 699-48-7 were dampened more than in well 699-37-E4. This difference in response at each of these wells may be caused by a difference in mean river-stage elevation between each of the periods (see Table 5.2). Time-series data for various mean river-stage elevations are lacking. The quick water-level responses in well 699-37-E4 to river-stage fluctuations also may reflect locally semi-confining aquifer conditions at this well. This would imply pressure waves caused, in part, by loading effects. Pressure waves felt at well 699-48-7 are not caused by loading effects because the aquifer is unconfined at this well.

For correlation and covariance statistics of water-level data at well 699-43-3, 1-day and 7-day running averages were applied to the river-stage data to smooth over variations of less than 1 day and 1 week, respectively. The values for correlation in Table 5.3 show that water-level fluctuations in well 699-43-3 correlate better with the averaged river-stage data. A hydrograph of well 699-43-3 and river stage in Figure 5.14 visually shows that short-term cycles of 1 day or less in river stage do not have the same shape as the well data, but that the well data and 7-day averaged river data do have a similar shape. This indicates that high-frequency river-stage changes do not propagate to well 699-43-3; such a result is expected because of the well's distance from the river.

5.5.4 Numerical Solution Results

Estimates of aquifer properties using the numerical solution described in Section 5.1 are presented below. The numerical solution was applied to water-level data from wells 699-43-3 and 699-48-7, along with their corresponding periods of river-stage data. The umerical solution was not applied to data from well 699-37-E4 because of semi-confining conditions at this well;

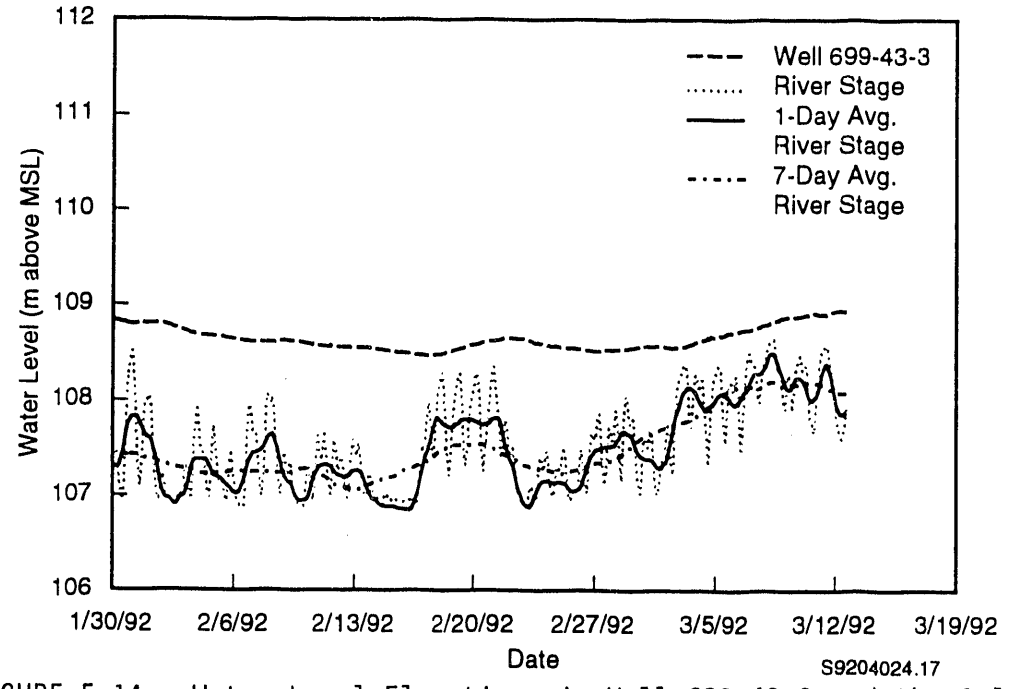

FIGURE 5.14. Water-Level Elevations in Well 699-43-3 and the Columbia River Stage, Including 1-Day and 7-Day Averages of Columbia River Stage

such conditions introduce the possibility of the water-level data being masked by loading effects from changes in river discharge.

Well 699-43-3

The numerical solution was applied to the same time series as that used to perform the statistical analyses discussed earlier, January 30 to March 12, 1992. The solutions were calculated with grid spacing Δx = 30 m (100 ft); time step Δt = 7200 s; and a range of values for $K\bar{h}/S = T/S$, for S between 0.1 and 0.3. The average aquifer thickness, bounded by the water table above and the top of a clayey unit below, between well 699-43-3 and the Columbia River is estimated to be 12 m (40 ft). With these parameters, the inverse modeling produced predicted time-series values for water-level elevation at the well, which are plotted in Figure 5.15.

Values of hydraulic conductivity ranged between 940 and 2800 m/day (3100 and 9200 ft/day), using estimates of 0.1 and 0.3, respectively, for

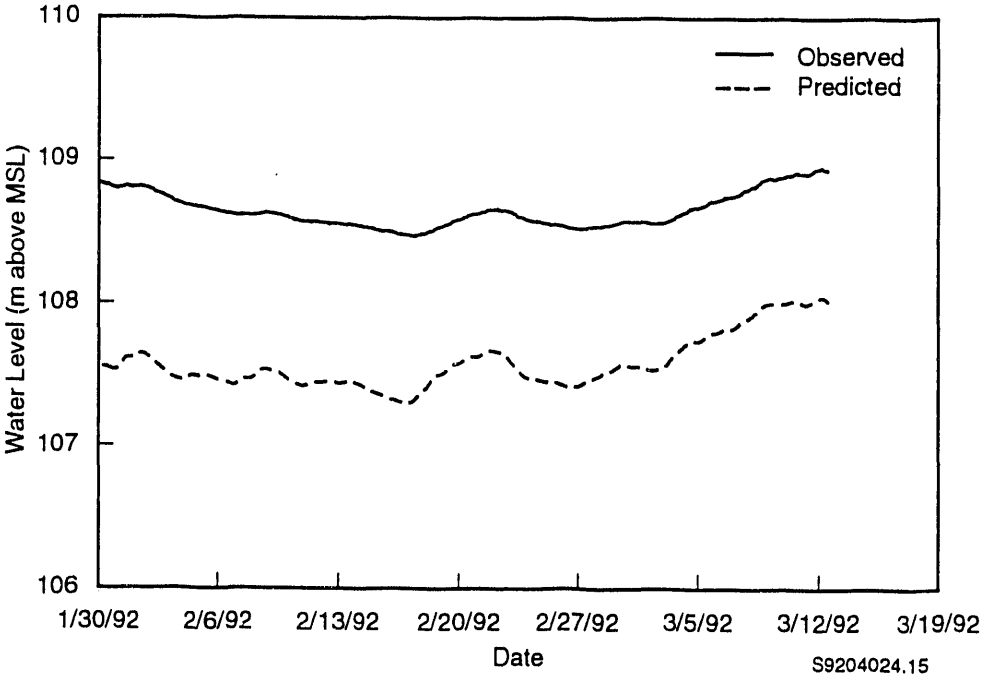

FIGURE 5.15. Observed and Predicted Water-Level Elevations for Well 699-43-3

specific yield. Transmissivity was estimated to be between 11,000 and 34,000 m^2/day (120,000 and 370,000 ft^2/day).

Well 699-48-7

The numerical solution was applied to the same time series as that used to perform the statistical analyses discussed earlier, September 13 to October 26, 1991. The solutions were calculated with grid spacing Δx = 3 m (10 ft); time step Δt = 1800 s; and a range of values for $K\bar{h}/S = T/S$, for S between 0.1 and 0.3. The aquifer thickness, bounded by the water table above and the top of a clayey unit below, between well 699-48-7 and the Columbia River is estimated to be 15 m (50 ft). With these parameters, the inverse modeling produced predicted time-series values for water-level elevation at the well, which are plotted in Figure 5.16.

Values of hydraulic conductivity ranged between 82 and 240 m/day (270 and 800 ft/day), using estimates of 0.1 and 0.3, respectively, for specific yield. Transmissivity was estimated to be between 1200 and 3700 m^2/day (13,000 and 40,000 ft^2/day).

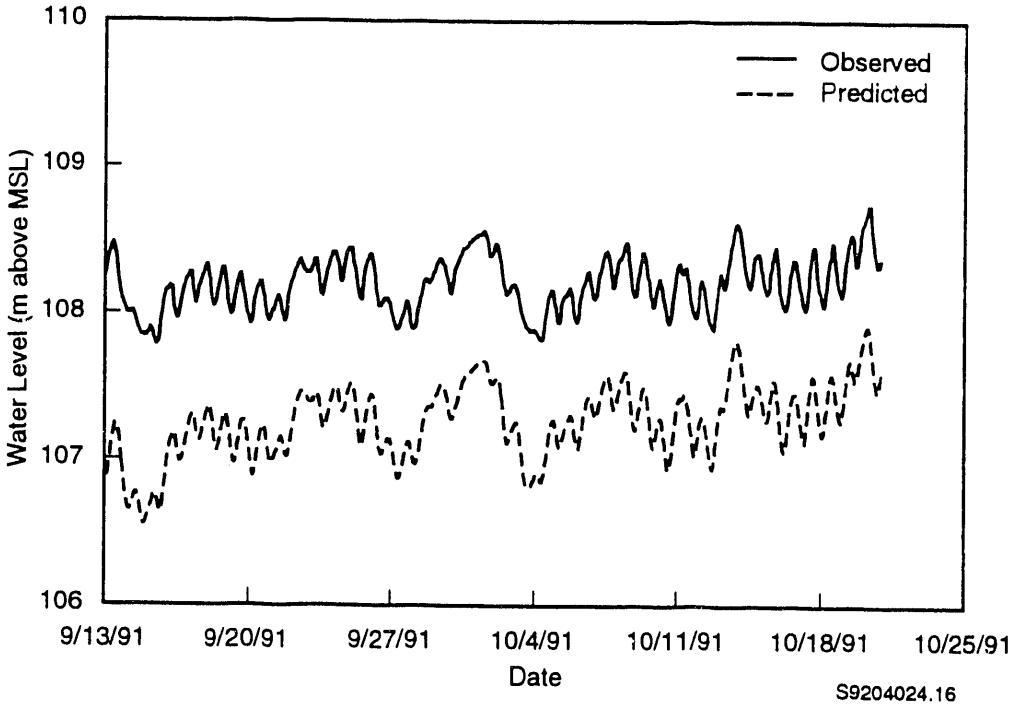

FIGURE 5.16. Observed and Predicted Water-Level Elevations for Well 699-48-7

5.6 GROUND-WATER AND SPRING CHEMISTRY

This section discusses general ground-water chemistry; distribution of major contaminants, including spatial and temporal effects; and river/aquifer relationships based on chemistry data.

5.6.1 Major Ion Chemistry

The chemistry of ground water in the Hanford Townsite study area is primarily of the calcium-bicarbonate type. Stiff diagrams for major ion chemistry of a number of wells are shown in Figure 5.17. These diagrams were constructed from water-chemistry analyses of samples collected in August, September, and October 1987 (Evans et al. 1988). The diagrams are plotted in milliequivalents per liter of the major anions and cations in water, modified slightly from the method given by Hem (1970). These patterns provide a relatively distinctive method of showing water-composition differences or similarities. The width of the pattern provides an approximate indication of total ionic content.

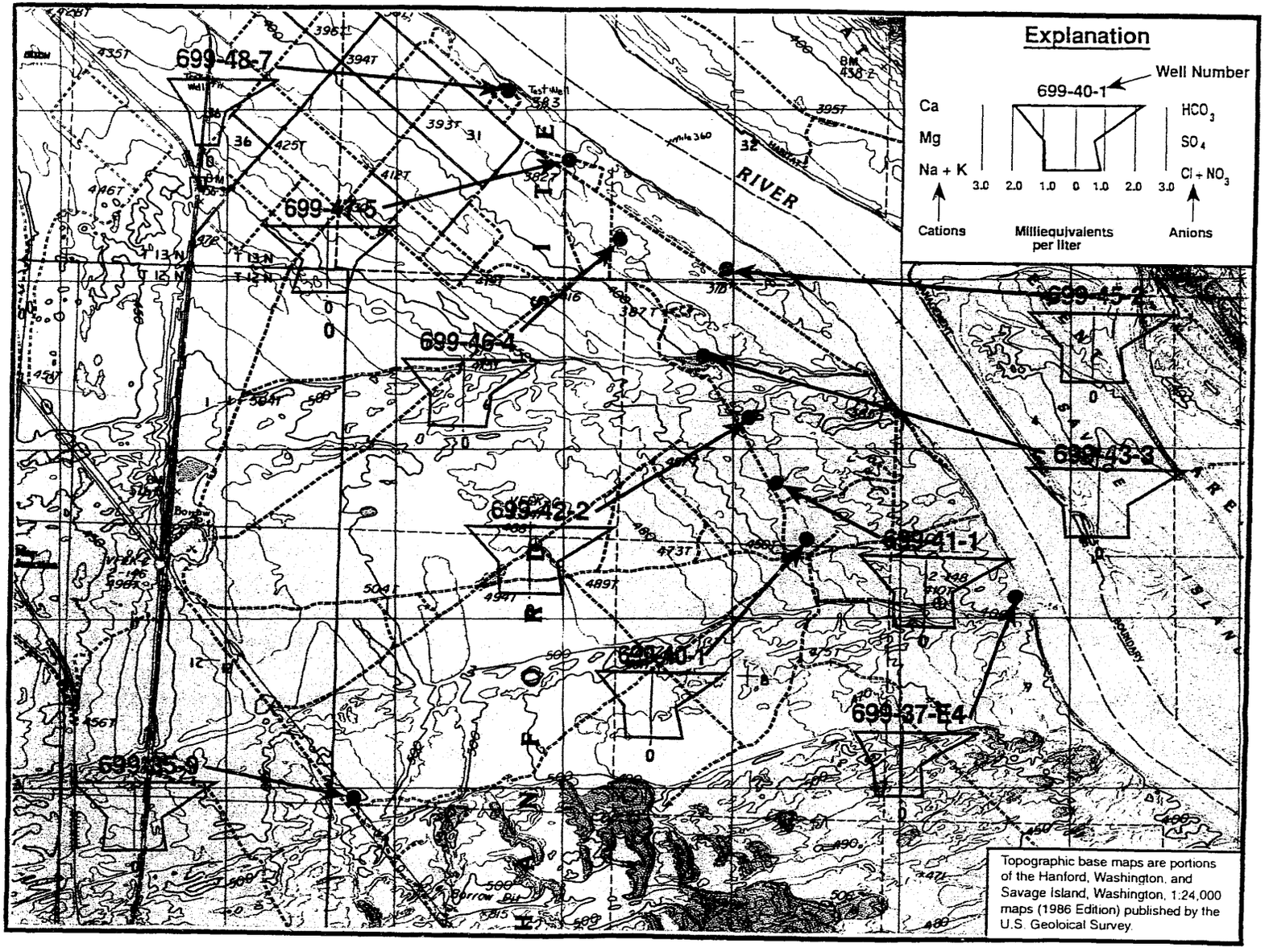

FIGURE 5.17. Major Ion Chemistry Analyses Presented as Stiff Diagrams for Water Samples Collected in Fall 1987

Although the dominant water-chemistry type is calcium bicarbonate, the stiff diagrams on Figure 5.17 indicate some subtle dissimilarity between water chemistry in some of the wells. Well 699-37-E4 has proportionally lower calcium than other wells. Well 699-47-5 has proportionally higher sodium plus potassium, lower magnesium, and lower nitrate than other wells. Well 699-48-7 has lower concentrations of all ions. Differences in ion water chemistry may be caused by geochemical differences in the sediment/water interaction. The ion chemistry differences in well 699-37-E4 may be a result of that well being open to sediments of the Ringold Formation rather than the Hanford formation, to which all the other wells are open. The lower concentration of all ions in well 699-48-7 is probably a result of dilution from the Columbia River.

In general, the major ion chemistry of ground water in the area does not vary by a large degree. The data used for constructing these stiff diagrams are provided in Appendix C.

Stiff diagrams for several times of sample collection, spanning more than 5 years, were constructed and evaluated. These diagrams did not reveal any obvious changes in ion chemistry between the different sampling times; therefore, these diagrams are not presented or discussed.

5.6.2 Distribution of Tritium and Nitrate

The distribution of tritium and nitrate concentrations from wells (Evans et al. 1989) and springs (Dirkes 1990) within the Hanford Townsite study area for fall 1988 is shown on Figure 5.18. Some data from spring sampling in 1983 (McCormack and Carlile 1984) also are presented. The general Site-wide distribution of tritium and nitrate was referred to earlier (see Figures 1.2 and 2.3, respectively). Tritium concentrations in ground water ranged from approximately 149,000 to 297,000 pCi/L. Tritium data for this time period were not available for well 699-48-7, located near the north end of the study area; however, the tritium concentrations in this well in fall 1987 and in fall 1989 were below the detection level of 500 pCi/L (Evans et al. 1990). The tritium concentration in well 699-49-13E was below the detection level of 500 pCi/L for the two samples collected in 1989 (Evans et al. 1990). Ground water in the vicinity of this well must be derived from a different source than the contaminated ground water entering the study area from the west.

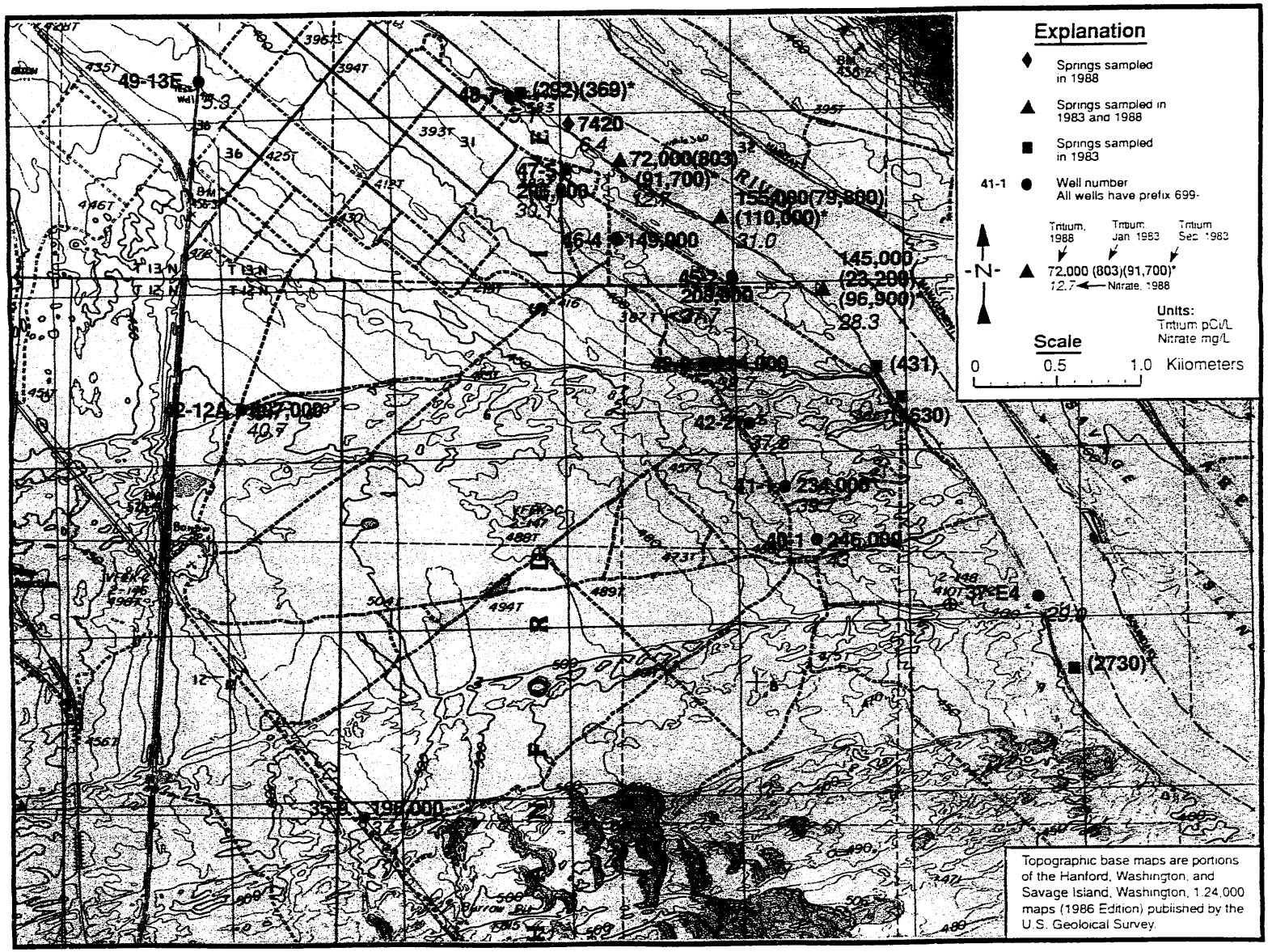

FIGURE 5.18. Distribution of Tritium and Nitrate in Samples from Ground Water and Springs Collected Primarily in Fall 1988

This clearly indicates the distinct northern boundary of the tritium plume. Nitrate concentrations ranged from approximately 5.1 parts per million (ppm) in well 699-48-7 to 43 ppm in well 699-40-1. Note that tritium and nitrate concentrations vary with river stage in many of these wells; this variance is discussed later in detail.

Tritium concentrations in the springs ranged from approximately 7420 pCi/L (near the north end of the study area) to 155,000 pCi/L (near the center of the study area). McCormack and Carlile (1984) reported concentrations of tritium and also nitrate in spring samples collected in January and September 1983. They sampled three springs that were not sampled by Dirkes (1990), south along the river to a location near well 699-37-E4. These sample locations and results of samples collected in January and September 1983 also were shown on Figure 5.18. These results indicate that spring discharges characterized by elevated tritium concentrations (greater than 20,000 pCi/L) were confined primarily to a region beginning near well 699-47-5 and extending downstream a distance of approximately 1.6 km (1 mi), below which the tritium concentration of springs is less than 2000 pCi/L.

The tritium concentration of wells inland from these downstream springs is more than 200,000 pCi/L. The lower tritium concentrations in springs may be a result of the influence of a clay unit that runs parallel to the river in this vicinity (see Section 4.0). This clay unit, which has an elevation above the water table in some locations, apparently acts as a partial barrier to ground-water flow between the river and the unconfined aquifer (Eddy et al. 1983). Data presented by Eddy et al. (1983) indicated that water levels in wells west of the clay unit (e.g., well 699-39-0) were quite stable, while water levels in wells the same distance from the river but located north of the clay unit (e.g., well 699-44-4) showed marked fluctuations. These authors concluded that this barrier may cause most ground-water flow to be diverted to the north and discharge to the river within the region where spring discharges have high tritium concentrations (Eddy et al. 1983). The springs with low tritium concentrations may be a result of the overwhelming influence of bank storage over the ground water residing in lower-permeability materials beneath or intercalated with the clay unit.

The investigations of springs discussed above did not evaluate the transient nature of spring discharges, which would consist of a large component of ground water affected by bank storage for much of the year. Those springs sampled by McCormack and Carlile (1984) in both January and September had higher tritium concentrations in September; however, these data are inadequate to make any generalizations regarding the time distribution of tritium concentrations in springs discharging to the river.

5.6.3 Long-Term Trends

Long-term tritium concentration trend plots provide an indication of the migration of tritium throughout the Hanford Townsite study area. These trend plots are shown combined in Figure 5.19. The trend plot for well 699-42-12A, located in the western portion of the study area, indicates that tritium concentration peaked some time in the late 1970s and has been decreasing steadily for approximately the past 5 years. The data also indicate some annual fluctuations (the cause for these is unknown). The trend plot for well 699-35-9, located in the southwest portion of the study area, indicates that tritium has not yet peaked in this vicinity and in fact shows a significantly delayed and

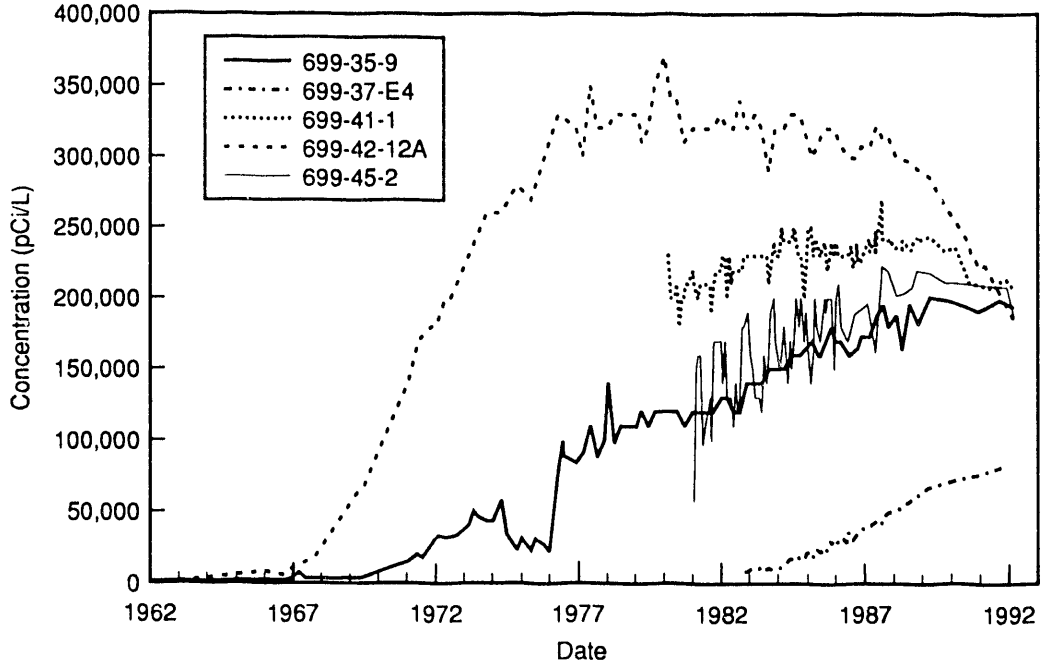

FIGURE 5.19. Long-Term Trends of Tritium Concentration in Five Wells

dampened tritium trend as compared with that of well 699-42-12A. These data suggest that the tritium plume from the 200-East Area arrived at well 699-42-12A much sooner, and was less dispersed, than at well 699-35-9 (the effect of radioactive decay on these trends has not been evaluated). Ground-water velocity between the 200-East Area and well 699-42-12A is therefore assumed to be greater than the velocity between the 200-East Area and well 699-35-9. Hydrologic test data, which were presented in Section 5.2, indicate that the transmissivity is approximately one order of magnitude greater in the vicinity of well 699-42-12A than in the vicinity of well 699-35-9. These data also are consistent with results provided by Poeter and Gaylord (1990) that described the lithologic controls on migration of tritium. They suggested that the percent of mud-dominated lithofacies, as well as the lateral continuity of the mud-dominated lithofacies, plays an important role in impeding tritium migration in some regions (including the region in the vicinity of well 699-35-9).

The trend plot for well 699-41-1 indicates that tritium concentration fluctuates within a given year. Data collected in 1981 (Eddy et al. 1983) indicate that changes in tritium concentrations in this well are not largely affected by changes in Columbia River flow. The long-term trend data also indicate that tritium concentration may have peaked in the mid to late 1980s and has been decreasing approximately since 1989. The plot for well 699-45-2 indicates that tritium concentration fluctuates largely within a given year and that the trend appears to have leveled off in the past couple of years. The large fluctuations are likely a direct result of bank storage effects from the Columbia River. The peak tritium concentration may have reached well 699-41-1 in the mid 1980s, lagging a few years behind the peak in well 699-42-12A. The trend of well 699-41-1 more closely resembles the trend in well 699-42-12A than does the trend of well 699-45-2, and tritium concentration in well 699-41-1 appears to be less dispersed and thus is higher than in well 699-45-2. This indicates that the ground-water flow path may be continuous and velocity may be greatest between well 699-42-12A and well 699-41-1 (however, other influences also may affect tritium concentration trends in well 699-41-1). If this is the case, a means of ground-water outflow must be present between well 699-41-1 and the river or some other discharge point.

The tritium concentration trend in well 699-27-8, located south of the study area (see Figure 1.2), was reviewed (this trend plot is not shown in this report). The maximum tritium concentration in this well was greater than 1×10^6 pCi/L, peaking in the early to mid '970s. These data indicate an earlier arrival and less dispersion of the tritium plume at this well than at well 699-42-12A. The aquifer at this location obviously is highly permeable, and it is possible that these highly permeable materials extend northeast toward the river and into the Hanford Townsite study area and influence tritium concentration trends and contaminant discharge in the study area. This was also demonstrated in the work by Poeter and Gaylord (1990). The lower-permeability aquifer materials in the vicinity of well 699-35-9 may result in a restriction of ground-water flow and contaminant migration in at least a portion of the region between wells 699-27-8 and 699-42-12A.

The data trend for well 699-37-E4 shows a much later and dampened response in tritium concentration than for any other wells. This well is completed within the Ringold Formation; therefore, the transmissivity of the sediments at this well is expected to be less than the transmissivity in the Hanford formation. The lower transmissivity of the Ringold Formation and associated lower ground-water velocity in this formation explain why tritium concentrations lag much behind in this well. Note, however, that the tritium concentration in this well has increased steadily over time. Because of the lower transmissivity of the Ringold Formation, the contaminant flux to the Columbia River from this formation will be significantly less than from the Hanford formation.

5.6.4 Bank Storage Effects on Ground-Water Chemistry

The effects of the Columbia River and associated bank storage on ground-water chemistry were studied by Eddy et al. (1982, 1983). They documented that tritium concentrations decline as the river flow rate increases in the spring months and the river water enters the bank; the trend is reversed when the river flow rate decreases later in the year. Tritium concentrations in well 699-47-5 fluctuated from approximately 25,000 pCi/L to approximately 185,000 pCi/L in 1981 in response to changes in the flow rate of the river. This general trend (but not the magnitude of changes in concentration) was

true for three wells (699-43-3, 699-44-4, and 699-47-5) from which tritium concentrations were determined approximately monthly in 1980, 1981, and most of 1982. This general trend did not hold true in well 699-46-4, in which tritium concentrations increase as the river flow rate increases, and tritium concentrations decrease as the river flow rate decreases.

Ground-water tritium concentrations and ground-water elevations were determined in wells 699-42-12A, 699-43-3, 699-46-4, and 699-47-5 between August 1990 and early March 1991 as part of the current study (Figures 5.20 through 5.23, respectively). Figure 5.24 shows tritium concentration plots for all these wells combined. The same general relationships between tritium concentrations and ground-water elevations were observed as between tritium concentrations and river flow rate discussed above. The relationships between river stage (flow rate) and ground-water elevations have been established and were discussed in Sections 5.4 and 5.5. Although tritium did not fluctuate as much in 1991 as in 1981, the strong inverse relationship to the Columbia River stage and ground-water elevations is obvious. The same relationship holds true for well 699-43-3, although it is not affected to the same extent as well 699-47-5. A direct, rather than inverse, relationship between ground-water elevations and tritium concentrations occurs in well 699-46-4. Tritium concentrations in well 699-42-12A are not affected by Columbia River stage, but rather are a result of the regional trend of tritium concentrations, which was discussed in Section 5.6.3.

The changes in tritium concentrations as a result of changes in river stage are a direct result of bank storage. When the Columbia River stage is high, water migrates inland, mixing with ground water and causing an increase in ground-water elevations. When the river stage is low, the mixed water returns to the river, and ground-water elevations decrease again. The cause of the increase in tritium concentrations as ground-water elevations increase in well 699-46-4 is unknown. One hypothesis is that well 699-46-4 may be separated from ground water with higher tritium concentration and somewhat isolated (geologically) from direct mixing (and subsequent dilution) with water from bank storage. As water levels increase, ground water containing higher tritium concentration migrates toward well 699-46-4.

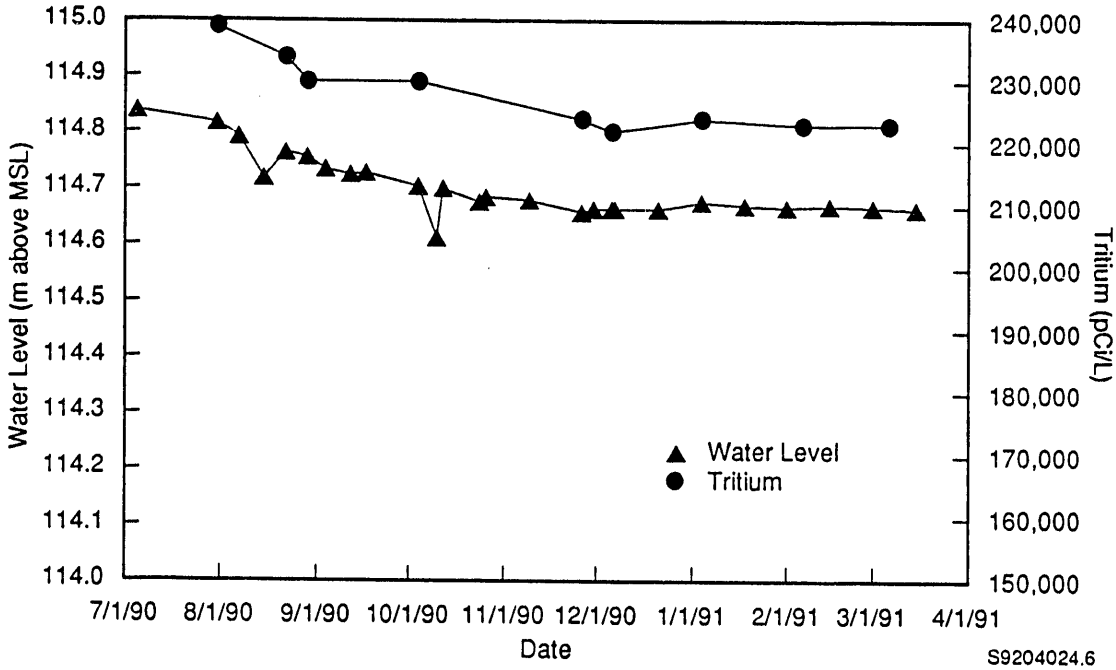

FIGURE 5.20. Water-Level Elevation and Tritium Concentration in Well 699-42-12A

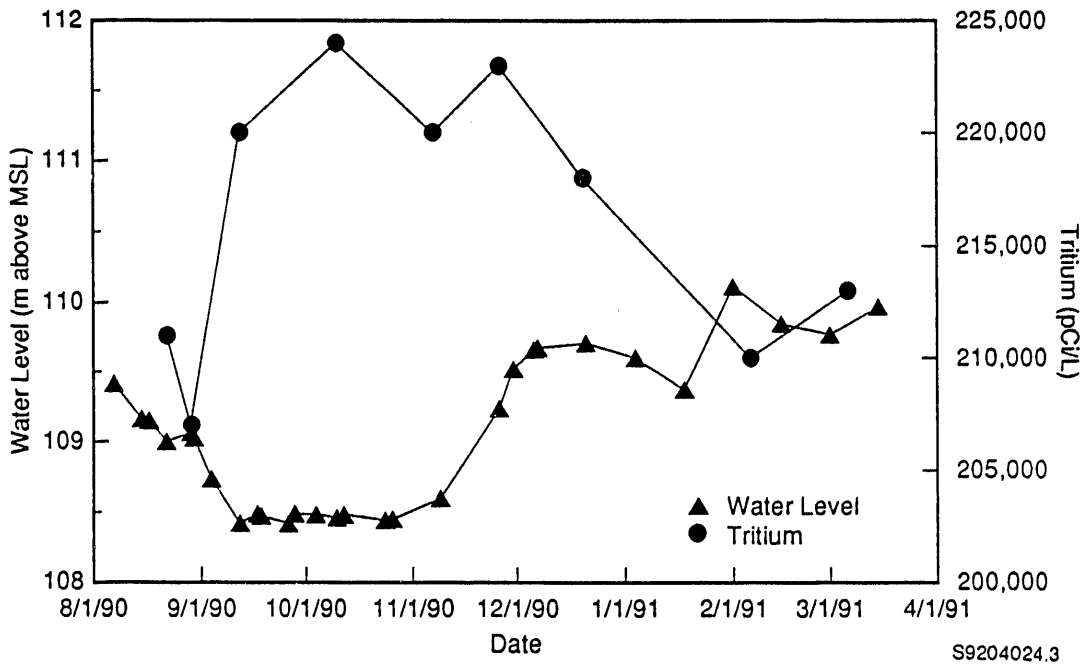

FIGURE 5.21. Water-Level Elevation and Tritium Concentration in Well 699-43-3

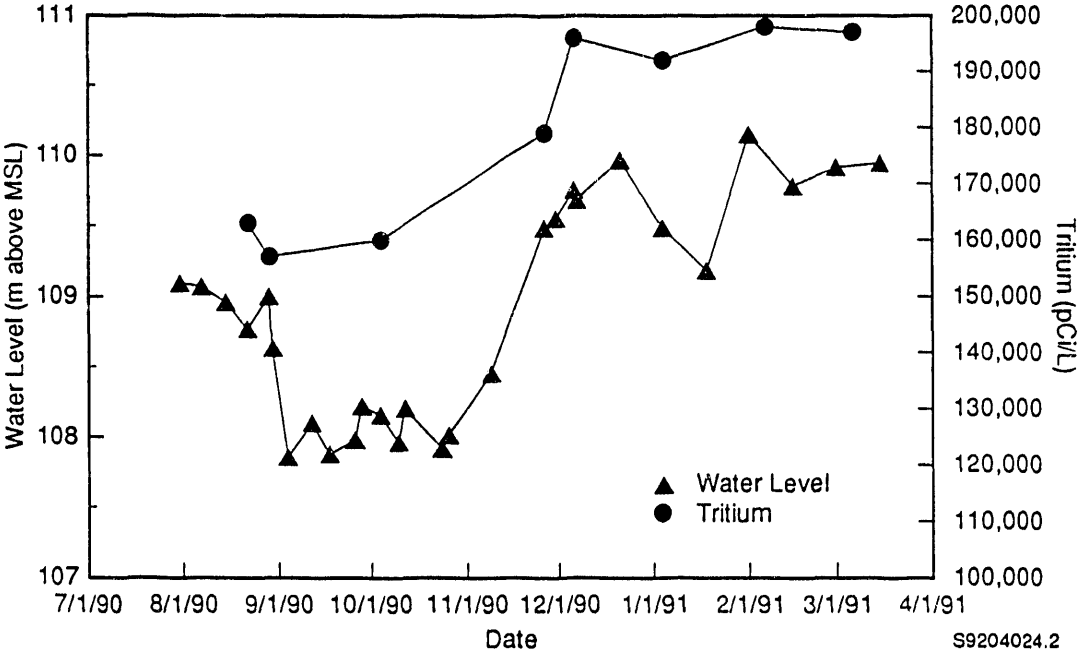

FIGURE 5.22. Water-Level Elevation and Tritium Concentration in Well 699-46-4

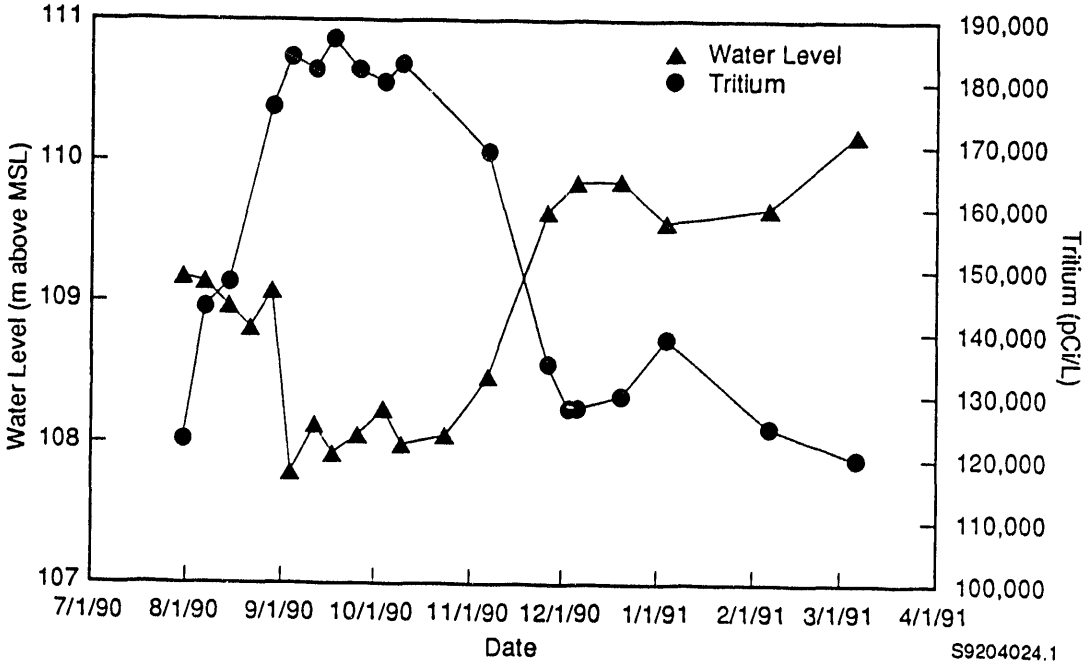

FIGURE 5.23. Water-Level Elevation and Tritium Concentration in Well 699-47-5

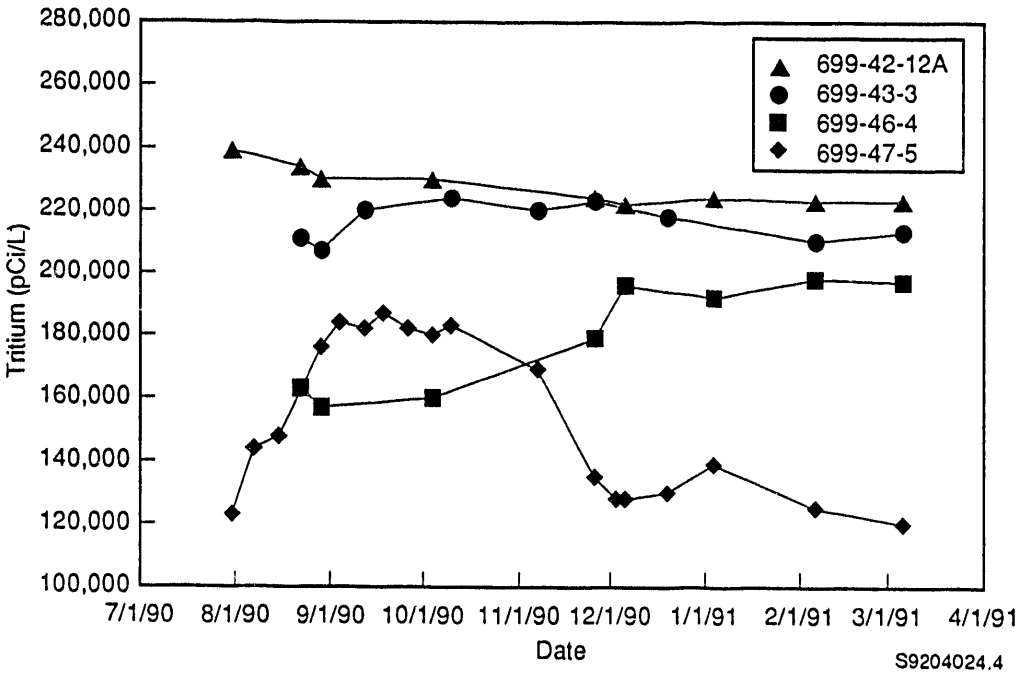

FIGURE 5.24. Tritium Concentration in Wells 699-42-12A, 699-43-3, 699-46-4, and 699-47-5

Two different transient effects occur as a result of the Columbia River fluctuations and bank storage. One is the pressure wave that is transferred inland and is observed as water-level fluctuations in wells. The other is the actual movement of water from the river into bank storage, causing an interchange or mixing with ground water. The pressure wave is observed much farther inland than the distance traveled in the aquifer by water derived from the Columbia River. This is evidenced by water-level fluctuations and associated tritium concentration changes in wells 699-43-3 and 699-47-5. The tritium concentration change in well 699-43-3 is approximately 25% of the change in well 699-47-5 when the magnitude of the water-level change in well 699-43-3 is approximately 75% of the change in well 699-47-5. It cannot be ascertained how far inland the dilution effects of bank storage occur because of the lack of appropriate data.

5.7 GROUND-WATER MODELING

5.7.1 Modeling Objectives

The primary modeling objective in this study was to incorporate geologic heterogeneity into a numeric model of flow and, ultimately, contaminant transport. Utilizing alternate realizations of geologic heterogeneity will improve our understanding of how much detail, with respect to heterogeneity, is required to describe contaminant transport; this information will be valuable to site characterization activities.

In 1990 and 1991, D. R. Gaylord and coworkers at WSU developed multiple geologic realizations using a geostatistical technique called multiple indicator conditional stochastic simulation. Indicator simulations retain information on extreme values of hydraulic conductivity and their connectivity between known points. Because extreme values are very important in contaminant transport, it is not difficult to discern the advantages of indicator analysis over kriged conductivity fields that smooth away much of this information.

A second modeling objective was to address the transient nature of the model's discharge boundary condition, the Columbia River. Currently, wells completed in the unconfined aquifer near the Columbia River have annual water-table variations of as much as 2 m (7 ft). These variations should not affect the regional flow of the Hanford formation unconfined aquifer. However, such variations may affect the timing of contaminant delivery to the river, with high river stage impeding near-river transport. To model this bank storage phenomenon in cross section, a code that can simulate variably saturated conditions must be used. As wetting fronts advance and then recede from the bank in response to river-stage fluctuations, nodes within the zone of water-table fluctuation will move through various levels of saturation. Because this zone consists of relatively coarse materials in the Hanford Townsite study area, the capillary fringe will be small and wetting fronts will change rapidly. These conditions require high-resolution spatial discretization in the zone of water-table fluctuation to ensure numeric stability.

5.7.2 Code Selection

The above modeling objectives were considered in the selection of a code that could be used to construct a two-dimensional, cross sectional model of the Hanford Townsite study area. Several codes were considered, of which two were selected for further investigations.

PORFLO-3 is a three-dimensional, variably saturated, integrated finite-difference code that meets all of the above objectives. Its ability to simulate the variably saturated conditions resulting from the bank storage phenomenon provides marked advantages over other codes. However, the high-resolution discretization required to generate a stable numeric solution in this zone of variable saturation results in a model that requires substantial computational resources. For example, discretizing the entire model domain, while constraining the discretization in the zone of variable saturation to 0.76 m (2.5 ft) vertically and 1.5 m (5 ft) horizontally, resulted in a 31,000-node model.

The other code investigated was CFEST, a three-dimensional, saturated finite-element code. CFEST is formulated to model confined aquifers; however, through an iterative approach that adjusts the surface nodes to match the water-table elevation at the previous time step, unconfined aquifers can be simulated. To implement this methodology, all variations in water-table elevation must be absorbed by the surface elements (i.e., if the water table fluctuates 3 m, the surface elements must be positioned such that the surface nodes of each surface element can be moved through the 3-m water-table fluctuation). This limitation can cause problems if material properties are such that more than one element is needed to accurately represent the zone of water-table fluctuation.

Each of the above codes has its advantages and disadvantages when considering ability to meet the modeling objectives. However, because the PORFLO-3 code was less restrictive, it was selected for this study. By initially ignoring the river-stage fluctuations (i.e., using annual average river-stage as the model's downstream boundary condition) and concentrating instead on simulating the effect of geologic heterogeneity, constraints placed on discretization of the zone affected by bank storage can be relaxed. This

approach resulted in a model of manageable size able to adequately represent geologic heterogeneity. In addition, by selecting PORFLO-3, the ability to simulate variably saturated conditions is retained; if warranted, a submodel could be developed near the downstream boundary to study bank storage effects.

5.7.3 Conceptual Model

As mentioned in Section 5.7.1, D. R. Gaylord and coworkers at WSU developed multiple geologic realizations using geostatistical techniques (see Figure 4.6). The cross section runs perpendicular to the Columbia River near the old Hanford Townsite along most of the length of section B-B' (see Figure 4.1). The model domain extends horizontally 3700 m (12,000 ft) from the Columbia River and vertically from the top of basalt to the land surface. Neutron-neutron, gamma-gamma, and descriptive geologic logs were supplemented with grain size data to delineate the following four hydrofacies: 1) gravels, 2) sandy gravels, 3) sands, and 4) clays and silts.

In 1988, D. R. Gaylord and E. P. Poeter at WSU assessed some existing aquifer test data to identify a representative hydraulic conductivity for each of the hydrofacies. Of the available aquifer tests, only one representative test was identified for each hydrofacies. Other test data exhibited anomalies or were from wells completed in more than one of the defined hydrofacies (resulting in a composite conductivity). Based on this limited data set, hydraulic conductivity was assigned to each of the hydrofacies as follows: 1) 12,000 m/day (40,000 ft/day) for gravel, 2) 3000 m/day (10,000 ft/day) for sandy gravel, 3) 60 m/day (200 ft/day) for sand, and 4) 0.2 m/day (0.6 ft/day) for clays and silts. Gaylord and Poeter noted that, because of the limited information available on the hydraulic conductivity of each of the defined hydrofacies, these values should be used with caution.

Boundary conditions were specified as Dirichlet (held head) at the model's upstream and downstream boundaries; all other boundaries were specified as no-flux boundaries. This designation assumes that surficial recharge can be neglected as well as recharge of the unconfined aquifer by the underlying basalts. Quantification of these possible sources of aquifer recharge, and the solution's sensitivity to recharge, was not within the scope of this

study; for purposes of performing a preliminary modeling study of aquifer heterogeneity, the boundary conditions discussed above were deemed adequate.

The downstream boundary consisted of the Columbia River. As discussed previously, for this preliminary modeling study of aquifer heterogeneity, bank storage effects were not considered; instead, the downstream boundary, from the river surface to the river bottom, was held at the annual average river stage. From the elevation of the river bottom to the top of basalt, the boundary was specified as no flux; this designation stems from the fact that regional ground-water contour maps indicate that the Columbia River acts as a sink for the unconfined aquifer on both sides of the river. For the upstream boundary, well hydrographs were analyzed to identify the distance from the river where river-stage fluctuations were no longer affecting the water table; well hydrographs indicated that at 3700 m (12,000 ft) from the river, river-stage fluctuations had no appreciable effect on the water table. Because no information was available on the hydraulic potential distribution at depth, hydraulic potential was held constant at depth.

The initial hydraulic potential distribution was specified linearly between the downstream and upstream boundaries and was specified as constant with depth. This designation was true everywhere except in the basalt formation. Because of the formulation of PORFLO-3, a finite-difference code with no implementation of interior no-flow nodes, the basalt formation had to be included in the model domain. To ensure that the unconfined and confined flow systems were simulated as having no intercommunication, the basalts were assigned a conductivity of 3×10^{-9} m/day (1×10^{-8} ft/day). Contour maps of hydraulic potential in the confined and unconfined aquifers were compared for the study area; in general, hydraulic potential in the confined aquifer was 3 m (10 ft) higher than in the unconfined aquifer. For clarity in delineating the confined from the unconfined aquifer in the contour plots of hydraulic potential distribution, initial conditions in the confined aquifer were set 3 m (10 ft) higher than those in the unconfined aquifer.

5.7.4 Model Development

The model domain was discretized into grid blocks measuring 30 m (100 ft) in the horizontal direction (dx) and 3 m (10 ft) in the vertical

direction (dy). This discretization resulted in a model requiring a solution at approximately 4500 nodes. After some preliminary analysis, this discretization was chosen for its ability to adequately represent the heterogeneity simulated with the geostatistical technique while adhering to numerical stability criteria and keeping the model of manageable size; in a preliminary study of heterogeneity, all of these factors are important and must be considered when discretizing the model domain.

The stochastic simulation results, in digital format, were supplied to PNL along with a code used to interpolate results contained in the stochastic simulation grid onto a user-defined grid. The stochastic simulation grid was discretized into grid blocks of 30 m (100 ft) in the horizontal direction (dx) and of variable vertical thickness (dy); the variable vertical thickness was a result of the stochastic simulation process. Several options were available for the interpolation; in this study, the hydrofacies were assigned to each grid block by determining the hydrofacies occupying the greatest percentage of the user-specified grid block. A code was then developed to incorporate this geologic heterogeneity into the PORFLO-3 model.

5.7.5 Modeling Results and Discussion

For several of the geologic realizations, transient simulations were run for a duration of 100 years. An example of a resulting hydraulic potential distribution is shown in Figure 5.25. This figure indicates that flow would be notably impeded where the potential lines a very closely spaced. This area corresponds to a zone of low-permeability silt and clay facies downgradient of the basalt anticline. Although little information on hydraulic potential distribution with depth exists in this area, the simulated hydraulic potential distribution is not consistent with the current concept of the hydrologic system. There are several possible explanations for this discrepancy:

- The first and most probable explanation is that the conductivity value of the silt and clay facies was set too low. Note that conductivity values for each of the facies are based on the results of one aquifer test, and hence representativeness of these values is suspect.

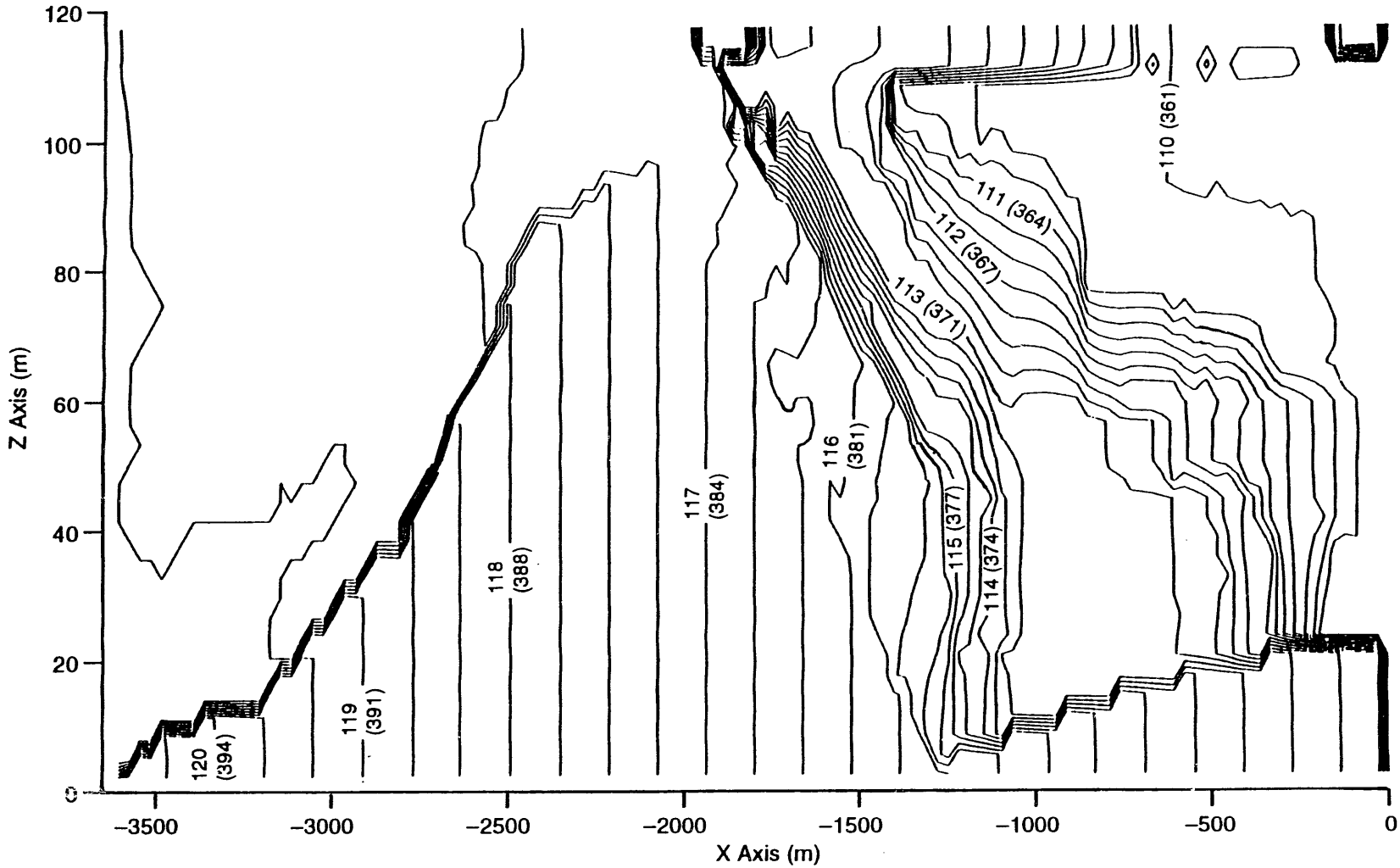

FIGURE 5.25. Two-Dimensional Cross Section of Hydraulic Potential Distribution Produced from Ground-Water Flow Modeling

- The realizations may be biased toward the silt and clay facies and contain a higher percentage of this facies than actually is present.

- In a two-dimensional, cross sectional model, the geology specified at the cross section is assumed to be areally continuous. In real three-dimensional space, this may be a poor assumption; the clay and silt facies may extend laterally only a short distance, allowing ground water to flow through surrounding, higher-permeability materials.

6.0 CONTAMINANT DISCHARGE TO THE COLUMBIA RIVER

This section summarizes much of the information presented in previous sections and provides a conceptual model of the Hanford Townsite study area. Mechanisms of discharge to the river and estimates of ground-water flux and contaminant mass discharge to the river are provided.

6.1 CONCEPTUAL MODEL OF THE HANFORD TOWNSITE STUDY AREA

A general conceptual model, or a framework from which to estimate ground-water flux and contaminant mass discharge to the Columbia River, was constructed based on hydrogeologic and hydrochemistry data presented in Sections 4.0 and 5.0.

6.1.1 Aquifer Geometry

The saturated Hanford formation, which is unconfined throughout the study area, makes up the total aquifer thickness for the purpose of constructing the conceptual model. This can be justified on the basis that the transmissivity of the Hanford formation is more than an order of magnitude greater than that of the Ringold Formation, which is reasonable based on the previously documented hydraulic conductivity values of both the Ringold Formation and the Hanford formation and on the results of hydrograph analyses presented in Section 5.5. Also, the tritium concentration in wells completed within the Ringold Formation is much lower than in wells completed within the Hanford formation. It is also prudent to represent only the Hanford formation as the total aquifer because data are available on the hydraulic head within the Hanford formation but not within the Ringold Formation. Further, contaminant distribution data are available for only one well within the Ringold Formation.

A map of the bottom of the Hanford formation was shown in Figure 4.7, Section 4.2. Figure 6.1 shows the generalized saturated thickness of the aquifer. The map indicates that the aquifer thickness is variable. The aquifer is not present adjacent to the Columbia River where the clay unit rises to an elevation above the water table and in the northeastern part of

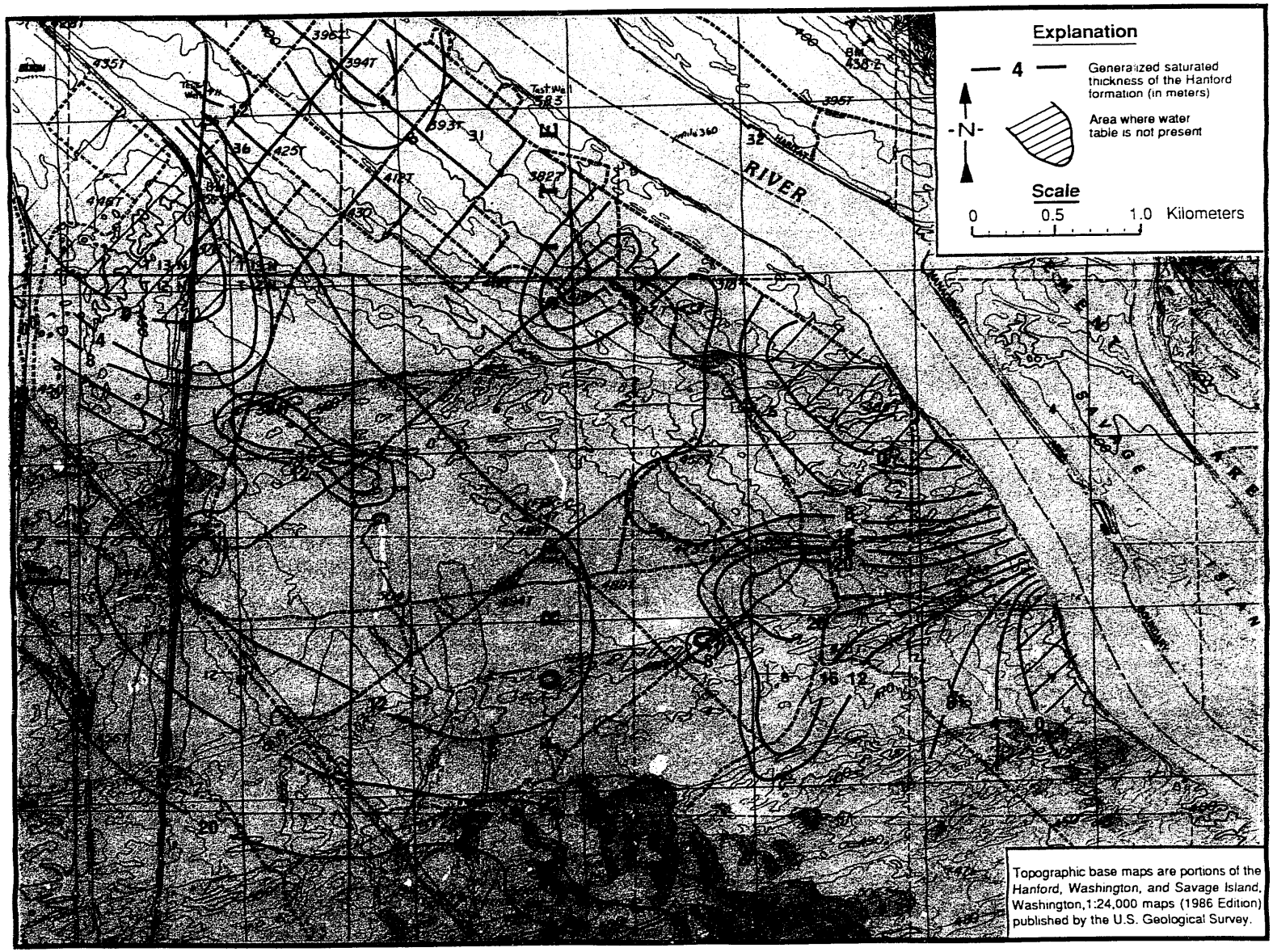

FIGURE 6.1. Generalized Hanford Formation Aquifer Thickness Map for the Hanford Townsite Study Area

the study area where the Elephant Mountain basalt associated with the Gable Mountain anticline rises above the water table.

Variations occur in the permeability of the saturated Hanford formation. These heterogeneities, as discussed in some detail by Poeter and Gaylord (1990), influence ground-water flow and tritium migration. The aquifer in the vicinity of well 699-35-9 has relatively lower permeability than in the vicinity of well 699-42-12A.

6.1.2 Ground-Water Flow

Flow nets depicting the conceptual water-table elevation and ground-water flow lines are shown in Figure 6.2. These flow nets were constructed considering hydrogeologic controls and boundaries. The flow lines indicate that ground water flows south of the basalt anticline in the northeastern part of the study area and is restricted somewhat in the southwest part of the study area (where the hydraulic gradient is steeper). Ground water is diverted around the clay unit that is adjacent to the Columbia River. Ground water discharges to the river north and also south of the clay unit. It is further concluded, based on geologic and water-chemistry data, that ground water also flows from the north along the east edge of the basalt anticline and converges with ground water flowing from the west. This former flow path contains ground water with essentially background levels of tritium (see Section 5.6.2). As the flow paths from the north and west converge, a very sharp delineation of the north edge of the tritium plume is formed (see Figure 1.2).

A simplified cross section of the aquifer and part of the west side of the river channel north of the clay unit is shown in Figure 6.3 (the location of the section is shown in Figure 6.2). The surface of the water table and the river are shown for the two time periods depicting high and low ground-water elevations. Three separate space intervals indicating the generalized nature of the hydraulic gradient for the two time periods are shown. The first interval (A) is between the upgradient edge of the study area and a location where bank storage has no influence on water levels. This interval serves as essentially a "constant gradient" condition that is influenced only by regional ground-water flow. The second interval (B) is between the

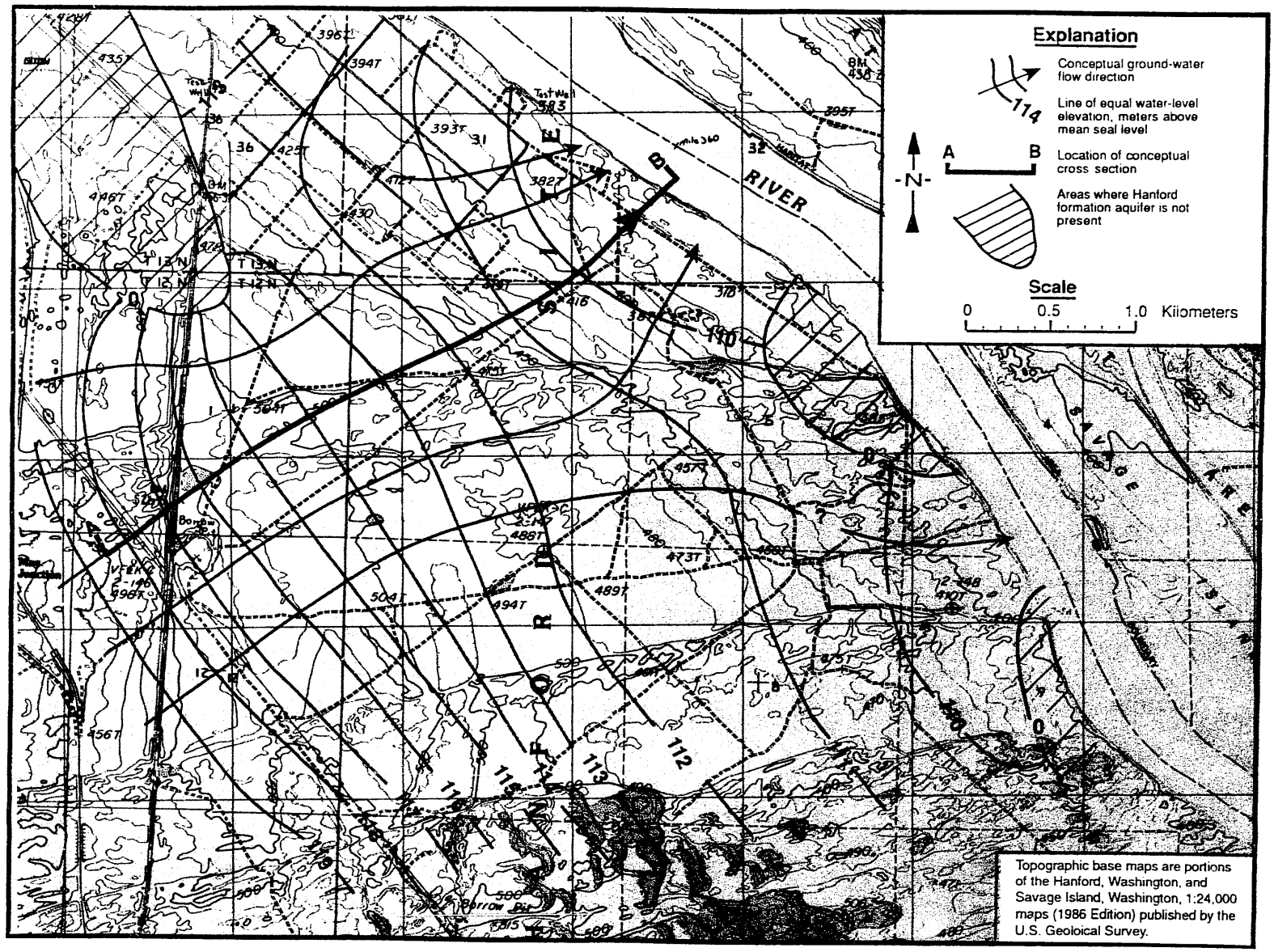

FIGURE 6.2. Generalized Ground-Water Flow Net of the Water Table in the Hanford Townsite Study Area

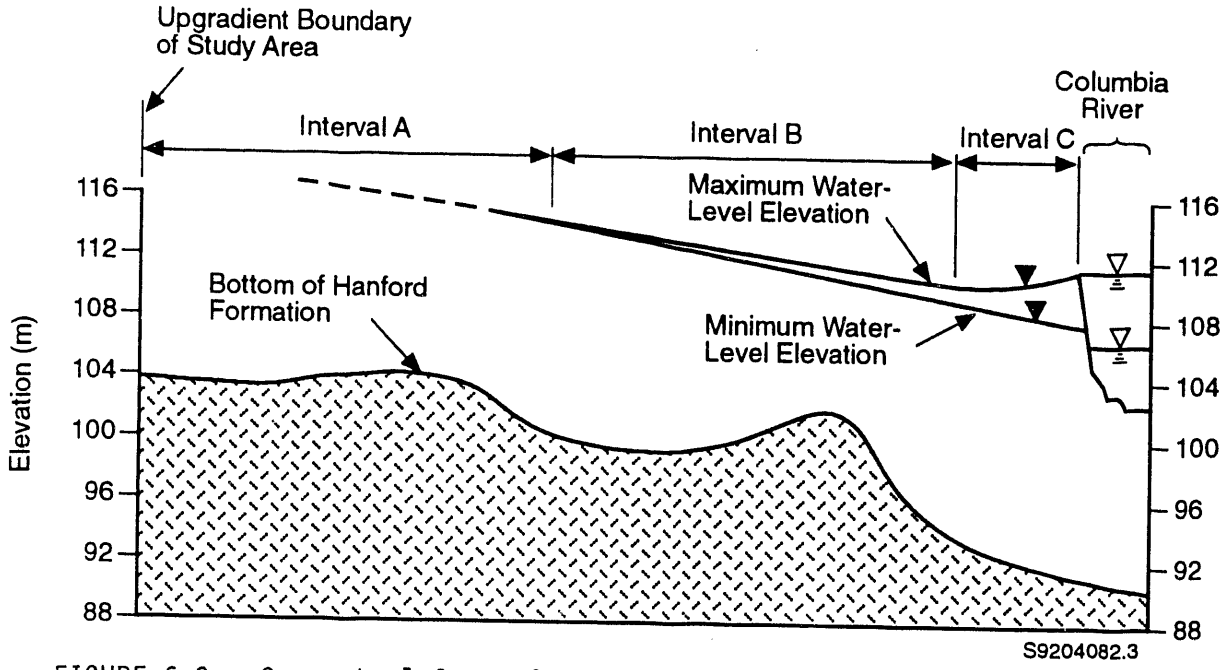

FIGURE 6.3. Conceptual Cross Section Showing the Maximum and Minimum Ground-Water and River-Stage Elevations (location of cross section is shown in Figure 6.2)

downgradient end of interval A and a location where water levels fluctuate minimally in response to river fluctuations. This interval represents conditions that are affected by river fluctuations but where flow is always toward the river, or the gradient is always positive. The third interval (C) is located between the downgradient edge of interval B and a location where water levels fluctuate greatly in response to river fluctuations. Within this interval, ground-water flow is toward the river for some periods and is away from the river for other periods; in other words, the gradient is positive for some periods and negative for some periods. The gradient within interval A is essentially constant at all times of the year. The gradient within intervals B and C are greatest during low river stage, and the gradient within interval C is negative during high river stage.

Figure 6.3 also clearly shows that the Columbia River does not penetrate the entire thickness of the Hanford formation in this location. Ground-water discharge to the river in this location will occur beneath the bed, or bottom, of the river as well as from springs and seeps along the riverbank. Discharge

to the bed of the river will be controlled by the hydraulic head differential between the aquifer and the river and by the hydraulic characteristics (i.e., leakage) of the riverbed material. It is assumed that the hydraulic head in the aquifer materials below the river is, on the average, greater than the elevation of the river stage (this condition is necessary for net ground-water discharge to the river to occur). However, when the upward hydraulic head differential is largest, which would occur when the Columbia River stage is low, ground-water discharge to the bed of the river is greatest. When the upward hydraulic head differential is small (when the Columbia River stage is high), ground-water discharge to the bed of the river is small. If the hydraulic head differential reverses, which may occur when the Columbia River stage is high, leakage from the river into the aquifer materials underlying the river would result. This is obviously a complex relationship, which would require unavailable data to characterize, and further discussion is beyond the scope of this report.

6.2 GROUND-WATER DISCHARGE TO THE COLUMBIA RIVER

Based on the conceptual model, ground-water flow is controlled by variations in hydraulic conductivity within the Hanford formation and by channels incised into the Ringold Formation in which the Hanford formation was deposited. Most ground water entering the Hanford Townsite study area from the west appears to flow through the vicinity of well 699-42-12A. Therefore, the discharge rate was estimated by assuming a flow path to the river from this location. Hydraulic conductivity within this flow path was estimated from available test data. The hydraulic gradient for each interval shown in Figure 6.3 was determined from water-level measurements in nearby wells.

Ground-water flow volumes were calculated for two periods corresponding to high and low river stage (and associated ground-water levels) and for each of the intervals shown in Figure 6.3. This allowed both an evaluation of the effects of river-stage fluctuations on the time distribution of ground-water discharge to the river and an evaluation of ground-water flow under a constant gradient. The ground-water discharge for a unit width was calculated across the boundaries corresponding to the downgradient edge of each interval. The

thickness and width of the aquifer were multiplied by the unit discharge to arrive at the total ground-water discharge for the interval of the aquifer being considered.

6.2.1 Method of Calculation and Data Used

The calculations of ground-water flow volumes were made by using Darcy's law, which can be stated as

$$Q = K \times I \times A \qquad (6.1)$$

where Q = ground-water discharge in m^3/s

K = hydraulic conductivity in m/day

I = hydraulic gradient in m/m

A = aquifer area in m^2.

The hydraulic conductivity and the aquifer area can be combined to result in the transmissivity T (hydraulic conductivity times thickness) multiplied by the aquifer width W. This approach is reasonable given the large uncertainties in many of the variables (Sections 6.2.2 and 6.2.3 discuss uncertainty). The equation then becomes

$$Q = T \times I \times W \qquad (6.2)$$

The hydrologic property values used for the calculations of ground-water discharge within each interval and for each time period are provided in Table 6.1. Maximum and minimum hydraulic gradient, aquifer thickness, and transmissivity values are provided. The hydraulic gradient data were taken from the water-table elevation maps in Section 5.2, and water-level elevations in wells were used to obtain the specific values. Much of the information was not taken from wells along the flow path shown in Figure 6.3 because of the lack of wells along the section. Rather, the information was derived from wells assumed to be directly perpendicular to the flow path and also assumed

TABLE 6.1. Hydrologic Values Used for Ground-Water Discharge Calculations

Interval	Hydraulic Gradient (I)		Hydraulic Conductivity (m/day)	Aquifer Thickness (m)		Transmissivity (m^2/day)	
	Minimum Gradient	Maximum Gradient		Maximum Gradient	Minimum Gradient	Maximum Gradient	Minimum Gradient
A	0.003	0.003	300	20	20	6000	6000
B	0.002	0.003	540	10	12	5400	6500
C	-0.001	0.002	540	10	12	5400	6500

to represent hydrologic conditions along the flow path. The hydraulic properties were taken from values provided in Sections 5.2 and 5.5. The most quantitative hydraulic conductivity values, derived from aquifer test analyses, that were assumed representative of the higher-permeability materials were used for the analyses.

The gradient and thickness are constant within interval A. The maximum gradient within intervals B and C occurs when the thickness is at the minimum; therefore, the transmissivity is smallest when the gradient is greatest. The minimum gradient in interval B corresponds to a period when the gradient is negative in interval C. The transmissivity in these intervals is the largest when the gradient is at its minimum.

6.2.2 Results of Ground-Water Discharge Calculations

The results of the ground-water discharge calculations for each interval and for each gradient condition are provided in Table 6.2. The total width of the discharge areal cross section was assumed to be 1000 m. This value for the width assumes that the area of discharge would be of uniform thickness for the entire width. This is the approximate width where the average thickness is approximately 11 m. This value was multiplied by the unit width discharge values to obtain the total estimated ground-water discharge for each gradient condition. The total ground-water discharge passing the downgradient side of interval A is approximately 6.6×10^6 m^3/year (or 6.6×10^9 L/year) under the assumed conditions. (For comparison, approximately 2.4×10^{10} L of liquid was disposed in the 200 Areas during 1988.) The total discharge through interval A should approximate the total discharge to the Columbia River, by the

TABLE 6.2. Minimum and Maximum Calculated Unit Width Discharge and Total Ground-Water Discharge for Each Space Interval

Interval	Unit Width Discharge (m^3/day/m)		Total Discharge (m^3/day)	
	Minimum	Maximum	Minimum	Maximum
A	18	18	18,000	18,000
B	13	16	13,000	16,000
C	-6.5	11	-6,500	11,000

principle of conservation of mass. The total estimated discharge in interval B should bracket the discharge in interval A if the total discharge passing through A is equal to the total discharge passing through B. The results for interval C do not bracket the results of either interval A or interval B. These results for interval C indicate the large time-variant fluctuation in ground-water discharge to the Columbia River. To accurately quantify the discharge and these variations, the calculation would require integration of many representative time periods.

The discharge in interval A may be larger than both the maximum and the minimum discharge in intervals B and C for several reasons. The width of the discharge regions may vary significantly, the hydraulic conductivity of the discharge regions may also vary, and/or ground water may be going into storage as a result of a generally rising water level. The discharge calculation made for interval A is considered to be the most representative because the water-level data for this interval are nearest to the flow path through which calculations were made, and because dynamic water-level changes will not affect these calculations significantly as they may for the other intervals.

These results provide a qualitative estimate of the magnitude of ground-water flow and discharge in the vicinity where large ground-water discharge via springs has been documented previously. Prater et al. (1984) provided an estimated discharge rate of 0.085 m^3/s (3 ft^3/s) or 7300 m^3/day (2.6 x 10^5 ft^3/day) to the Columbia River between river miles 360 and 356 (U.S.

Geological Survey river-mile system), which primarily encompasses the Hanford Townsite study area. This ground-water discharge rate was based on results of Site-wide numerical modeling.

6.2.3 Uncertainty and Limitations

The major limitations of the approach and uncertainty in results provided for ground-water discharge are the following:

- The hydraulic properties are not known with certainty for the section through which ground-water discharge estimates were made. In addition, the distribution and variability of hydraulic properties are not known. These uncertainties have the largest impact on the discharge calculations.

- The thickness and extent of the aquifer are not known with certainty throughout the region where most ground-water discharge is believed to occur. Thickness variations will affect the transmissivity estimates used for the calculations.

- The width of the region of ground-water discharge is not known with certainty. The region where the Hanford formation may extend to the river south of the "clay barrier" also may contribute ground water to the Columbia River.

- The hydraulic gradient along the section through which the calculations were made is not known with certainty. The impact of using data from wells that do not lie directly in the flow path is not known.

- It is assumed that the gradient through the entire saturated thickness is horizontal and that the changes in water-table elevations are propagated vertically essentially instantaneously. Because this is a ground-water discharge region, this assumption is very likely not valid; however, no other data are available with which to define the vertical gradients. The uncertainty associated with this assumption is unknown.

- The tritium concentration is assumed to be constant throughout the full saturated thickness of the Hanford formation. This assumption is reasonable given the amount of dispersion that would occur over the distance from the source area to the study area.

- The ground-water discharge was calculated for only two periods within the period of record for the current study. It is unknown how representative these periods are for "average" ground-water and Columbia River discharge conditions.

The total uncertainty in the ground-water discharge estimates is a factor of plus or minus approximately five times the calculated values. Transmissivity within the more permeable portions of the Hanford formation calculated from aquifer tests and from indirect numerical methods ranges from approximately 1200 to 34,000 m^2/day. This is the only variable that was used to assign a total uncertainty to the calculations, because it is by far the largest variable that will affect the calculation of ground-water discharge. The transmissivity values used in the calculations ranged from 5400 to 6500 m^2/day; therefore, the range on either side of these values was considered for assigning the total uncertainty.

6.3 CONTAMINANT MASS DISCHARGE TO THE COLUMBIA RIVER

The contaminant mass discharge calculated in this section includes only calculations for tritium. The same approach could be used for other constituents if desired. The tritium mass discharge will vary as a function of both ground-water discharge and tritium concentration in ground water. The concentration of tritium in ground water adjacent to the river will be lowest when the river stage and associated ground-water elevations are highest. The hydraulic gradient is reversed and the maximum effects of bank storage are conceived to occur at this time. When the river stage drops, the gradient again becomes positive and the mixed ground water returns to the river. The gradient is expected to reach a maximum at the lowest river stage. The tritium concentration in ground water discharging to the river and to springs would be expected to reach a maximum during the later period of low river stage, especially just prior to another large rise in river stage. However, the fluctuations in tritium concentration shown very little lag time in response to water-level fluctuations based on data collected during the current study.

A numerical modeling study by Yim and Mohsen (1992) established that tidal fluctuation has a major effect on exit concentration of a contaminant plume discharging to the surface water body. The conservation of mass is maintained by the increased ground-water velocity (and thus discharge) occurring during periods when the surface water is at low stage. This is likely

the same phenomenon that maintains conservation of mass (in this case, tritium) during contaminated ground-water discharge within the Hanford Townsite study area.

6.3.1 Method of Calculation and Data Used

Estimates of tritium mass discharging to the river during high and low river-stage periods were made based on the calculated discharge across intervals A, B, and C. Tritium mass discharging from interval C was estimated primarily to indicate the large changes that occur in tritium mass discharged during the year. The tritium mass discharge was calculated for each period from the equation

$$M = Q \times C \qquad (6.3)$$

where M is the tritium mass discharge rate (Ci/day), Q is the ground-water discharge volume (m^3/day), and C is the average tritium concentration for the period (pCi/L).

The maximum ground-water discharge through interval B occurs at low river stage and is associated with the lowest water-level elevation (largest gradient) and the highest tritium concentration. The tritium concentration values used for the period of maximum discharge were taken from measurements made during the period of study. Tritium concentration values used for the period of minimum discharge for interval A were taken from measured values; however, values used for intervals B and C were assumed based on relative trends from previous years' measurements and extrapolation of the current year's measured values.

6.3.2 Results of Mass Discharge Calculations

Results of tritium mass discharge calculations are provided in Table 6.3. The maximum and minimum mass discharge rates in curies per day are provided for each interval. The total estimated tritium mass discharge for 1 year also is provided. The mass discharge through interval A does not change because the gradient and tritium concentration are essentially constant within this interval. The total annual tritium mass discharge to the Columbia

TABLE 6.3. Calculated Tritium Mass Discharge to the Columbia River

Interval	Ground-Water Discharge (m^3/day)		Tritium Concentration (pCi/L)		Tritium Mass Discharge (Ci/day)		Total Annual Tritium Mass Discharge (Ci/year)
	Minimum	Maximum	Minimum	Maximum	Minimum	Maximum	
A	18,000	18,000	2.2×10^5	2.3×10^5	4.0	4.0	1,400
B	13,000	16,000	2.1×10^5	2.2×10^5	2.7	3.5	1,100
C	-6,500	11,000	1.0×10^5	1.8×10^5	-0.65	2.0	Not determined

River was estimated by assuming the daily mass discharge rate is constant for the year. The total annual tritium mass discharge for interval B was calculated from an average of the maximum and minimum daily mass discharge rates.

Prater et al. (1984) calculated a ground-water discharge rate of approximately 7300 m^3/day for the Hanford Townsite vicinity. The annual tritium mass discharge to the Columbia River from within the Hanford Townsite study area was estimated to be approximately 540 Ci/year based on the ground-water discharge rate calculated by Prater et al. (1984) and using an average tritium concentration of 200,000 pCi/L. The value calculated for the current study is approximately two to two and one-half times this estimate.

The tritium concentration in the river contributed from ground-water discharge in the Hanford Townsite study area was calculated using the approach previously used by Prater et al. (1984) and Freshley and Thorne (1992):

$$C_{river} = C_{well} \, (Q_{gw}/Q_{river})$$

where C_{river} = the resulting radionuclide concentration in the river (pCi/L)

C_{well} = the average radionuclide (or maximum and minimum) concentration in the ground water (pCi/L)

Q_{gw} = the average ground-water discharge to the Columbia River (m^3/s)

Q_{river} = the average (or maximum and minimum) flow rate of the river (m^3/s).

An average ground-water discharge to the Columbia River of 18,000 m^3/day was assumed for the Hanford Townsite study area. The average flow rate of the Columbia River at Priest Rapids Dam during 1991 was 4070 m^3/s (3.52 x 10^8 m^3/day), with a maximum monthly flow of 5490 m^3/s (4.74 x 10^8 m^3/day) and a minimum monthly flow of 2460 m^3/s (2.12 x 10^8 m^3/day). The concentration of tritium measured in wells minimally affected by bank storage at the Hanford Townsite study area and assumed to represent tritium concentrations in ground water was approximately 200,000 pCi/L. Based on the average Columbia River flow rates and average ground-water concentrations, tritium concentration in the river from ground-water discharge in the Hanford Townsite study area was estimated to be 10 pCi/L. A maximum concentration of approximately 17 pCi/L in the river was calculated using the minimum river flow rate. A minimum concentration of approximately 8 pCi/L in the river was estimated with the maximum river flow rate. These results agree favorably with those of Freshley and Thorne (1992). These numbers provide an estimate of the possible range of concentrations in the river resulting from ground-water discharge.

Contaminant mass discharge to the Columbia River from the Ringold Formation is considered at this time to be insignificant in relation to the discharge from the Hanford formation. This is because of the much lower transmissivity and tritium concentration in ground water within the Ringold Formation than within the Hanford formation.

6.3.3 Uncertainty and Limitations

The same limitations apply to the calculation of contaminant mass discharge to the Columbia River that applied to ground-water discharge calculations. These were discussed in Section 6.2.3. In addition, uncertainties in tritium concentrations apply to the contaminant mass discharge calculations; however, the uncertainties within this variable are very small in comparison to other uncertainties and limitations previously discussed. The total uncertainty factor assigned to the contaminant mass discharge calculation is plus or minus five.

7.0 CONCLUSIONS

Results provided in previous reports and obtained from the current study demonstrate that ground-water movement, contaminant distribution, and discharge to the Columbia River in the Hanford Townsite study area are influenced 1) by the local geology, 2) by regional ground-water conditions, and 3) significantly by river-stage fluctuations. These results led to the following major conclusions.

- Ground water containing tritium concentrations greater than the Drinking Water Standard of 20,000 pCi/L discharges to the Columbia River via several springs within the study area. The concentration of tritium in these springs, however, is lower than the concentration of tritium in ground water from wells as a result of dilution from bank storage. Tritium concentration in springs was as high as 155,000 pCi/L, and tritium concentration in wells was as high as 246,000 pCi/L for a similar sampling period.

- Ground-water velocity and tritium migration rate appear to be greater in the east-central part of the study area, just south of the subcrop of the Gable Mountain anticline structure, than in the southeast part of the study area. This region of higher hydraulic conductivity appears to be continuous to the river. Tritium concentration trends and aquifer test data support this conclusion.

- Fluctuations in Columbia River discharge (and stage) affect ground-water elevations in wells located as far as 800 m from the river. Wells near the river exhibit an increase in ground-water elevations during high river stage and a decrease in ground-water elevations during low river stage. Statistical analyses indicated a high degree of correlation between the river-stage fluctuations and well water-level fluctuations. The magnitude of river fluctuations was approximately 6 m, and the maximum magnitude of water-level fluctuations in wells affected by the river was approximately 3.5 m for the period of study. By contrast, the maximum magnitude of water-level fluctuations in wells influenced by regional ground-water flow alone was less than 0.4 m. The magnitude of the average horizontal hydraulic gradient across the length of the study area varied from approximately 3.1×10^{-3} when the river stage was low in October 1990 to approximately 2.4×10^{-3} when the river stage was high in May 1991.

- Fluctuations in Columbia River discharge and associated bank storage affect concentrations of tritium in wells. As the river stage rises, water from the river moves inland, resulting in dilution of tritium concentrations in wells near the river. During a period of approximately 5 months, tritium concentration fluctuated

approximately 70,000 pCi/L in a well located approximately 200 m from the river and fluctuated approximately 17,000 pCi/L in a well located approximately 800 m from the river. The fluctuations in tritium concentration were proportionally less than the fluctuations in water-level elevation within the well located farther from the river. This result indicates that water-level responses are seen farther from the river than are the dilution effects of the river.

- By far the majority of ground-water discharge to the Columbia River is from the Hanford formation aquifer. This formation has higher transmissivity and higher contaminant concentrations than seen in the underlying Ringold Formation. The saturated thickness of the Hanford formation ranges from zero to approximately 25 m. The aquifer is not present in the northwest portion of the study area where the Elephant Mountain basalt subcrops above the water table, and in two locations adjacent to the Columbia River in the east portion of the study area where clay- and silt-dominated facies of the Ringold Formation subcrop above the water table.

- Ground-water flow and the areas of greatest discharge to the river are very likely controlled by the areas where the Ringold Formation or Elephant Mountain basalt subcrop above the water table. Ground water is diverted around these areas where the Hanford formation aquifer is not present and discharges to the river in one (and quite possibly a second) restricted region. One of these regions, which is approximately 1500 m in width, coincides with the region where spring discharges have the highest concentrations of tritium; this region is located in the north-central portion of the river reach passing through the study area.

- Ground-water and contaminant discharge to the Columbia River was calculated based on best estimates of the aquifer hydraulic properties, aquifer geometry, and hydraulic gradients. The total ground-water discharge to the Columbia River was calculated to be approximately 6.6×10^6 m^3/year, which is about two and one-half times greater than a previously reported estimate. The total tritium mass discharge to the Columbia River was calculated to range from approximately 1100 to 1400 Ci/year. The tritium concentration in the river contributed from ground-water discharge was calculated to be approximately 10 pCi/L. The total uncertainty factor assigned to the calculated contaminant mass discharge calculations is plus or minus five. Although ground-water and contaminant discharge fluctuates based on the Columbia River stage, no estimates of the time-variant nature of contaminant discharge were made.

8.0 REFERENCES

Anderson, D. A., J. C. Tannehill, and R. H. Pletcher. 1984. Computational Fluid Mechanics and Heat Transfer. Hemisphere Publishing Corp., New York.

Bear, J. 1979. Hydraulics of Groundwater. McGraw-Hill, Inc., New York.

Bendat, J. S., and A. G. Piersol. 1986. Random Data; Analysis and Measurement Procedures. 2nd ed. John Wiley & Sons, Inc., New York.

Bjornstad, B. N. 1985. "Late Cenozoic Stratigraphy and Tectonic Evolution Within a Subsiding Basin, South-Central Washington." Geological Society of America Abstracts with Programs, no. 70805, v. 17, no. 7, p. 524.

Bjornstad, B. N., and K. R. Fecht. 1989. "Pre-Wisconsin Glacial-Outburst Floods: Pedogenic and Paleomagnetic Evidence from the Pasco Basin and Adjacent Channeled Scabland." Geological Society of America Abstracts with Programs, no. 1577, v. 21, no. 5, p. 58.

Bjornstad, B. N., K. R. Fecht, and A. M. Tallman. 1991. "Quaternary Stratigraphy of the Pasco Basin, South-Central Washington." In The Geology of North America, vol. K-2, Quaternary Nonglacial Geology; Conterminous U.S., ed. R. B. Morrison, pp. 228-238. Geological Society of America, Boulder, Colorado.

Brown, R. E. 1960. The Surface of the Ringold Formation Beneath the Hanford Works Area. HW-62530, General Electric Company, Richland, Washington.

Buske, N., and K. Josephson. 1986. Spring 1986 Data Report. Search Technical Services, Davenport, Washington.

Carslaw, H. S., and J. C. Jaeger. 1959. Conduction of Heat in Solids. Oxford University Press, Inc., London.

Cooney, F. M., and S. P. Thomas. 1989. Westinghouse Hanford Company Effluent Discharges and Solid Waste Management Report for Calendar Year 1988: 200/600 Areas. WHC-EP-0141-1, Westinghouse Hanford Company, Richland, Washington.

Dirkes, R. L. 1990. 1988 Hanford Riverbank Springs Characterization Report. PNL-7500, Pacific Northwest Laboratory, Richland, Washington.

DOE (see U.S. Department of Energy)

Eddy, P. A., C. S. Cline, and L. S. Prater. 1982. Radiological Status of the Ground Water Beneath the Hanford Site, January - December, 1981. PNL-4237, Pacific Northwest Laboratory, Richland, Washington.

Eddy, P. A., L. S. Prater, and J. T. Rieger. 1983. Ground-Water Surveillance at the Hanford Site for CY-1982. PNL-4659, Pacific Northwest Laboratory, Richland, Washington.

EPA (see U.S. Environmental Protection Agency)

Evans, J. C., R. W. Bryce, D. J. Bates, and M. L. Kemner. 1990. Hanford Site Ground-Water Surveillance for 1989. PNL-7396, Pacific Northwest Laboratory, Richland, Washington.

Evans, J. C., R. W. Bryce, D. R. Sherwood, M. L. Kemner, and D. R. Newcomer. 1989. Hanford Site Ground-Water Monitoring for July Through December 1988. PNL-7120, Pacific Northwest Laboratory, Richland, Washington.

Evans, J. C., D. I. Dennison, R. W. Bryce, P. J. Mitchell, D. R. Sherwood, K. M. Krupka, N. W. Hinman, E. A. Jacobson, and M. D. Freshley. 1988. Hanford Site Ground-Water Monitoring for July Through December 1987. PNL-6315-2, Pacific Northwest Laboratory, Richland, Washington.

Fecht, K. R., S. P. Reidel, and A. M. Tallman. 1987. "Paleodrainage of the Columbia River System on the Columbia Plateau of Washington State - A Summary." In Selected Papers on the Geology of Washington, ed. J. E. Schuster, pp. 219-248. Washington Division of Geology and Earth Resources Bulletin 77, Washington State Department of Natural Resources, Olympia, Washington.

Fletcher, C.A.J. 1988. Computational Techniques for Fluid Dynamics 1 - Fundamental and General Techniques. Springer-Verlag New York, Inc., New York.

Freshley, M. D., and M. J. Graham. 1988. Estimation of Ground-Water Travel Time at the Hanford Site: Description, Past Work, and Future Needs. PNL-6328, Pacific Northwest Laboratory, Richland, Washington.

Freshley, M. D., and P. D. Thorne. 1992. Ground-Water Contribution to Dose from Past Hanford Operations. PNL-7978 HEDR, Pacific Northwest Laboratory, Richland, Washington.

Gee, G. W. 1987. Recharge at the Hanford Site: Status Report. PNL-6403, Pacific Northwest Laboratory, Richland, Washington.

Gephart, R. E., R. C. Arnett, R. G. Baca, L. S. Leonhart, and F. A. Spane, Jr. 1979. Hydrologic Studies Within the Columbia Plateau, Washington: An Integration of Current Knowledge. RHO-BWI-ST-5, Rockwell Hanford Operations, Richland, Washington.

Graham, M. J., M. D. Hall, S. R. Strait, and W. R. Brown. 1981. Hydrology of the Separations Area. RHO-ST-42, Rockwell Hanford Operations, Richland, Washington.

Hem, J. D. 1970. Study and Interpretation of the Chemical Characteristics of Natural Water. 2nd ed. USGS Water-Supply Paper 1473, U.S. Geological Survey, Washington, D.C.

Jaquish, R. E., and R. W. Bryce, eds. 1990. Hanford Site Environmental Report for Calendar Year 1989. PNL-7346, Pacific Northwest Laboratory, Richland, Washington.

Kipp, K. L., and R. D. Mudd. 1973. Collection and Analysis of Pump Test Data for Transmissivity Values. BNWL-1709, Pacific Northwest Laboratory, Richland, Washington.

Lindsey, K. A. 1991. Revised Stratigraphy for the Ringold Formation, Hanford Site, South-Central Washington. WHC-SD-EN-EE-004, Rev. 0, Westinghouse Hanford Company, Richland, Washington.

McCormack, W. D., and J.M.V. Carlile. 1984. Investigation of Ground-Water Seepage from the Hanford Shoreline on the Columbia River. PNL-5289, Pacific Northwest Laboratory, Richland, Washington.

Mullineaux, D. R., R. E. Wilcox, W. F. Ebaugh, R. Fryxell, and M. Rubin. 1978. "Age of the Last Major Scabland Flood of the Columbia Plateau in Eastern Washington." Quaternary Research 10:171-180.

Murthy, K. S., L. A. Stout, B. A. Napier, A. E. Reisenauer, and D. K. Landstrom. 1983. Assessment of Single-Shell Tank Residual Liquid Issues at Hanford Site, Washington. PNL-4688, Pacific Northwest Laboratory, Richland, Washington.

Myers, C. W., S. M. Price, J. A. Caggiano, M. P. Cochran, W. J. Czimer, N. J. Davidson, R. C. Edwards, K. R. Fecht, G. E. Holmes, M. G. Jones, J. R. Kunk, R. D. Landon, R. K. Ledgerwood, J. T. Lillie, P. E. Long, T. H. Mitchell, E. H. Price, S. P. Reidel, and A. M. Tallman. 1979. Geologic Studies of the Columbia Plateau: A Status Report. RHO-BWI-ST-4, Rockwell Hanford Operations, Richland, Washington.

Newcomb, R. C., and S. G. Brown. 1961. Evaluation of Bank Storage Along the Columbia River Between Richland and China Bar, Washington. USGS Water-Supply Paper 1539-I, U.S. Geological Survey, Washington, D.C.

Newcomb, R. C., J. R. Strand, and F. J. Frank. 1972. Geology and Ground-Water Characteristics of the Hanford Reservation of the U.S. Atomic Energy Commission, Washington. USGS Professional Paper 717, U.S. Geological Survey, Washington, D.C.

Pacific Northwest Laboratory (PNL). 1987. Environmental Monitoring at Hanford for 1986. PNL-6120, Pacific Northwest Laboratory, Richland, Washington.

Pacific Northwest Laboratory (PNL). 1989. Procedures for Ground-Water Investigations. PNL-6894, Pacific Northwest Laboratory, Richland, Washington.

Pinder, G. F., J. D. Bredehoeft, and H. H. Cooper, Jr. 1969. "Determination of Aquifer Diffusivity from Aquifer Response to Fluctuations in River Stage." Water Resources Research 5(4):850-855.

PNL (see Pacific Northwest Laboratory)

Poeter, E. P., and D. R. Gaylord. 1990. "Influence of Aquifer Heterogeneity on Contaminant Transport at the Hanford Site." Ground Water 26(6):900-909.

Prater, L. S., J. T. Rieger, C. S. Cline, E. J. Jensen, T. L. Liikala, and K. R. Oster. 1984. Ground-Water Surveillance at the Hanford Site for CY-1983. PNL-5041, Pacific Northwest Laboratory, Richland, Washington.

Press, W. H., B. P. Flannery, S. A. Teukolsky, and W. T. Vetterling. 1986. Numerical Recipes, The Art of Scientific Computing. Cambridge University Press, Cambridge.

Price, K. R. 1986. Environmental Monitoring at Hanford for 1985. PNL-5817, Pacific Northwest Laboratory, Richland, Washington.

Puget Sound Power and Light Company (PSPL). 1982. Skagit/Hanford Nuclear Project, Preliminary Safety Analysis Report. Puget Sound Power and Light Company, Bellevue, Washington.

Serkowski, J. A., and W. A. Jordan. 1989. Operational Groundwater Monitoring at the Hanford Site - 1988. WHC-EP-0260, Westinghouse Hanford Company, Richland, Washington.

Tallman, A. M., K. R. Fecht, M. C. Marratt, and G. V. Last. 1979. Geology of the Separation Areas, Hanford Site, South-Central Washington. RHO-ST-23, Rockwell Hanford Operations, Richland, Washington.

U.S. Department of Energy (DOE). 1987. Final Environmental Impact Statement - Disposal of Hanford Defense High-Level, Transuranic and Tank Wastes. DOE/EIS-0113, U.S. Department of Energy, Richland, Washington.

U.S. Department of Energy (DOE). 1988. Consultation Draft, Site Characterization Plan, Reference Repository Location, Hanford Site, Richland, Washington. DOE/RW-0164, Vol. 1, U.S. Department of Energy, Washington, D.C.

U.S. Environmental Protection Agency (EPA). 1976. National Interim Primary Drinking Water Regulations. EPA-570/9-76-003, U.S. Environmental Protection Agency, Washington, D.C.

U.S. Geological Survey (USGS). 1987. Subsurface Transport of Radionuclides in Shallow Deposits of the Hanford Nuclear Reservation, Washington--Review of Selected Previous Work and Suggestions for Further Study. USGS Open-File Report 87-222, Tacoma, Washington.

Webster, G. D., and J. W. Crosby III. 1982. "Stratigraphic Investigation of the Skagit/Hanford Nuclear Project." In Skagit/Hanford Nuclear Project, Preliminary Safety Analysis Report, pp. 2R-i to 2R-35. Puget Sound Power and Light Company, Bellevue, Washington.

Woodruff, R. K., and R. W. Hanf. 1991. Hanford Site Environmental Report for Calendar Year 1990. PNL-7930, Pacific Northwest Laboratory, Richland, Washington.

Yim, C. S., and M.F.N. Mohsen. 1992. "Simulation of Tidal Effects on Contaminant Transport in Porous Media." Ground Water 30(1):78-86.

APPENDIX A

GEOPHYSICAL LOGGING INFORMATION

TABLE A.1. Summary of Pacific Northwest Laboratory Geophysical Logs for the Hanford Townsite Study Area (all units in feet)

WELL NUMBER	DATE	NAT. GAMMA	DENSITY	NEUTRON	TEMPERATURE	SONIC	MAGNETIC	SP&R	CALIPER	CAMERA
699-33-6	2/2/82	178-5	178-4	178-8	178-110	178-120				
699-33-14	5/13/82	119-5	120-4	120-5	119-70					
699-34-8	NONE									
699-35-3	NONE									
699-35-3A	NONE									
699-35-6	NONE									
699-35-9	2/9/62				166-121					YES
	2/26/62				166-121					
	4/24/62				166-120					
	5/22/62				164-121					
	7/3/62				164-121					
	8/29/62				166-120					
	10/24/62				166-120					
	1/9/63				166-120					
	4/22/63	166-0								
	7/25/63				120-166					
	12/13/63				120-166					
	7/24/64				120-166					
	4/26/67				116-168					
	3/12/68				116-166					
	1/29/74				163-120					
	5/20/80	168-5	168-4	196-5	170-122					
699-36-E3	1/25/82	352-4	353-4	353-7	354-90	353-100				
	2/1/82						353-256			

TABLE A.1. (contd)

WELL NUMBER	DATE	NAT. GAMMA	DENSITY	NEUTRON	TEMPERATURE	SONIC	MAGNETIC	SP&R	CALIPER	CAMERA
699-36-1	2/2/82	114-5	114-4	114-7						
	1/21/82									YES
699-36-2	2/2/82	286-5	286-4	286-6	287-90	286-110	285-220			
	8/22/90									285-0
699-36-10	8/23/90									141-0
699-37-E1	1/20/82									YES
	1/25/82	165-5	165-4	165-7	165-90					
	2/1/82						164-158			
	9/27/90									157-0
699-37-E4	NONE									
699-37-4	NONE									
699-38-E0	2/1/82	110-6	110-4	113-8	110-100					
	1/20/82									YES
699-38-3	NONE									
699-38-8	NONE									
699-38-9	2/2/82	82-5	83-4	79-7						
	1/21/82									YES
699-38-15	3/10/82	136-6	136-5	137-9	136-60					
699-39-E2	NONE									

TABLE A.1. (contd)

WELL NUMBER	DATE	NAT. GAMMA	DENSITY	NEUTRON	TEMPERATURE	SONIC	MAGNETIC	SP&R	CALIPER	CAMERA
699-39-0	10/27/80	99-6	100-4	100-7	100-87					
699-39-1	NONE									
699-39-2A	NONE									
699-39-7A	2/2/82	190-5	190-6	193-7	190-4	193-8				
	2/25/92	181-2.9					180-2.8			181-0
699-39-7B	3/3/92									139-0
699-39-12	NONE									
699-40-0	1/23/92									65-0
699-40-1	2/9/62				192-78					
	2/26/62				240-78					
	4/24/62				390-79					
	5/22/62				390-78					
	5/31/62				388-77					
	7/3/62				388-74					
	8/29/62				388-77					
	10/24/62				388-77					
	1/9/63				388-78					
	4/22/63	383-0								
	7/25/63				385-74					
	12/13/63				385-78					
	7/24/64				388-71					
	4/26/67				388-76					
	3/12/68				384-76					

TABLE A.1. (contd)

WELL NUMBER	DATE	NAT. GAMMA	DENSITY	NEUTRON	TEMPERATURE	SONIC	MAGNETIC	SP&R	CALIPER	CAMERA
	1/29/74				385-76					
	5/20/80	89-5	90-4	90-5	91-84					
	?									YES
699-40-2	NONE									
699-40-6	2/1/82	102-5	104-5	112-7						
	1/20/82									YES
699-40-12B	3/9/82	364-5	366-5							
	3/10/82			367-7						
699-40-13	2/11/82	500-4	501-5	501-6	500-10					
699-41-1	4/17/81				82-72					
	4/21/81	83-5	83-4	83-6						
699-41-4	NONE									
									264-164	
699-41-5	2/1/82	262-5	263-4	265-7	263-110	263-117		264-179		
	1/20/82									YES
	8/22/90									160-0
	1/23/92	261-2.4					260-4.9			151-0
699-41-10	NONE									
699-41-11	NONE									
699-42-2	4/21/81	95-4	95-4	95-5						
699-42-3	NONE									

TABLE A.1. (contd)

WELL NUMBER	DATE	NAT. GAMMA	DENSITY	NEUTRON	TEMPERATURE	SONIC	MAGNETIC	SP&R	CALIPER	CAMERA
699-42-10	5/14/82	222-4	222-3	222-6	222-125					
	8/22/90									221-0
699-42-12A	2/9/62				154-144					
	2/23/62				153-143					
	4/24/62				153-143					
	5/22/62				152-144					
	7/3/62				153-142					
	8/29/62				152-143					
	10/24/62				152-144					
	1/9/63				152-143					
	4/22/63	145-0								
	7/25/63				153-141					
	12/13/63				153-142					
	7/24/64				152-140					
	4/26/67				146-139					
	3/11/68				235-140					
	1/29/74				235-139					
	6/15/77									YES
699-42-12B	3/6/80	150-5								
	4/28/80		151-4	150-5						
699-42-12C	5/11/76									YES
699-43-2	NONE									
699-43-3	4/21/81	76-4	76-3	76-7						
	5/2/84									YES

TABLE A.1. (contd)

WELL NUMBER	DATE	NAT. GAMMA	DENSITY	NEUTRON	TEMPERATURE	SONIC	MAGNETIC	SP&R	CALIPER	CAMERA
699-43-8	NONE									
699-43-9	5/14/82	218-3	219-2	219-6	220-120					
	8/22/90									218-0
699-44-4	4/21/81	52-4	52-5	52-6						
699-44-7	5/13/82	475-3		475-7	476-60					
	2/23/91	473.3 - 1.9			473 - 0.8					
	2/25/91						473-10	473-5		
	8/23/90									473-0
699-45-2	10/27/80	47-4	48-4	48-8	49-27					
699-45-6A	NONE									
699-46-3	2/8/82	124-6	124-3	124-6	124-22					
	8/24/90									51-0
699-46-4	4/21/81	44-4	45-4	45-8						
699-46-5	2/8/82	380-6	380-5	380-5	380-9	380-12	380-300			
	2/22/91	379 - 2.5			1.4 - 382.5					
	2/26/91							377-10		
	8/24/90									381-0
699-46-15	1/21/82									YES
699-46-21B	9/2/80	150-5	149-4	150-8	139-132					
699-47-5	4/21/81	46-5	46-5	46-6						

TABLE A.1. (contd)

WELL NUMBER	DATE	NAT. GAMMA	DENSITY	NEUTRON	TEMPERATURE	SONIC	MAGNETIC	SP&R	CALIPER	CAMERA
699-48-7	2/9/62				40-26					
	2/23/62				46-32					
	4/23/62				46-24					
	5/22/62				46-24					
	5/31/62				45-19					
	7/3/62				45-20					
	8/29/62				45-28					
	10/24/62				45-32					
	1/9/63				45-31					
	7/25/63				45-23					
	12/13/63				45-32					
	7/24/64				45-18					
	4/26/67				43-28					
	3/11/68				44-27					
	1/29/74				44-24					
	5/5/76									YES
699-48-17	NONE									
699-48-18	1/29/74				76-63					
	6/28/76		82-3							
	4/28/80	81-5	82-4	82-6	84-64					
	5/5/76									YES
699-48-22	1/19/82									YES
699-49-10	NONE									
699-49-12A	NONE									

TABLE A.1. (contd)

WELL NUMBER	DATE	NAT. GAMMA	DENSITY	NEUTRON	TEMPERATURE	SONIC	MAGNETIC	SP&R	CALIPER	CAMERA
699-49-12B	NONE									
699-49-13A	NONE									
699-49-13B	NONE									
699-49-13C	NONE									
699-49-13D	NONE									
699-49-13E	2/9/62				81-52					
	2/23/62				80-51					
	4/23/62				81-52					
	5/22/62				80-51					
	7/3/62				80-49					
	8/29/62				80-51					
	10/24/62				81-51					
	1/9/63				84-51					
	7/25/63				80-49					
	12/13/63				80-51					
	7/23/74				81-45					
	4/26/67				81-51					
	3/11/68				80-50					
	1/29/74				82-51					
	3/15/77									YES
699-49-21	4/7/82	127-6	127-5	127-8	127-90					

APPENDIX B

ELEVATIONS OF THE TOP OF BASALT AND THE BOTTOM OF THE HANFORD FORMATION

TABLE B.1. Elevations of the Top of Basalt and the Bottom of the Hanford Formation Observed in Wells Within the Hanford Townsite Study Area

Well	Top of Basalt (m)	Bottom of Hanford Formation (m)	Top of Basalt (ft)	Bottom of Hanford Formation (ft)
699-31-8	-20.1	105.8	-66	347
699-31-11	-24.4	97.5	-80	320
699-31-17	-36.0	93.0	-118.1	305
699-33-6	-13.4	98.1	-44	322
699-33-14	-24.1	104.9	-79	344
699-33-21A	-37.2	102.4	-122	336
699-34-8	-11.6	96.0	-38	315
699-34-20	-33.8	94.2	-111	309
699-35-3	7.3	100.9	24.0	331.0
699-35-03B	25.3	101.5	83	333
699-35-6	0.3	102.7	1	337
699-35-9		102.1		335
699-35-16	-19.5	100.6	-64	330
699-35-19A	-25.3	100.6	-83	330
699-36-1	66.1	95.7	216.9	314
699-36-2	55.8	99.7	183	327
699-36-10	-7.6	101.8	-25	334
699-36-17	-12.8	100.0	-42	328
699-36-E3	42.4	104.5	139	343
699-37-4	77.7	101.2	255	332
699-37-E1	72.5	101.8	238	334
699-37-E4		110		361
699-38-3	87.5	100.9	287	331
699-38-8	21.3	103.3	70	339
699-38-9	2.1	107.6	7	353
699-38-15	-5.8	101.7	-19	333.7
699-38-19	-8.8	102.4	-29	336
699-38-E0	77.1	98.5	253	323
699-39-1	67.4	86.9	221.1	285
699-39-2	64.3	85.6	211.0	281
699-39-7A	103	107.0	337.9	351
699-39-7B	103	105.5	337.9	346
699-39-E2	66.4	85.0	217.8	279
699-40-0	29	106.4	95.1	349
699-40-1	38.4	95.1	126	312
699-40-2	32.0	104.5	105	343
699-40-6	78.0	101.8	256	334
699-40-12B	15.4	106.71	50.4	350.1

TABLE B.1. (contd)

Well	Top of Basalt (m)	Bottom of Hanford Formation (m)	Top of Basalt (ft)	Bottom of Hanford Formation (ft)
699-40-13	5.8	105.9	19	347.4
699-40-20	-4.6	103.9	-15	341
699-41-4	41.1	103.9	135	341
699-41-5	79.6	100.9	261.2	331
699-41-10	66.4	92.4	217.8	303
699-41-11	39.9	102.4	130.9	336
699-41-20	4.6	94.8	15	311
699-42-3	14	99.7	45.9	327
699-42-10	86.6	100.3	284.1	329
699-42-12A	100.6	95.1?	330	312?
699-42-21	0.6	103.3	2	339
699-43-1		107		350
699-43-2	20	104.9	65.6	344
699-43-3		100.6		330.04
699-43-8	63.4	98.1	208	322
699-43-9	98.8	98.8	324.1	324
699-43-18	18.6	99.7	61	327
699-44-2		104		340
699-44-7	4.3	104.9	14.1	344.3
699-44-16	28	94.5	91.9	310
699-45-2		103.0		338
699-45-6A	13.4	93.0	44	305
699-46-3	21	89.9	68.9	295
699-46-5	17	93.6	55.8	307
699-46-15	126	126	413.4	413
699-47-5		104.5		343
699-48-7		102.0		334.7
699-49-7A		103.1		338.1
699-49-10		108.9		357.2
699-49-12B		98.5		323.2
699-49-13E		102.63		336.72
699-49-21	118	118	387.1	387
699-51-19	105	109.4	344.5	359
699-52-17	15	93.9	49.2	308
699-54-15	18	92.4	59.1	303
Boring #1		108		355
Boring #2		111		364

APPENDIX C

WATER-LEVEL AND WATER-CHEMISTRY DATA

TABLE C.1. Water-Level Measurements and Elevations from Wells

Well Number	Casing Elevation ft, MSL	Date of Measure-ment	Depth to Water, ft	Water-Level Elevation above Mean Sea Level feet	meters
699-35-09	499.83	7/5/90	113.15	386.68	117.86
		7/20/90	113.21	386.62	117.84
		7/25/90	113.23	386.6	117.84
		8/17/90	113.2	386.63	117.84
		8/31/90	113.23	386.6	117.84
		9/17/90	113.26	386.57	117.83
		9/28/90	113.3	386.53	117.81
		10/12/90	113.24	386.59	117.83
		10/26/90	113.36	386.47	117.80
		11/9/90	113.31	386.52	117.81
		11/30/90	113.43	386.4	117.77
		12/6/90	113.43	386.4	117.77
		12/7/90	113.39	386.44	117.79
		12/21/90	113.5	386.33	117.75
		1/4/91	113.43	386.4	117.77
		1/18/91	113.44	386.39	117.77
		2/1/91	113.45	386.38	117.77
		2/15/91	113.49	386.34	117.76
		3/1/91	113.45	386.38	117.77
		3/15/91	113.57	386.26	117.73
		3/29/91	113.63	386.2	117.71
		4/26/91	113.64	386.19	117.71
		5/24/91	113.66	386.17	117.70
		6/21/91	113.72	386.11	117.69
		8/16/91	113.79	386.04	117.66
		9/13/91	113.79	386.04	117.66
		10/11/91	113.79	386.04	117.66
		11/25/91	113.88	385.95	117.64
		12/20/91	114.04	385.79	117.59
		1/16/92	114.08	385.75	117.58
		4/2/92	114.15	385.68	117.56
699-36-02	483.93	7/6/90	117.44	366.49	111.71
		12/6/90	118	365.93	111.54
699-36-10	526.99	7/5/90	140.68	386.31	117.75
699-37-E04	387.09	7/5/90	24.87	362.22	110.40
		12/6/90	27.24	359.85	109.68
		1/15/92	29.07	358.02	109.12
		1/16/92	28.84	358.25	109.19
		2/25/92	30.04	357.05	108.83
		4/2/92	29.41	357.68	109.02

TABLE C.1. (contd)

Well Number	Casing Elevation ft, MSL	Date of Measure-ment	Depth to Water, ft	Water-Level Elevation above Mean Sea Level feet	meters
699-37-04	488.87	1/16/92	111.89	376.98	114.90
699-38-15	454.75	7/5/90	59.54	395.21	120.46
		7/20/90	59.58	395.17	120.45
		7/25/90	59.59	395.16	120.44
		8/17/90	59.61	395.14	120.44
		8/30/90	59.64	395.11	120.43
		9/17/90	59.67	395.08	120.42
		9/28/90	59.68	395.07	120.42
		10/12/90	59.79	394.96	120.38
		10/26/90	59.73	395.02	120.40
		11/9/90	59.72	395.03	120.41
		11/30/90	59.78	394.97	120.39
		12/6/90	59.8	394.95	120.38
		12/7/90	59.79	394.96	120.38
		12/21/90	59.83	394.92	120.37
		1/4/91	59.84	394.91	120.37
		1/18/91	59.84	394.91	120.37
		2/1/91	59.86	394.89	120.36
		2/15/91	59.89	394.86	120.35
		3/1/91	59.89	394.86	120.35
		3/15/91	59.92	394.83	120.34
		3/29/91	59.95	394.8	120.34
		4/26/91	59.98	394.77	120.33
		5/24/91	60.02	394.73	120.31
		6/21/91	60.06	394.69	120.30
		8/16/91	60.11	394.64	120.29
		9/13/91	60.13	394.62	120.28
		10/11/91	60.16	394.59	120.27
		11/25/91	60.2	394.55	120.26
		12/20/91	60.26	394.49	120.24
		1/16/92	60.3	394.45	120.23
		4/2/92	60.35	394.4	120.21
699-39-E02	404.89	1/16/92	46.13	358.76	109.35
699-39-00	449.54	7/5/90	84.51	365.03	111.26
		12/6/90	85.39	364.15	110.99
		1/16/92	85.56	363.98	110.94
		2/25/92	85.62	363.92	110.92

TABLE C.1. (contd)

Well Number	Casing Elevation ft, MSL	Date of Measure-ment	Depth to Water, ft	Water-Level Elevation above Mean Sea Level feet	meters
699-39-07A	492.37	7/5/90	126.21	366.16	111.61
		7/20/90	126.23	366.14	111.60
		7/25/90	126.26	366.11	111.59
		8/17/90	126.27	366.1	111.59
		8/30/90	126.26	366.11	111.59
		9/17/90	126.27	366.1	111.59
		9/28/90	126.27	366.1	111.59
		10/12/90	126.23	366.14	111.60
		10/26/90	126.27	366.1	111.59
		11/9/90	126.31	366.06	111.58
		11/30/90	126.3	366.07	111.58
		12/6/90	126.3	366.07	111.58
		12/7/90	126.3	366.07	111.58
		12/21/90	126.31	366.06	111.58
		1/4/91	126.32	366.05	111.57
		1/18/91	126.31	366.06	111.58
		2/1/91	126.32	366.05	111.57
		2/15/91	126.33	366.04	111.57
		3/1/91	126.32	366.05	111.57
		3/15/91	126.33	366.04	111.57
		3/29/91	126.32	366.05	111.57
		4/26/91	126.32	366.05	111.57
		5/24/91	126.33	366.04	111.57
		6/21/91	126.32	366.05	111.57
		8/16/91	126.32	366.05	111.57
		9/13/91	126.33	366.04	111.57
		10/11/91	126.31	366.06	111.58
		11/25/91	126.31	366.06	111.58
		12/20/91	126.33	366.04	111.57
		1/16/92	126.34	366.03	111.57
		2/25/92	126.34	366.03	111.57
		4/2/92	126.38	365.99	111.55
699-40-01	438.71	6/18/90	74.31	364.4	111.07
		7/5/90	74.03	364.68	111.15
		1/15/92	75.29	363.42	110.77
		1/16/92	75.29	363.42	110.77
		2/25/92	75.38	363.33	110.74
		4/2/92	75.38	363.33	110.74

TABLE C.1. (contd)

Well Number	Casing Elevation ft, MSL	Date of Measure-ment	Depth to Water, ft	Water-Level Elevation above Mean Sea Level feet	meters
699-41-01	432.57	7/5/90	68.96	363.61	110.83
		8/30/90	70.77	361.8	110.28
		9/17/90	71.31	361.26	110.11
		9/28/90	71.51	361.06	110.05
		10/12/90	71.63	360.94	110.01
		10/26/90	71.77	360.8	109.97
		11/9/90	71.8	360.77	109.96
		11/30/90	71.04	361.53	110.19
		12/6/90	70.73	361.84	110.29
		12/7/90	70.7	361.87	110.30
		12/21/90	70.62	361.95	110.32
		1/4/91	70.28	362.29	110.43
		1/18/91	70.52	362.05	110.35
		2/1/91	69.98	362.59	110.52
		2/15/91	70.09	362.48	110.48
		3/1/91	70.25	362.32	110.44
		3/15/91	69.99	362.58	110.51
		3/29/91	69.87	362.7	110.55
		4/26/91	69.77	362.8	110.58
		5/24/91	69.72	362.85	110.60
		6/21/91	69.29	363.28	110.73
		8/16/91	69.94	362.63	110.53
		9/13/91	70.85	361.72	110.25
		10/11/91	71.49	361.08	110.06
		11/25/91	71.46	361.11	110.07
		12/20/91	71.65	360.92	110.01
		1/16/92	71.48	361.09	110.06
		2/25/92	71.88	360.69	109.94
		4/2/92	71.76	360.81	109.97
699-41-05	483.8	7/5/90	116.53	367.27	111.94
699-41-11	512.78	7/6/90	142.08	370.7	112.99
		7/20/90	142.08	370.7	112.99
		7/25/90	142.37	370.41	112.90
		8/17/90	142.59	370.19	112.83
		8/30/90	142.75	370.03	112.79
		9/17/90	142.88	369.9	112.75
		9/28/90	142.95	369.83	112.72
		10/12/90	142.98	369.8	112.72
		10/26/90	143.04	369.74	112.70
		11/9/90	143.05	369.73	112.69
		11/30/90	143.07	369.71	112.69
		12/7/90	143	369.78	112.71
		12/21/90	143	369.78	112.71

TABLE C.1. (contd)

Well Number	Casing Elevation ft, MSL	Date of Measure-ment	Depth to Water, ft	Water-Level Elevation above Mean Sea Level feet	meters
699-41-11	512.78	1/4/91	142.85	369.93	112.75
		1/18/91	142.84	369.94	112.76
		2/1/91	142.79	369.99	112.77
		2/15/91	142.75	370.03	112.79
		3/1/91	142.75	370.03	112.79
		3/15/91	142.72	370.06	112.79
		3/29/91	142.62	370.16	112.82
		4/26/91	142.44	370.34	112.88
		5/24/91	142.37	370.41	112.90
		6/21/91	141.78	371	113.08
		8/16/91	142.32	370.46	112.92
		9/13/91	142.53	370.25	112.85
		10/11/91	142.74	370.04	112.79
		11/25/91	142.83	369.95	112.76
		12/20/91	142.93	369.85	112.73
		1/16/92	142.93	369.85	112.73
		4/2/92	142.98	369.8	112.72
699-42-02	433.5	7/5/90	70.35	363.15	110.69
		1/16/92	75.45	358.05	109.13
		2/25/92	76.36	357.14	108.86
699-42-10	495.5	7/5/90	128.43	367.07	111.88
		7/20/90	128.53	366.97	111.85
		7/25/90	128.96	366.54	111.72
		8/17/90	129.26	366.24	111.63
		8/30/90	129.5	366	111.56
		9/17/90	129.63	365.87	111.52
		9/28/90	129.73	365.77	111.49
		10/12/90	129.76	365.74	111.48
		10/26/90	129.86	365.64	111.45
		11/9/90	129.88	365.62	111.44
		11/30/90	129.92	365.58	111.43
		12/6/90	129.83	365.67	111.46
		12/7/90	129.81	365.69	111.46
		12/21/90	129.8	365.7	111.47
		1/4/91	129.66	365.84	111.51
		1/18/91	129.68	365.82	111.50
		2/1/91	129.61	365.89	111.52
		2/15/91	129.59	365.91	111.53
		3/1/91	129.67	365.83	111.50
		3/15/91	129.6	365.9	111.53
		3/29/91	129.5	366	111.56
		4/26/91	129.31	366.19	111.61
		5/24/91	129.26	366.24	111.63

TABLE C.1. (contd)

Well Number	Casing Elevation ft, MSL	Date of Measure-ment	Depth to Water, ft	Water-Level Elevation above Mean Sea Level feet	meters
699-42-10	495.5	6/21/91	128.49	367.01	111.86
		8/16/91	129.3	366.2	111.62
		9/13/91	129.57	365.93	111.54
		10/11/91	129.82	365.68	111.46
		11/25/91	129.97	365.53	111.41
		12/20/91	130.09	365.41	111.38
		1/16/92	130.14	365.36	111.36
		4/2/92	130.27	365.23	111.32
699-42-12A	514.27	6/18/90	137.73	376.54	114.77
		7/5/90	137.51	376.76	114.84
		7/31/90	137.58	376.69	114.82
		8/7/90	137.66	376.61	114.79
		8/15/90	137.9	376.37	114.72
		8/22/90	137.75	376.52	114.76
		8/29/90	137.78	376.49	114.75
		9/4/90	137.85	376.42	114.73
		9/12/90	137.88	376.39	114.72
		9/17/90	137.87	376.4	114.73
		10/4/90	137.95	376.32	114.70
		10/10/90	138.25	376.02	114.61
		10/12/90	137.96	376.31	114.70
		10/24/90	138.04	376.23	114.67
		10/26/90	138.01	376.26	114.68
		11/9/90	138.03	376.24	114.68
		11/26/90	138.1	376.17	114.66
		11/30/90	138.08	376.19	114.66
		12/6/90	138.08	376.19	114.66
		12/7/90	138.08	376.19	114.66
		12/21/90	138.08	376.19	114.66
		1/4/91	138.04	376.23	114.67
		1/18/91	138.06	376.21	114.67
		2/1/91	138.07	376.2	114.67
		2/15/91	138.06	376.21	114.67
		3/1/91	138.07	376.2	114.67
		3/15/91	138.08	376.19	114.66
		3/29/91	138.05	376.22	114.67
		4/26/91	138.02	376.25	114.68
		6/21/91	137.82	376.45	114.74
		8/16/91	138.06	376.21	114.67
		9/13/91	138.19	376.08	114.63
		1/16/92	138.41	375.86	114.56
		2/25/92	138.55	375.72	114.52
		4/2/92	138.59	375.68	114.51

TABLE C.1. (contd)

Well Number	Casing Elevation ft, MSL	Date of Measure-ment	Depth to Water, ft	Water-Level Elevation above Mean Sea Level feet	meters
699-42-12B	514	8/30/90	138.77	375.23	114.37
		9/17/90	138.85	375.15	114.35
		9/28/90	138.89	375.11	114.33
		10/12/90	138.95	375.05	114.32
		10/26/90	138.99	375.01	114.30
		11/9/90	139	375	114.30
		11/30/90	139.06	374.94	114.28
		12/7/90	139.05	374.95	114.28
		12/21/90	139.05	374.95	114.28
		1/4/91	139.04	374.96	114.29
		1/18/91	139.05	374.95	114.28
		2/1/91	139.06	374.94	114.28
		2/15/91	139.05	374.95	114.28
		3/1/91	139.07	374.93	114.28
		3/15/91	139.07	374.93	114.28
		3/29/91	139.04	374.96	114.29
		4/26/91	139	375	114.30
		5/24/91	139	375	114.30
		8/16/91	139.05	374.95	114.28
		9/13/91	139.18	374.82	114.25
		10/11/91	139.22	374.78	114.23
		11/25/91	139.38	374.62	114.18
		12/20/91	139.43	374.57	114.17
		2/25/92	139.54	374.46	114.14
		4/2/92	139.68	374.32	114.09
699-43-03	419.64	7/5/90	56.65	362.99	110.64
		7/20/90	58.94	360.7	109.94
		7/25/90	60.89	358.75	109.35
		7/31/90	61.16	358.48	109.26
		8/7/90	60.66	358.98	109.42
		8/15/90	61.5	358.14	109.16
		8/17/90	61.54	358.1	109.15
		8/22/90	62.02	357.62	109.00
		8/29/90	61.82	357.82	109.06
		8/30/90	61.94	357.7	109.03
		9/4/90	62.9	356.74	108.73
		9/12/90	63.92	355.72	108.42
		9/17/90	63.7	355.94	108.49
		9/18/90	63.76	355.88	108.47
		9/26/90	63.93	355.71	108.42
		9/28/90	63.7	355.94	108.49
		10/4/90	63.72	355.92	108.48
		10/10/90	63.8	355.84	108.46
		10/12/90	63.72	355.92	108.48

TABLE C.1. (contd)

Well Number	Casing Elevation ft, MSL	Date of Measure-ment	Depth to Water, ft	Water-Level Elevation above Mean Sea Level feet	meters
699-43-03	419.64	10/24/90	63.85	355.79	108.44
		10/26/90	63.83	355.81	108.45
		11/9/90	63.34	356.3	108.60
		11/26/90	61.25	358.39	109.24
		11/30/90	60.32	359.32	109.52
		12/6/90	59.86	359.78	109.66
		12/7/90	59.82	359.82	109.67
		12/21/90	59.71	359.93	109.71
		1/4/91	60.05	359.59	109.60
		1/18/91	60.8	358.84	109.37
		2/1/91	58.37	361.27	110.12
		2/15/91	59.25	360.39	109.85
		3/1/91	59.51	360.13	109.77
		3/15/91	58.85	360.79	109.97
		3/29/91	58.29	361.35	110.14
		4/26/91	57.78	361.86	110.29
		5/24/91	57.29	362.35	110.44
		6/21/91	57.49	362.15	110.38
		8/16/91	58.91	360.73	109.95
		9/13/91	62.64	357	108.81
		10/11/91	63.46	356.18	108.56
		11/25/91	62.45	357.19	108.87
		12/20/91	62.16	357.48	108.96
		1/16/92	61.93	357.71	109.03
		1/22/92	61.81	357.83	109.07
		2/25/92	63.51	356.13	108.55
		4/2/92	62.89	356.75	108.74
699-43-09	490.74	7/5/90	127.28	363.46	110.78
699-44-04	391.27	7/5/90	28.54	362.73	110.56
		1/16/92	33.9	357.37	108.93
		2/25/92	36.36	354.91	108.18
699-44-07	437.78	7/6/90	70.81	366.97	111.85
		7/20/90	70.96	366.82	111.81
		7/25/90	71.16	366.62	111.75
		8/17/90	71.22	366.56	111.73
		8/30/90	71.25	366.53	111.72
		9/17/90	71.39	366.39	111.68
		9/28/90	71.45	366.33	111.66
		10/12/90	71.42	366.36	111.67
		10/26/90	71.5	366.28	111.64
		11/9/90	71.4	366.38	111.67
		11/30/90	71.33	366.45	111.69

TABLE C.1. (contd)

Well Number	Casing Elevation ft, MSL	Date of Measure-ment	Depth to Water, ft	Water-Level Elevation above Mean Sea Level feet	meters
699-44-07	437.78	12/6/90	71.4	366.38	111.67
		12/7/90	71.36	366.42	111.68
		12/21/90	71.35	366.43	111.69
		1/4/91	71.24	366.54	111.72
		1/18/91	71.23	366.55	111.72
		2/1/91	71.04	366.74	111.78
		2/15/91	71.12	366.66	111.76
		3/1/91	71.02	366.76	111.79
		3/15/91	71.07	366.71	111.77
		3/29/91	71.05	366.73	111.78
		4/26/91	70.9	366.88	111.83
		5/24/91	70.83	366.95	111.85
		6/21/91	70.6	367.18	111.92
		7/19/91	70.63	367.15	111.91
		8/16/91	70.84	366.94	111.84
		9/13/91	71.06	366.72	111.78
		10/11/91	71.19	366.59	111.74
		11/25/91	71.18	366.6	111.74
		12/20/91	71.27	366.51	111.71
		1/16/92	71.27	366.51	111.71
		4/2/92	71.42	366.36	111.67
699-45-02	379.89	7/5/90	17.43	362.46	110.48
		12/6/90	19..	359.99	109.72
		1/16/92	22.85	357.04	108.83
699-46-03	381.53	7/5/90	20.84	360.69	109.94
		12/6/90	22.85	358.68	109.33
		1/16/92	24.98	356.55	108.68
699-46-04	382.45	7/5/90	19.81	362.64	110.53
		7/31/90	24.53	357.92	109.09
		8/7/90	24.62	357.83	109.07
		8/15/90	24.98	357.47	108.96
		8/22/90	25.6	356.85	108.77
		8/29/90	24.84	357.61	109.00
		8/30/90	26.05	356.4	108.63
		9/4/90	28.6	353.85	107.85
		9/12/90	27.8	354.65	108.10
		9/18/90	28.53	353.92	107.87
		9/26/90	28.2	354.25	107.96
		9/28/90	27.4	355.05	108.22
		10/4/90	27.62	354.83	108.15

TABLE C.1. (contd)

Well Number	Casing Elevation ft, MSL	Date of Measure-ment	Depth to Water, ft	Water-Level Elevation above Mean Sea Level feet	meters
699-46-04	382.45	10/10/90	28.25	354.2	107.96
		10/12/90	27.45	355	108.20
		10/24/90	28.4	354.05	107.91
		10/26/90	28.08	354.37	108.01
		11/9/90	26.64	355.81	108.45
		11/26/90	23.25	359.2	109.48
		11/30/90	23.02	359.43	109.55
		12/6/90	22.36	360.09	109.76
		12/7/90	22.59	359.86	109.69
		12/21/90	21.67	360.78	109.97
		1/4/91	23.25	359.2	109.48
		1/18/91	24.25	358.2	109.18
		2/1/91	21.07	361.38	110.15
		2/15/91	22.27	360.18	109.78
		3/1/91	21.83	360.62	109.92
		3/15/91	21.74	360.71	109.94
		3/29/91	21.02	361.43	110.16
		4/26/91	20.45	362	110.34
		5/24/91	19.53	362.92	110.62
		6/21/91	21.4	361.05	110.05
		8/16/91	21.47	360.98	110.03
		9/13/91	26.77	355.68	108.41
		10/11/91	27.26	355.19	108.26
		11/25/91	26.52	355.93	108.49
		12/20/91	25.32	357.13	108.85
		1/16/92	25.23	357.22	108.88
		2/25/92	27.83	354.62	108.09
		4/2/92	26.39	356.06	108.53
699-46-05	384.3	7/5/90	6.92	377.38	115.03
		7/20/90	7.78	376.52	114.76
		7/25/90	8.07	376.23	114.67
		8/17/90	8.3	376	114.60
		8/30/90	8.59	375.71	114.52
		9/28/90	9.06	375.24	114.37
		10/12/90	9.03	375.27	114.38
		10/26/90	9.21	375.09	114.33
		11/9/90	8.78	375.52	114.46
		11/30/90	8	376.3	114.70
		12/6/90	8.02	376.28	114.69
		12/7/90	7.95	376.35	114.71
		12/21/90	7.71	376.59	114.78
		1/4/91	8.05	376.25	114.68
		1/18/91	8.11	376.19	114.66

TABLE C.1. (contd)

Well Number	Casing Elevation ft, MSL	Date of Measure-ment	Depth to Water, ft	Water-Level Elevation above Mean Sea Level feet	meters
699-46-05	384.3	2/1/91	7.28	377.02	114.92
		2/15/91	7.54	376.76	114.84
		3/1/91	7.12	377.18	114.96
		3/15/91	7.43	376.87	114.87
		3/29/91	7.34	376.96	114.90
		4/26/91	7.08	377.22	114.98
		5/24/91	6.81	377.49	115.06
		6/21/91	7.34	376.96	114.90
		7/19/91	7.67	376.63	114.80
		8/16/91	7.5	376.8	114.85
		9/13/91	8.61	375.69	114.51
		10/11/91	8.84	375.46	114.44
		11/25/91	8.63	375.67	114.50
		12/20/91	8.54	375.76	114.53
		1/16/92	8.4	375.9	114.57
		2/25/92	9.06	375.24	114.37
		4/2/92	8.67	375.63	114.49
699-47-05	382.25	7/5/90	19.54	362.71	110.55
		7/31/90	24.07	358.18	109.17
		8/7/90	24.2	358.05	109.13
		8/15/90	24.75	357.5	108.97
		8/22/90	25.26	356.99	108.81
		8/29/90	24.41	357.84	109.07
		9/4/90	28.6	353.65	107.79
		9/12/90	27.5	354.75	108.13
		9/18/90	28.17	354.08	107.92
		9/26/90	27.74	354.51	108.05
		10/4/90	27.14	355.11	108.24
		10/10/90	27.95	354.3	107.99
		10/24/90	27.75	354.5	108.05
		11/7/90	26.38	355.87	108.47
		11/26/90	22.53	359.72	109.64
		12/6/90	21.85	360.4	109.85
		12/20/90	21.81	360.44	109.86
		1/4/91	22.78	359.47	109.57
		2/6/91	22.46	359.79	109.66
		3/6/91	20.74	361.51	110.19
		7/19/91	22.35	359.9	109.70
		1/16/92	25.24	357.01	108.82

TABLE C.1. (contd)

Well Number	Casing Elevation ft, MSL	Date of Measure-ment	Depth to Water, ft	Water-Level Elevation above Mean Sea Level feet	meters
699-48-07	384.72	6/18/90	20.02	364.7	111.16
		7/5/90	21.95	362.77	110.57
		7/20/90	24.48	360.24	109.80
		7/25/90	25.18	359.54	109.59
		8/3/90	25.18	359.54	109.59
		8/17/90	27.69	357.03	108.82
		8/30/90	28.27	356.45	108.65
		8/31/90	28.27	356.45	108.65
		9/17/90	31.03	353.69	107.80
		9/28/90	29.3	355.42	108.33
		10/12/90	30.14	354.58	108.08
		10/26/90	30.15	354.57	108.07
		11/9/90	28.18	356.54	108.67
		11/30/90	24.72	360	109.73
		12/6/90	24.16	360.56	109.90
		12/7/90	24.48	360.24	109.80
		12/21/90	23.4	361.32	110.13
		1/4/91	25.27	359.45	109.56
		1/18/91	26.27	358.45	109.26
		2/1/91	22.87	361.85	110.29
		2/15/91	24.46	360.26	109.81
		3/1/91	23.74	360.98	110.03
		3/15/91	23.59	361.13	110.07
		3/29/91	23.05	361.67	110.24
		4/26/91	22.38	362.34	110.44
		5/24/91	21.49	363.23	110.71
		6/21/91	23.84	360.88	110.00
		7/19/91	24.15	360.57	109.90
		8/16/91	23.2	361.52	110.19
		9/13/91	29.15	355.57	108.38
		10/11/91	29.43	355.29	108.29
		11/25/91	28.94	355.78	108.44
		12/20/91	27.63	357.09	108.84
		1/16/92	27.8	356.92	108.79
		2/25/92	30.12	354.6	108.08
		4/2/92	28.59	356.13	108.55

TABLE C.2. Tritium Concentration Data Collected During the Study Period

Well Number	Sample Collection Date	Tritium Concentration (pCi/L)
699-42-12A	7/31/90	239,000
	8/22/90	234,000
	8/29/90	230,000
	10/4/90	230,000
	11/26/90	224,000
	12/6/90	222,000
	1/4/91	224,000
	2/6/91	223,000
	3/6/91	223,000
699-43-3	8/22/90	211,000
	8/29/90	207,000
	9/12/90	220,000
	10/10/90	224,000
	11/7/90	220,000
	11/26/90	223,000
	12/20/90	218,000
	2/6/91	210,000
	3/6/91	213,000
699-46-4	8/22/90	163,000
	8/29/90	157,000
	10/4/90	160,000
	11/26/90	179,000
	12/6/90	196,000
	1/4/91	192,000
	2/6/91	198,000
	3/6/91	197,000
699-47-5	7/31/90	123,000
	8/7/90	144,000
	8/15/90	148,000
	8/29/90	176,000
	9/4/90	184,000
	9/12/90	182,000
	9/18/90	187,000
	9/26/90	182,000
	10/4/90	180,000
	10/10/90	183,000
	11/7/90	169,000
	11/26/90	135,000
	12/6/90	128,000
	12/20/90	130,000
	1/4/91	139,000
	2/6/91	125,000
	3/6/91	120,000

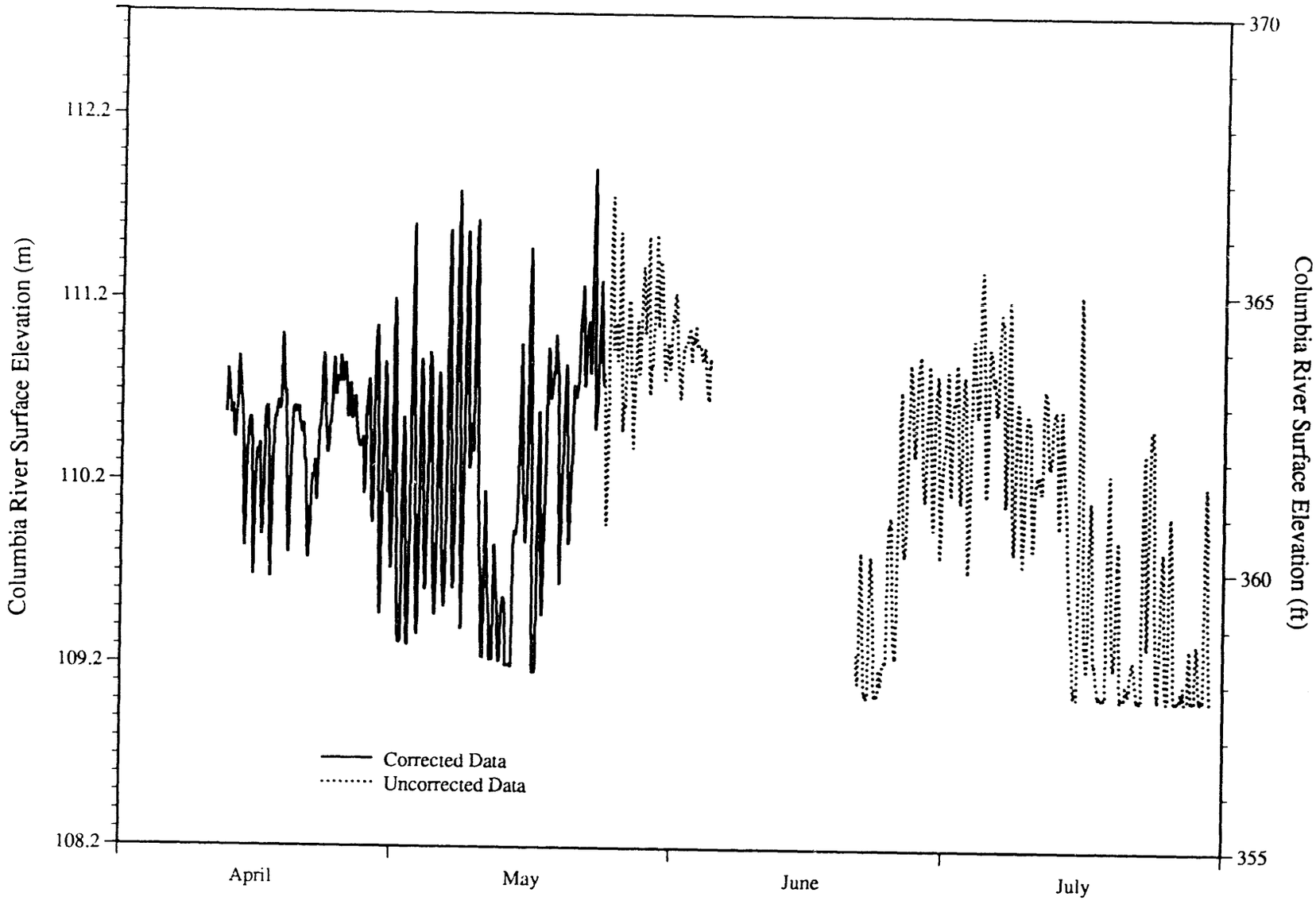

FIGURE C.1. Hanford Townsite River-Stage Data: April 1991 Through July 1991

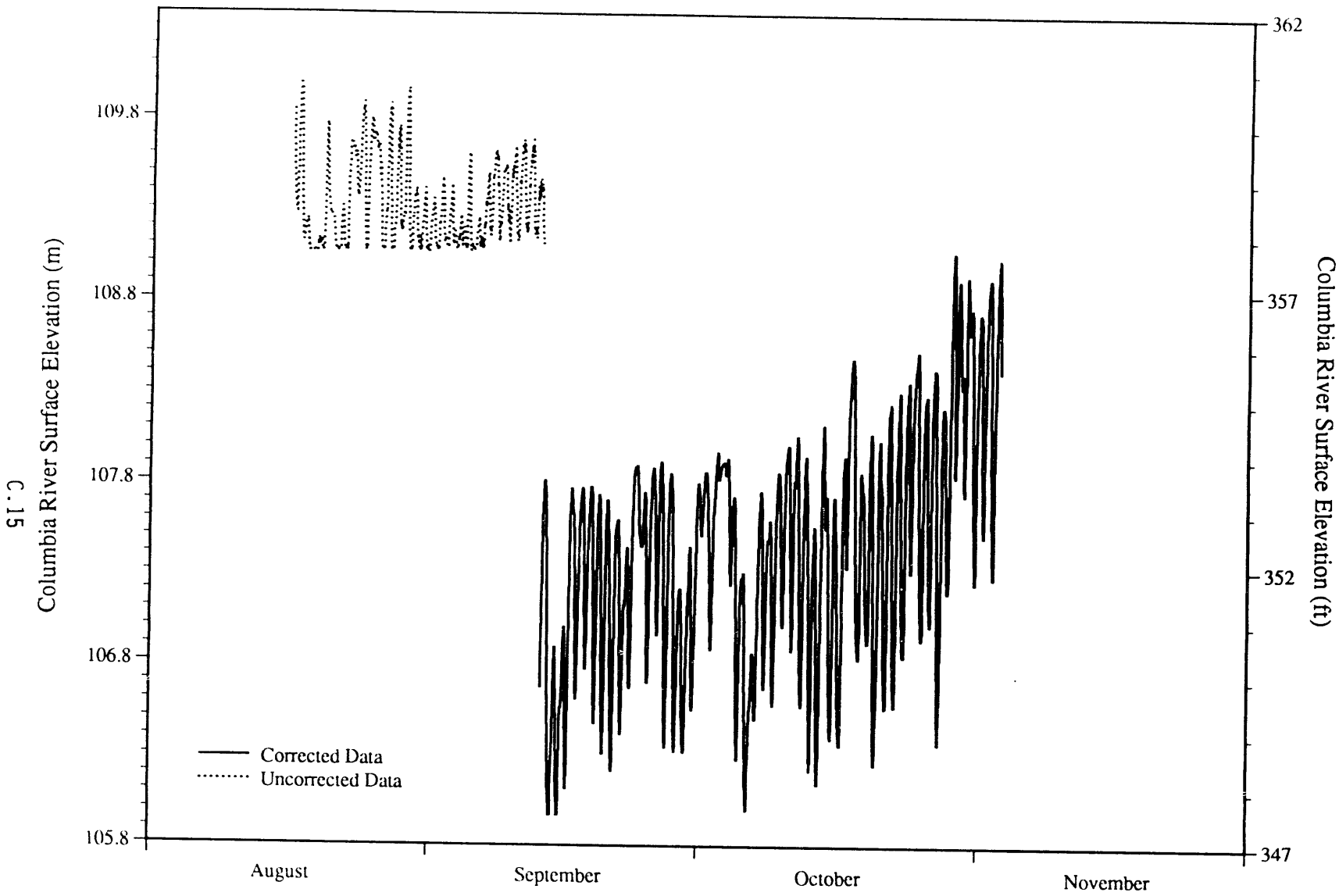

FIGURE C.2. Hanford Townsite River-Stage Data: August 1991 Through November 1991

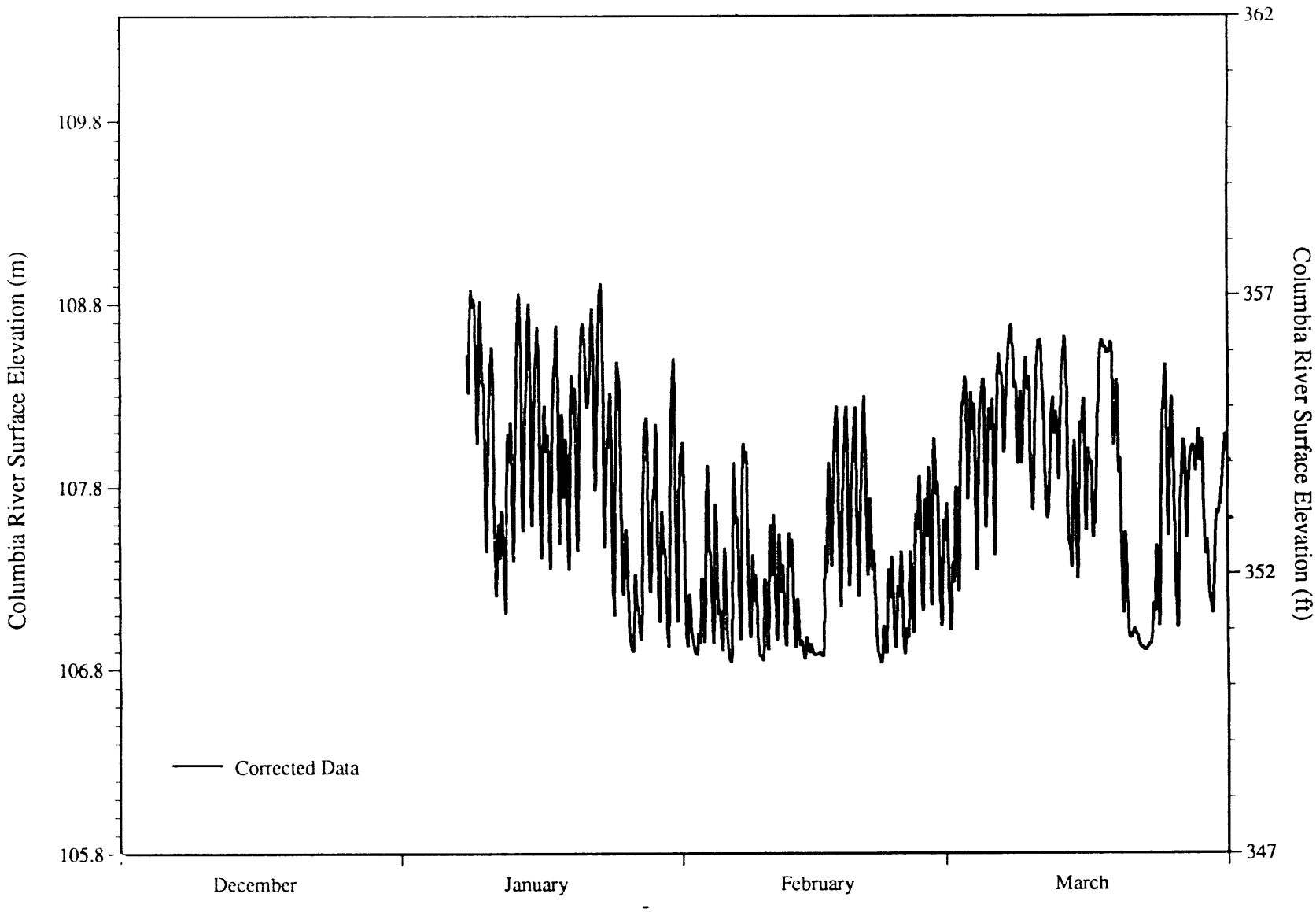

FIGURE C.3. Hanford Townsite River-Stage Data: December 1991 Through March 1992

TABLE C.3. Water-Chemistry Data from Fall 1987 Used for Constructing Stiff Diagrams

Constituent	Conversion	mg/L	meq/L	Percent
Well 699-35-9				
Anions				
HCO_3	0.02	122	2.440	56.3
SO_4	0.02082	44.1	0.918	21.2
Cl	0.02821	13.3	0.375	8.7
NO_3	0.01613	37.3	0.602	13.9
Cl + NO_3			0.977	22.5
		Total Anions	4.335	100.0
Cations				
Ca	0.0499	37	1.846	49.6
Mg	0.08226	11.3	0.930	25.0
Na	0.0435	18.6	0.809	21.7
K	0.02557	5.37	0.137	3.7
Na + K			0.946	25.4
		Total Cations	3.722	100.0
		Balance	16.5%	
Well 699-37-E4				
Anions				
HCO_3	0.02	117	2.340	65.8
SO_4	0.02082	26.8	0.558	15.7
Cl	0.02821	7.73	0.218	6.1
NO_3	0.01613	27.2	0.439	12.3
Cl + NO_3			0.657	18.5
		Total Anions	3.555	100.0
Cations				
Ca	0.0499	31.6	1.577	46.9
Mg	0.08226	11.7	0.962	28.6
Na	0.0435	15.8	0.687	20.5
K	0.02557	5.22	0.133	4.0
Na + K			0.821	24.4
		Total Cations	3.360	100.0
		Balance	5.8%	

TABLE C.3. (contd)

Well 699-40-1

Constituent	Conversion	mg/L	meq/L	Percent
Anions				
HCO_3	0.02	120	2.400	61.0
SO_4	0.02082	33.9	0.706	17.9
Cl	0.02821	9.3	0.262	6.7
NO_3	0.01613	35.1	0.566	14.4
$Cl + NO_3$			0.829	21.1
		Total Anions	3.934	100.0
Cations				
Ca	0.0499	38.2	1.906	49.4
Mg	0.08226	12.4	1.020	26.4
Na	0.0435	18.3	0.796	20.6
K	0.02557	5.36	0.137	3.6
Na + K			0.933	24.2
		Total Cations	3.859	100.0
		Balance	1.9%	

Well 699-41-1

Constituent	Conversion	mg/L	meq/L	Percent
Anions				
HCO_3	0.02	124	2.480	58.1
SO_4	0.02082	39.5	0.822	19.3
Cl	0.02821	11.1	0.313	7.3
NO_3	0.01613	40.4	0.652	15.3
$Cl + NO_3$			0.965	22.6
		Total Anions	4.267	100.0
Cations				
Ca	0.0499	40.8	2.036	50.4
Mg	0.08226	12.7	1.045	25.9
Na	0.0435	18.8	0.818	20.2
K	0.02557	5.58	0.143	3.5
Na + K			0.960	23.8
		Total Cations	4.041	100.0
		Balance	5.6%	

TABLE C.3. (contd)

Well 699-42-2

Constituent	Conversion	mg/L	meq/L	Percent
Anions				
HCO_3	0.02	125	2.500	58.6
SO_4	0.02082	39.2	0.816	19.1
Cl	0.02821	10.9	0.307	7.2
NO_3	0.01613	39.7	0.640	15.0
Cl + NO_3			0.948	22.2
		Total Anions	4.264	100.0
Cations				
Ca	0.0499	40.1	2.001	49.5
Mg	0.08226	12.8	1.053	26.0
Na	0.0435	19.4	0.844	20.9
K	0.02557	5.66	0.145	3.6
Na + K			0.989	24.5
		Total Cations	4.043	100.0
		Balance	5.5%	

Well 699-43-3

Constituent	Conversion	mg/L	meq/L	Percent
Anions				
HCO_3	0.02	125	2.500	58.1
SO_4	0.02082	41.2	0.858	19.9
Cl	0.02821	11.8	0.333	7.7
NO_3	0.01613	38	0.613	14.2
Cl + NO_3			0.946	22.0
		Total Anions	4.304	100.0
Cations				
Ca	0.0499	42.8	2.136	50.0
Mg	0.08226	13.7	1.127	26.4
Na	0.0435	20	0.870	20.4
K	0.02557	5.28	0.135	3.2
Na + K			1.005	23.5
		Total Cations	4.268	100.0
		Balance	0.8%	

TABLE C.3. (contd)

Well 699-45-2

Constituent	Conversion	mg/L	meq/L	Percent
Anions				
HCO_3	0.02	124	2.480	58.4
SO_4	0.02082	40.3	0.839	19.8
Cl	0.02821	11.4	0.322	7.6
NO_3	0.01613	37.4	0.603	14.2
$Cl + NO_3$			0.925	21.8
		Total Anions	4.244	100.0
Cations				
Ca	0.0499	39.8	1.986	50.5
Mg	0.08226	12	1.987	25.1
Na	0.0435	19	0.826	21.0
K	0.02557	5.1	0.130	3.3
Na + K			0.957	24.3
		Total Cations	3.930	100.0
		Balance	8.0%	

Well 699-46-4

Constituent	Conversion	mg/L	meq/L	Percent
Anions				
HCO_3	0.02	121	2.420	58.3
SO_4	0.02082	45.3	0.943	22.7
Cl	0.02821	11.8	0.333	8.0
NO_3	0.01613	28.4	0.458	11.0
$Cl + NO_3$			0.791	19.0
		Total Anions	4.154	100.0
Cations				
Ca	0.0499	39.1	1.951	47.6
Mg	0.08226	12.8	1.053	25.7
Na	0.0435	22.2	0.966	23.6
K	0.02557	5.04	0.129	3.1
Na + K			1.095	26.7
		Total Cations	4.099	100.0
		Balance	1.4%	

TABLE C.3. (contd)

Well 699-47-5

Constituent	Conversion	mg/L	meq/L	Percent
Anions				
HCO_3	0.02	121	2.420	56.7
SO_4	0.02082	50.7	1.056	24.7
Cl	0.02821	12.1	0.341	8.0
NO_3	0.01613	28	0.452	10.6
Cl + NO_3			0.793	18.6
		Total Anions	4.269	100.0
Cations				
Ca	0.0499	42.7	2.131	50.8
Mg	0.08226	10.5	0.864	20.6
Na	0.0435	24.3	1.057	25.2
K	0.02557	5.43	0.139	3.3
Na + K			1.196	28.5
		Total Cations	4.190	100.0
		Balance	1.9%	

Well 699-48-7

Constituent	Conversion	mg/L	meq/L	Percent
Anions				
HCO_3	0.02	104	2.080	76.0
SO_4	0.02082	20.6	0.429	15.7
Cl	0.02821	4.49	0.127	4.6
NO_3	0.01613	6.35	0.102	3.7
Cl + NO_3			0.229	8.4
		Total Anions	2.738	100.0
Cations				
Ca	0.0499	28	1.397	54.9
Mg	0.08226	8.18	0.673	26.4
Na	0.0435	9.77	0.425	16.7
K	0.02557	1.93	0.049	1.9
Na + K			0.474	18.6
		Total Cations	2.544	100.0
		Balance	7.6%	

DISTRIBUTION

No. of Copies

OFFSITE

12 DOE/Office of Scientific and Technical Information

C. Cline
Washington State Department of Ecology
MS 7600
99 South Sound Center
Olympia, WA 98504-7600

P. T. Day B5-01
U.S. Environmental Protection Agency
P.O. Box 550
Richland, WA 99352

J. Erickson
Washington State Department of Health
Division of Radiation Protection
Airdustrial Center
Building 5, MS L-13
Olympia, WA 98503

D. Jansen
Washington State Department of Ecology
MS 7600
99 South Sound Center
Olympia, WA 98504-7600

K. Kowalic
Washington State Department of Ecology
MS 7600
99 South Sound Center
Olympia, WA 98504-7600

No. of Copies

D. Nilander
Washington State Department of Ecology
7601 West Clearwater
Suite 102
Kennewick, WA 99336

D. R. Sherwood B5-01
U.S. Environmental Protection Agency
P.O. Box 550
Richland, WA 99352

ONSITE

14 DOE Richland Field Office

G. M. Bell	A5-52
J. K. Erickson	A5-19
M. J. Furman	A5-21
E. D. Goller	A5-19
J. D. Goodenough	A5-19
A. C. Harris	A5-19
R. D. Hildebrand	A5-55
R. G. Holt	A5-15
R. G. McLeod	A5-19
P. M. Pak	A5-19
R. K. Stewart	A5-19
K. M. Thompson	A5-15
M. W. Tiernan	A5-55
Public Reading Room	

26 Westinghouse Hanford Company

M. R. Adams	H4-55
J. W. Cammann	H4-14
G. D. Carpenter	B2-16
L. B. Collard	H4-14
C. D. Delaney	H4-56

No. of Copies

	L. P. Diediker	T1-30
	J. J. Dorian	B2-16
	K. R. Fecht	H4-56
	K. A. Gano	XO-21
	E. M. Greager	L6-60
	L. C. Hulstrom	H4-55
	R. L. Jackson	H4-56
	V. G. Johnson	H5-29
	A. J. Knepp	H4-56
	M. J. Lauterbach	H4-55
	A. G. Law	H4-56
	S. M. McKinney	T1-30
	D. L. Parker	H4-55
	R. E. Peterson	G4-08
	J. W. Roberts	H4-55
	J. A. Serkowski	H4-56
	K. R. Simpson	H5-29
	L. C. Swanson	H5-29
	S. J. Trent	H4-56
	S. E. Vukelich	H4-55
	C. D. Wittreich	H4-55
54	Pacific Northwest Laboratory	
	M. P. Bergeron	K6-77
	B. N. Bjornstad	K6-96
	J. V. Borghese	K6-96
	R. W. Bryce	K6-96
	M. A. Chamness	K6-96
	R. L. Dirkes	K6-13
	P. G. Doctor	K6-96
	J. C. Evans	K6-81
	M. D. Freshley	K6-77
	R. E. Gephart	K1-22
	T. J Gilmore	K6-96

No. of Copies

	R. H. Gray	K1-33
	S. H. Hall	K6-96
	M. S. Hanson	K1-51
	D. C. Lanigan	K6-84
	G. V. Last	K6-96
	T. L. Liikala	k6-96
	S. P. Luttrell (10)	K6-96
	D. L. McAlister	K6-96
	P. D. Meyer	K6-77
	D. R. Newcomer (3)	K6-96
	A. W. Pearson	K6-96
	D. A. Perez	K6-86
	K. D. Pohlod	K6-96
	J. T. Rieger	K6-96
	R. Schalla	K6-96
	F. A. Spane	K6-96
	S. S. Teel (3)	K6-96
	P. D. Thorne	K6-96
	V. R. Vermeul (3)	K6-77
	R. W. Wallace	K6-77
	R. K. Woodruff	K6-13
	Publishing Coordination	
	Technical Report Files (5)	

Routing

R. M. Ecker	SEQUIM
J. W. Falco	K6-78
M. J. Graham	K6-80
C. J. Hostetler	K6-81
P. M. Irving	K6-98
R. L. Skaggs	K6-77
C. S. Sloane	K6-04
P. C. Hays (last)	K6-86

END

DATE
FILMED
6/8/93